

REAL TIME OPTIMISATION
OF AN
ACTIVE FILTER'S PERFORMANCE
AND APPLICATIONS TO THE POWER SYSTEM

A thesis
presented for the degree of
Doctor of Philosophy in Electrical and Electronic Engineering
in the
University of Canterbury,
New Zealand

by

Simon Douglas Round, B.E.(Hons.)

September 1992

Abstract

Power system loads have traditionally drawn a sinusoidal current. Due to recent advances in power electronics, many loads now draw a nonsinusoidal or distorted current from the supply. Regulations limit the level of distortion larger loads may draw, but small loads are excluded. However, the smaller loads collectively create a distortion problem which needs to be compensated for. To reduce the distortion drawn from the power system, a shunt active filter has been developed. Computer simulations which have been performed, demonstrate that the active filter can compensate for distortive load currents, resulting in near sinusoidal supply currents.

Single and three phase analogue controlled active filters have been constructed to compensate for harmonic and phase displaced current distortion. The three phase active filter can also balance the supply currents for unbalanced harmonic loads. For different load types, the power amplifier switching frequency and DC bus voltage affect the active filter's efficiency and ability to reduce the supply current distortion.

A digital controller has been developed which allows the active filter to operate at an optimum level of supply current and efficiency, independent of the load type. A financially based savings calculation has been developed to determine the relationship between distortion reduction and operational efficiency in order to perform this optimisation. The optimum operating point was determined using a simplex optimisation algorithm which climbs the calculated savings surface to achieve maximum savings. The ability of the optimisation algorithm to find the point of maximum savings and to adapt to load changes has been demonstrated. The optimisation algorithm has been extended to include phase displacement compensation in the calculation of the maximum savings point.

A novel application of the active filter, where passive filters can not be used, is presented. This involves providing compensation for nonlinear loads operating from a weak, variable frequency AC system. The ability of the active filter to compensate for both the generator's current and voltage distortion is demonstrated. An initial investigation of a resonant link active filter to reduce the switching losses is also presented.

Acknowledgements

I would like to thank my supervisor Richard Duke for his enthusiasm, encouragement and support throughout the three and half years of my research. Additional thanks to Richard for the occasions when he has gone the extra mile, working at night helping with diagrams and papers and especially coping with the pressure of reading this thesis in a hurry. I would also like to thank Jos Arrillaga for his advice and expertise in the area of Power System harmonics.

I would like to thank the people in Power Electronics Lab for the fruitful discussions we have had on the world, life and sometimes power electronics. Especially thanks to my colleagues who have helped proof read this thesis. Thanks to Chris Kaiser for his suggestions on optimisation and model aeroplanes, Mark Tomlinson for his mathematical and computer ability, and to Ross Walker, Hamish Laird and Rodger Brough. A general thanks to all the other people to whom I've had discussions with, including the technical staff of my department, and especially to Bernice "Bernie" Hintz for bringing us back to the real world!

To Ken Henderson, who started this work, Bart Schroder and Paul Handley, my thanks for their advice on some of the finer points on the design of power electronic equipment.

I extend my gratitude for the financial support from the University Grants Committee, Institute of Professional Engineers of NZ, Tait Electronics Ltd for the scholarships granted to me. Also thanks to the GEC (NZ) Ltd and NZ Lotteries Commission for the financial contribution which enabled us to obtain the DSP hardware for this project.

A big thanks to Mum and Dad for their support and encouragement throughout my BE and this thesis work. I am sorry it has been so difficult for them to understand what I have been doing! My final thanks is to Jane Piper for her wonderful support and understanding during my studies at University. Jane has kept me going throughout all of this work.

Nomenclature

Abbreviations

AC	alternating current
ADC	analogue to digital converter
BPF	band pass filter
DAC	digital to analogue converter
DC	direct current
DSP	digital signal processor
EMI	electromagnetic interference
EPROM	erasable programmable read only memory
FFT	fast fourier transform
FIR	finite impulse response (filter)
IGBT	insulated gate bipolar transistor
KVL	Kirchoff's voltage law
MCT	MOS controlled thyristor
MOS	metal oxide semiconductor
PC	personal computer
PI	proportional-integral (control)
PID	proportional-integral-derivative (control)
PI+FF	proportional-integral and feed forward (control)
PLL	phase locked loop
PWM	pulse width modulation
RMS	root mean square
SPU	signal processing unit
THD	total harmonic distortion
ZCD	zero crossing detector
ZCS	zero current switching
ZVS	zero voltage switching

Symbols

I_c	compensating current
I_c'	compensating current signal
I_L	load current
I_s	supply current
P	real power
S	apparent power
ΔP	extra power consumed to active filter
ζ	efficiency of the active filter
$\cos\theta$	displacement factor
μ	distortion factor
pf	power factor (harmonic and displacement)

Chg()	charge for power
R_c	energy cost ratio (charging ratio of real to apparent power)
C_{NAF}	cost of a distortive load
C_{AF}	cost of a compensated supply current
SAV	actual savings made from active filtering
SAV_R	percentage savings referenced to cost of not active filtering
PEN	penalty function
THD	total harmonic distortion
THD_{MAX}	maximum allowed total harmonic distortion

Publications Associated With This Thesis

The following publications have been made as a result of the work contained in this thesis:

- 1/ "Novel use of a synthetic sinusoid in the measurement of power system harmonics", Duke R.M, Round S.D, Proc. 6th Conf. on Power Electronics and Motion Control, Budapest, Hungary. Oct.1-3 1990, Vol. 2, pp.368-373.
- 2/ "An active filter for current distortion compensation in power systems", Duke R.M., Round S.D. and Henderson K.C, Proc. 4th Intl. Conf. on Harmonics in Power Systems, Budapest, Hungary. Oct.4-6 1990, pp.367-73.

Also included in: Electric Power Research Institute (USA) Research Publication RP2951-7, Survey of Active Power Line Conditioning Methodologies, 1991.

- 3/ "An Active Distortion Compensation System", Round S.D, Duke R.M, Proc. NELCON, Vol. 28, Palmerston North, New Zealand, August 1991, pp. 99-104.
- 4/ "The steady state performance of a controlled current active filter", Duke R.M., Round S.D., IEEE Trans. on Power Electronics, submitted in revised form August 1991, accepted for publication October 1991.
- 5/ "A controlled current inverter for active distortion compensation and power factor correction", Round S.D, Duke R.M, IECON, Kobe, Japan, Oct 28 - Nov 2, 1991, Vol. 1, pp. 735-740.
- 6/ "Design of an Intelligent Controller for an Active Filter", Duke R.M., Round S.D., Proc. Singapore International Conference on Intelligent Control and Instrumentation, Singapore, Feb. 1992, Vol. 2, pp. 1168-73.
- 7/ "Energy Savings from Active Filtering", Round S.D., Duke R.M., Proc. NELCON, Vol. 29, Wellington, New Zealand, August 18-20, 1992, pp. 147-152.

TABLE OF CONTENTS

Abstract	iii
Acknowledgements	v
Nomenclature	vii
Publications Associated With This Thesis	ix
 1 INTRODUCTION	 1
1.1 Definitions of Power System Distortion	3
1.2 Scope of Thesis	4
 2 HARMONIC REDUCTION TECHNIQUES	 7
2.1 Passive Filters	7
2.2 Pulse Number Modification	9
2.3 Active Filters	9
2.3.1 Series Active Filter	10
2.3.2 Shunt Active Filter	11
2.3.2.1 Power Amplifier Configurations	13
2.3.2.2 Compensating Signal Generation	13
2.3.2.3 Switching Strategy	14
2.4 Proposed Method of Current Distortion Compensation	15
 3 MODELLING AND COMPUTER SIMULATION	 17
3.1 Mathematical Model	18
3.2 Active filter Model	21
3.2.1 Implementation of the Computer Model	25
3.3 Computer Simulation of the Active Filter's Performance	25
3.3.1 Steady State Operation	26
3.3.2 Transient Performance	28
3.4 Summary	30
 4 ANALOGUE ACTIVE FILTER	 31
4.1 Single Phase Hardware Description	31
4.1.1 Signal Processing	32
4.1.1.1 Compensating Current Signal Generation	32
4.1.1.2 Magnitude Control	33
4.1.2 Power Amplifier	36
4.1.2.1 Switching Strategy	37
4.1.2.2 Reinjection Transformer	38

4.2 Three Phase Active Filtering System	38
4.3 Summary	39
5 PERFORMANCE OF THE ANALOGUE ACTIVE FILTER	41
5.1 Single Phase Steady State Performance	41
5.1.1 Harmonic Current Compensation	41
5.1.2 Distortion Compensation	44
5.2 Three Phase Steady State Operation	46
5.2.1 Performance	46
5.2.2 Phase Balancing	48
5.3 Transient Performance	53
5.3.1 Single Phase	53
5.3.2 Three Phase	54
5.4 Operational Performance of the Single Phase Active Filter	56
5.5 Summary	60
6 DIGITAL CONTROLLER FOR THE ACTIVE FILTER	63
6.1 Requirements of a Digital Controller	63
6.2 Hardware Description	65
6.3 Software Description	69
6.3.1 Interrupt Functions	69
6.3.2 Non Interrupt Functions	72
6.4 Steady State Performance	73
6.5 Transient Performance	73
6.5.1 Bus Voltage Control	75
6.5.2 Feed-Forward Control	80
6.6 Summary	84
7 OPTIMISATION OF ENERGY SAVINGS	85
7.1 Cost Function	86
7.1.1 Derivation of the Cost Function	87
7.1.2 Energy Cost Ratio	91
7.1.3 Setting the Maximum Allowed Supply Current THD	93
7.2 Maximisation of Savings	95
7.3 Results of Optimisation	97
7.3.1 Changing the Starting Point	98
7.3.2 Effect of Load Changes	99
7.4 Power Factor Correction	100
7.4.1 Displacement Correction	100
7.4.2 Distortion and Displacement Correction	104

<i>TABLE OF CONTENTS</i>	xiii
7.4.3 Three Variable Optimisation	105
7.5 Summary	106
8 NOVEL APPLICATIONS OF ACTIVE FILTERING	109
8.1 Variable Frequency Generation Systems	109
8.1.1 Hardware Model	110
8.1.2 Computer Simulation of a Large Isolated Generation System	112
8.2 Three Phase Rectifier with DC-Link Current Shaping	116
8.2.1 Computer Simulation	117
8.2.2 Hardware Model	118
8.3 Summary	120
9 RESONANT LINK ACTIVE FILTER	123
9.1 Analysis of Resonant Link Behaviour	124
9.2 Hardware Model	129
9.3 Computer Simulation of a Resonant Active Filter	133
9.4 Hardware Implementation of the Resonant Link Active Filter	136
9.5 Summary	138
10 DISCUSSION and CONCLUSION	141
10.1 Future Work	141
10.1.1 Optimisation Techniques	141
10.1.2 Bus Voltage Control	142
10.1.3 Phase Balancing	143
10.1.4 Adaptive Fundamental Tracking Filter	143
10.2 Conclusion	144
REFERENCES	147
APPENDIX A Mathematical Analysis of Resonant Link	153

LIST OF FIGURES

2.1 Shunt Passive Filters	7
2.2 Passive Filter Combination for a 6 Pulse Converter	8
2.3 Series and Shunt Active Filter	10
2.4 Single Phase Model of the Series Active Filter	11
2.5 Magnetic Flux Compensation Technique to Eliminate Power System Harmonics	12
2.6 Block Representation of Proposed Distortion Compensation System	15
3.1 Computer Model of the Active Filter	22
3.2 Two Model Configurations used for Simulating the Active Filter	23
3.3 Time Delayed Switching Strategy for the Controlled Current Inverter	24
3.4 Results of Steady State Simulation	27
3.5 Computed Transient Response of the Active Filter	29
4.1 Block Representation of Active Filtering System	31
4.2 Signal Processing Unit (SPU) of the Analogue Active Filter	32
4.3 Generation of Compensating Current Signal	34
4.4 Effect of Bus Voltage on Compensation Ability of the Active Filter	35
4.5 Power Amplifier Configuration	36
4.6 Hardware Implementation of the Time Delay Circuit	37
4.7 Connection of the Three Phase Active Filter	39
5.1 Single Phase Harmonic Load	41
5.2 Steady State Operation of the Active Filter for a Harmonic Load	43
5.3 Single Phase Harmonic and Displacement Load	44
5.4 Steady State Operation of the Active Filter to a Distorted Load	45
5.5 Three Phase Bridge Rectifier with Capacitive and Resistive Load	46
5.6 Steady State Results for a Three Phase Active Filter Compensating for a Bridge Rectifier with Capacitive and Resistive Load	47
5.7 Three Phase Bridge Rectifier with Inductive and Resistive Load	48
5.8 Active Filter Compensating for Three Phase Bridge Rectifier with Inductive and Resistive Load	48
5.9 Connection of the Three Phase Active Filter to provide Phase Balancing	49
5.10 Load to Provide Unbalanced and Harmonic Currents	49
5.11 Supply Current for an Unbalanced, Harmonic Load before Active Filtering	51
5.12 Supply Current for Active Filtering with an Unbalanced, Harmonic Load ..	52

5.13 DC Link Currents due to Phase Balancing	53
5.14 Single Phase Active Filter's Transient Response to a Step Increase in Harmonic Load	55
5.15 Transient Response for the Three Phase Active Filter for a Step Increase in Load Current using a Bus Voltage Controller	56
5.16 Switching Frequency Profiles for a DC Bus Voltage Increase from 190 V _{DC} to 350 V _{DC}	58
5.17 Performance of the Single Phase Active Filter	58
6.1 External Connection of the Active Filter to the TMS320C30 Digital Controller	65
6.2 Load Current's Measurement System	66
6.3 Lower Sampling Rate Analogue to Digital Converters	67
6.4 Low Sample Rate Digital Output for Time Delay Circuit	67
6.5 Digitally Controlled Time Delay	68
6.6 Interrupt Timing of TMS320C30	70
6.7 Operational Performance of the Digitally Controlled Active Filter	74
6.8 Implementation of PI Bus Voltage Controller	75
6.9 PI Controller Response to Different Integral Time Constants	78
6.10 Startup Transient of PI Controller	78
6.11 Sub-harmonics due to PI Controller	80
6.12 Addition of Feed-Forward to Bus Voltage Controller	81
6.13 Feed-Forward Controller	81
6.14 Output of Differentiator	82
6.15 Experimental Output of Feed-Forward Controller Due to Step Load Change	82
6.16 Response of Bus Voltage to Feed-Forward & PI and PI Controllers	83
7.1 Operating Characteristic of the Active Filter	86
7.2 Definition of Power Flow	87
7.3 Energy Savings Gained by Active Filtering	90
7.4 Effect of Harmonic Distortion on Energy Cost	92
7.5 Effect of Energy Cost Ratio R_C	94
7.6 Effect of setting maximum allowed THD	96
7.7 Modes of the Simplex Algorithm	98
7.8 Climbing the Savings Surface from Two Different Starting Points	99
7.9 Tracking Maximum under Load Change	101
7.10 Displacement Correction by the Digitally Controlled Active Filter	103
7.11 Possible Savings by Displacement Correction for various Resistive and Inductive Loads.	103

LIST OF FIGURES

xvii

7.12 Distortion and Displacement Compensation	104
7.13 Savings for Performing Power Factor Correction at a Cost Ratio of Five ..	105
7.14 Three Variable Optimisation Track	107
8.1 Hardware Connection for Active Filtering from a Variable Frequency Generation System	110
8.2 Experimental Results of Isolated Generator and Active Filtering System ...	111
8.3 Operation of the Active Filter during a Shift in Fundamental Frequency ...	113
8.4 12 Pulse DC System Supplied by Isolated Generation	113
8.5 Computer Simulation Results of 12 pulse DC Link and Isolated Generator .	115
8.6 Boost Converter Configuration	116
8.7 Active Filter Connection to the Controlled Current Boost Converter	117
8.8 Computer Simulation of the Active Filter and Controlled Current Boost Converter	118
8.9 Hardware Test Results of the Active Filter and Controlled Current Boost Converter	119
9.1 Block Diagram of Resonant Link Active Filter	124
9.2 Resonant Link Converter Circuit for Active Filter	125
9.3 Resonant Current and Voltage Analytically Calculated	127
9.4 Failure of the Resonant Cycle	129
9.5 Hardware Implementation of Resonant Link Model	130
9.6 Resonant Switching Cycles for the Hardware Model	131
9.7 Operation of the Resonant Capacitor Voltage as the Load Current Ramps Up	131
9.8 Ability of Resonant Link Converter to follow an Arbitrary Waveform	132
9.9 Multiresonant Link Circuit to Improve Performance at Low Load Current Levels	132
9.10 Computer Simulated Performance of the Resonant Active Filter	134
9.11 Final Hardware Implementation of the Resonant Link Active Filter	137
9.12 Supply, Compensating and Load Currents during Operation of the Resonant Link Active Filter	138
A.1 Resonant Link Configuration used in Resonant Cycle Analysis	153
A.2 Simplified Resonant Link Configuration when diode D is freewheeling	154
A.3 Simplified Resonant Link Configuration when Diode D is off	154

LIST OF TABLES

Table 5.1 Comparison of Supply Current Values for Phase Balancing	51
Table 6.1 Ziegler-Nichols Tuning Formula	76
Table 9.1 Comparison of Losses with and without a Resonant Link Converter .	136

CHAPTER 1

INTRODUCTION

The decline in the earth's environmental conditions, due to the production of greenhouse gases, depletion of the ozone layer and pollution produced by motor vehicles and industry, has slowly made the global community aware that action must be taken to protect the earth for both present and future generations [Leggett 1992]. The solution to these problems can not be achieved quickly since a country's economic survival is dependent on the industrial and personal productivity that uses these "environmentally unfriendly" processes. Over time these processes will be able to be modified, but only with a large monetary input and the necessary pressure from national and international bodies.

Promotion and education in the use of energy efficient products would help to protect the environment. The use of power electronics has enabled the efficient conversion of electrical energy into useable forms. Over recent years there has been a proliferation of products containing some form of power electronic control [Bose 1992a]. Power electronic devices tend to be nonlinear and are used in circuits which switch waveforms. When these devices are connected to the AC power system, they "pollute" the AC system by drawing nonsinusoidal or harmonic currents.

These harmonic currents do not produce any useful work and only contribute to the system losses. Harmonic currents increase the RMS level of supply current for the same rated power, thereby increasing transmission losses in the AC system. In three phase systems harmonic currents produce a neutral current, even if the loads are balanced [Arrillaga, Bradley, Bodger 1985]. The neutral conductor size may have to be increased to accommodate this larger current. Supply transformers may have to be derated to account for the additional heating due to the harmonic currents, resulting in additional capital and operating costs.

In a weak AC system, large consumers which draw current containing harmonic components can affect the supply voltage waveform to other consumers. This can result in other consumers drawing harmonic currents which may cause misoperation and/or failure in their equipment. Voltage and current harmonics in the presence of power factor correction capacitors may cause local system resonances, which in turn could lead to excessive currents and damage to the capacitors. Harmonic current flowing in transmission systems can also induce interference into nearby telecommunications circuits [Arrillaga et al. 1985].

Until relatively recently, harmonic currents have not been considered a problem,

as it was assumed that the AC power system was large enough to absorb the harmonic problem without any disturbance to the consumers. This is analogous to the earth's ability to absorb the production of say chemical pollutants. Today we realise that this is not the case and that the increase in the use of power electronic products is beginning to have an effect on the power system.

Since power electronics can be used to control the conversion of electrical energy from one form to another, it is possible to use power electronics in the prevention of harmonic currents. Previously this was not considered a viable option by designers, because of the additional cost and complexity of producing equipment that draws a sinusoidal supply current from the power system. Standards now exist, such as the IEEE-519 and IEC-555-2 [Duffey, Stratford 1989, IEC-555 1982], which limit the level of harmonic currents equipment can draw from the AC power system. With the new awareness of the potential problems produced by harmonic currents, these standards have brought about the development of power electronic equipment which draws sinusoidal currents. These standards do not expect all equipment presently drawing harmonic currents to be immediately changed to meet these new regulations. Therefore a large amount of equipment is already connected to the power system and drawing harmonic currents. The IEC-555-2 standard only covers equipment with a power rating above 300 W. This 300 W minimum power rating excludes a large amount of equipment, such as personal computers, which draw harmonic currents. Individually the low power equipment does not cause a problem, but when they are used collectively, such as personal computers in an office building, a harmonic problem can often occur.

Instead of retrofitting each item of equipment with a product which forces it to draw sinusoidal current from the supply, a possible solution is to position harmonic reduction equipment between the power system and the equipment drawing harmonic currents. Such harmonic reduction equipment would absorb the harmonic currents and therefore stop them from being drawn from the power system.

Traditionally tuned passive filters have been used to remove harmonic currents, however they suffer from problems such as the inability to remove uncharacteristic harmonics, and becoming overloaded as they absorb excessive harmonic currents from the power system [Arrillaga et al. 1985]. It is now possible to efficiently use power electronic devices to remove the harmonic components using active (power) filters. These active filters have flexible operational properties and are able to overcome the disadvantages of passive filters [Choe, Park 1988].

The work contained in this thesis involves the investigation of a single and three

phase active filter to compensate for current distortion in the power system. This current distortion may consist of both harmonic and phase displacement distortion. In a three phase power system the active filter also has the added advantage that it can balance the supply currents drawn by unbalanced harmonic loads. A digital controller is implemented in a single phase active filter to provide a form of intelligent control. The aim of the intelligent control is to operate the active filter so as to reduce the supply current distortion while maintaining a high level of efficiency. An automatic optimisation technique is used to find this operating point regardless of the type and level of load current. Incorporating resonant switching techniques in the active filter is investigated to improve the operating efficiency by reducing switching losses. A novel application which compensates for current distortion drawn from a weak, variable frequency AC power system is demonstrated. Passive filters are unable to be used in this application and an active filter is a suitable alternative.

1.1 DEFINITIONS OF POWER SYSTEM DISTORTION

Ideally every device connected to the power system should only consume real power. This however is not the case, some items of equipment draw a current component which is not converted into real power. These currents are defined in this thesis as distortion current and can contain both harmonic and phase displaced currents. A measure of the harmonic and displacement components can be defined by distortion and displacement factors respectively. This section defines the power system distortion terms.

A measure of the harmonic distortion can be given by a value of Total Harmonic Distortion (THD). THD is the square root of the sum of the squares of RMS harmonic currents divided by the RMS fundamental current as given in Equ. (1.1) [Arrillaga et al. 1985] and is often expressed as a percentage.

$$\text{THD} = \frac{\sqrt{\sum_{n=2}^{\infty} I_n^2}}{I_1} \times 100 \quad (\%) \quad (1.1)$$

Since harmonic currents increase the amount of supply current, a further factor can be determined to give a measure of harmonic contamination. This is called the distortion factor (μ) and is defined as the fundamental current component compared to the total supply current (Equ. (1.2)) [Arrillaga et al. 1985].

$$\mu = \frac{I_{1\text{ RMS}}}{I_{\text{RMS}}} \quad (1.2)$$

Distortion factor is usually incorporated into a term called power factor which describes the amount of harmonic distortion and the amount of phase angle displacement between the fundamental supply voltage and fundamental load current. Displacement factor ($\cos\theta$) is defined in Equ. (1.3) as the ratio of power (P) to the fundamental apparent power (S_1).

$$\cos\theta = \frac{P}{S_1} = \frac{P}{V_1 I_1} \quad (1.3)$$

The total power factor (pf) of the supply is the combination of harmonic and displacement distortion. Therefore power in the load can be determined from the apparent power (S) and power factor of the supply, and is defined by Equ. (1.4).

$$P = S \times \text{pf} \quad (1.4)$$

In the special case where the supply voltage is sinusoidal, the power factor can be defined in terms of displacement ($\cos\theta$) and distortion (μ) factors as in Equ. (1.5).

$$\text{pf} = \mu \cos\theta \quad (1.5)$$

1.2 SCOPE OF THESIS

Possible passive and active techniques for reducing harmonic current distortion in the power system are reviewed and the proposed active power filter discussed in Chapter 2. A computer model of the active filter is developed and typical operational waveforms are detailed in Chapter 3. Operation of analogue single and three phase versions of the active filter are discussed in Chapter 4, while Chapter 5 provides experimental results. A digital controller which is able to intelligently control the operation of the active filter is developed in Chapter 6. The power amplifier operating conditions of DC bus voltage and average switching frequency can be adjusted to alter

the performance of the active filter. In Chapter 7 a savings function which enables the operation of the digitally controlled active filter to be adjusted, to provide the greatest economical savings to the consumer, is derived. An optimisation technique is used to maximise these savings for any particular harmonic and phase displaced load combination. Two novel applications of active filtering are described in Chapter 8. The active filter is first used in a weak, variable frequency AC power system and then in combination with a boost converter to produce a sinusoidal input current and high DC output voltage from a conventional three phase diode bridge rectifier. In Chapter 9 a proposal for a resonant link active filter is investigated. Finally a discussion of possible future work relating to the active filter and a conclusion is presented in Chapter 10.

CHAPTER 2

HARMONIC REDUCTION TECHNIQUES

There are a number of different methods available to reduce harmonic currents and these are reviewed in this chapter. First of all, the traditional method of harmonic removal, passive filtering, is discussed in Section 2.1. Following this discussion, two other methods, pulse modification and active filtering, which overcome some of the limitations of passive filters are considered. Methods of pulse modification which are applicable to three phase converters are reviewed in Section 2.2. In Section 2.3 two different active filter approaches, series and shunt, are discussed. Finally, a new technique for harmonic reduction using a shunt active filter is proposed in Section 2.4.

2.1 PASSIVE FILTERS

A passive filter is a combination of inductive, capacitive and resistive components that produce a varying impedance that is dependent on frequency [Arrillaga et al. 1985]. Passive filters absorb current harmonics due to a low impedance at the harmonic current frequencies. Two types of passive filters (tuned and damped) with different impedance characteristics are used for passive power system harmonic filters.

Tuned shunt filters (Figure 2.1(a)) have a low impedance at one harmonic frequency. Therefore a tuned filter is required for each harmonic frequency component to be removed. Tuned passive filters are used to remove the lower order frequency harmonics (less than the 17th harmonic) since these generally have the largest magnitude [Arrillaga et al. 1985].

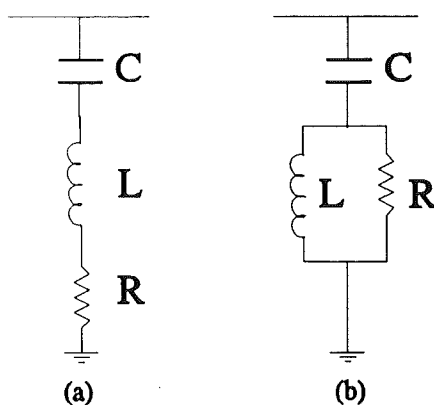


Figure 2.1 Shunt Passive Filters (a) Single Tuned (b) Second Order Damped

To eliminate the higher order harmonics a single second order damped shunt filter (Figure 2.1(b)) is generally used. This filter presents a low impedance for higher frequency components and is referred to as a high pass filter. Since the harmonic current's magnitudes are generally smaller at higher frequencies, a single filter, with a higher level impedance characteristic than the tuned filter and with a reduced capital cost, can still satisfactorily filter the higher order harmonics.

To economically construct a passive filter network to remove the harmonic currents produced by loads such as a 6 pulse converter, combinations of tuned and damped filters are used. A typical passive filter configuration for a 6 pulse converter is shown in Figure 2.2. Single tuned filters are used to remove the 5th, 7th, 11th and 13th harmonics, while the high pass filter removes the 17th and higher order harmonics.

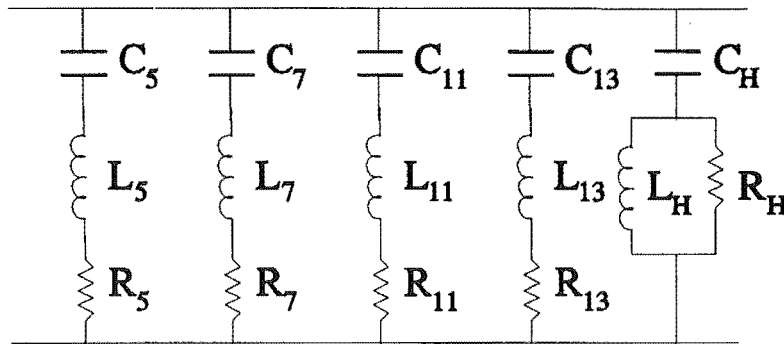


Figure 2.2 Passive Filter Combination for a 6 Pulse Converter

Passive filters suffer from some disadvantages. The single tuned filter's performance is affected by variations in the capacitor and inductor values caused by ageing and temperature drifts. Variations in supply frequency detune the passive filter, thus reducing the effectiveness of the filter in absorbing current harmonics. The passive filter can not compensate for any non characteristic current harmonic and they are designed for a specific load rating and system impedance. If the load size increases then the passive filter system could become overloaded due to the additional harmonic components.

Passive filters are unselective about which harmonic source to compensate for. Therefore it is possible for the passive filter to absorb harmonics from sources other than the one for which it was originally designed. This can lead to an overload situation and early failure of the passive filter. To overcome these disadvantages, pulse modification techniques can be used for reducing the harmonic currents flowing in three phase naturally commutated converter systems.

2.2 PULSE NUMBER MODIFICATION

The supply current harmonic content can be reduced for systems that use naturally commutating three phase static power converters by increasing the converter pulse number [Arrillaga 1982]. A 6 pulse rectifier system produces AC harmonics of the order $6n \pm 1$, where n is an integer. By connecting several 6 pulse rectifiers together, with appropriately phase shifted transformers, it is possible to increase the effective pulse number. A combination of two 6 pulse converters, one with a star and the other with a delta transformer, produces a 12 pulse converter with AC harmonics of $12n \pm 1$. Therefore the low frequency 5th and 7th harmonics are no longer present and the passive filter only has to remove the 11th, 13th and above harmonic currents.

Low voltage, high current converters, such as those used in aluminium smelters, often use very high pulse numbers (typically 48 pulse operation). When a rectifier is removed for maintenance or a failure occurs then low order harmonics are produced. Low order harmonics are also generated if an unbalance exists in the three phase supply voltages. Therefore in practice additional filters have to be added which can remove these low order harmonics during these times.

Using a low pulse number converter system it is possible to increase the pulse number by a technique of DC ripple reinjection [Arrillaga, Joosten, Baird 1983]. By addition of auxiliary transformer windings and DC side switches it is possible to increase the pulse multiplication factor indefinitely.

The reduction of harmonic current at lower frequencies by pulse multiplication is useful in variable speed generation systems where the fundamental frequency is not fixed [Arrillaga, Yonghe, Crimp, Villablanca 1992]. Pulse modification techniques can generally only reduce the harmonic currents drawn from the power system by three phase converter loads. Other harmonic loads, such as a single phase bridge rectifier, can not use pulse modification techniques to reduce harmonic distortion. The harmonic currents produced by these types of loads can however be removed by active filtering.

2.3 ACTIVE FILTERS

Active filters have the ability to compensate for harmonic current distortion produced by a variety of load types. An active filter can be used in two modes, either series connected to stop source harmonics (Figure 2.3(a)) or shunt connected to reduce the level of supply harmonics drawn by the load (Figure 2.3(b)) [Gyugyi, Strycula 1976].

The operation and limitations of series active filters are presented in Section 2.3.1 and is followed by a discussion of shunt active filters in Section 2.3.2.

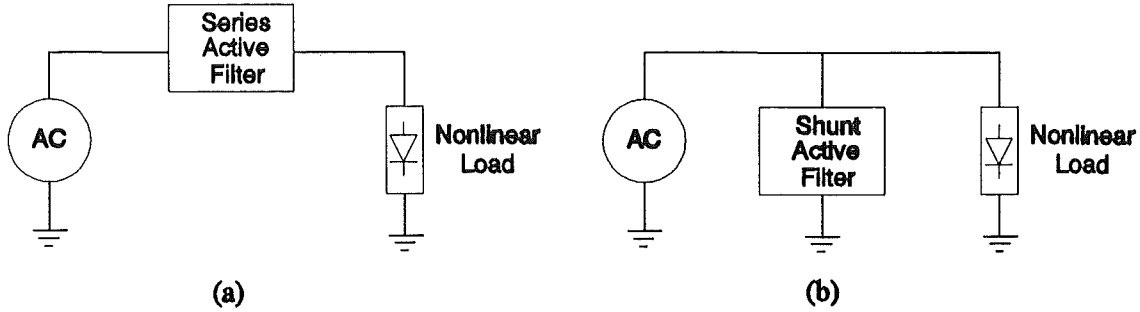


Figure 2.3 Series and Shunt Active Filter

2.3.1 Series Active Filter

Further investigations of the series active filter beyond the initial work of Gyugyi et al. [Gyugyi et al. 1976] has recently been carried out. The interest has been in the method of determining different control strategies for the series active filter. Two methods highlighted so far are the use of the instantaneous reactive power theory [Peng, Akagi, Nabae 1990] and the synchronous reference frame [Bhattacharya, Divan, Banerjee 1991]. The difference between these two methods is in the generation of the signal which is amplified to prevent the flow of source harmonics. This difference in the signal generation will not be discussed, only the overall operation of the series active filter is considered.

To achieve harmonic reduction, a series active filter is used in conjunction with a set of shunt passive filters. The passive filters absorb the current harmonics produced by the load, while the series active filter acts as a harmonic isolator to prevent the flow of harmonics in either direction between the supply and the load. The use of the series active filter allows the compensation provided by the passive filters not to be influenced by the power system impedance thus improving their performance and reducing the possibility of overloading.

A single phase model of the series active filter is presented in Figure 2.4. The harmonic producing load is represented by a current source i_L and the source impedance and impedance of the passive filter are represented by Z_s and Z_F respectively. The series active filter is realised by a voltage source inverter and therefore behaves as a controllable voltage source, v_C .

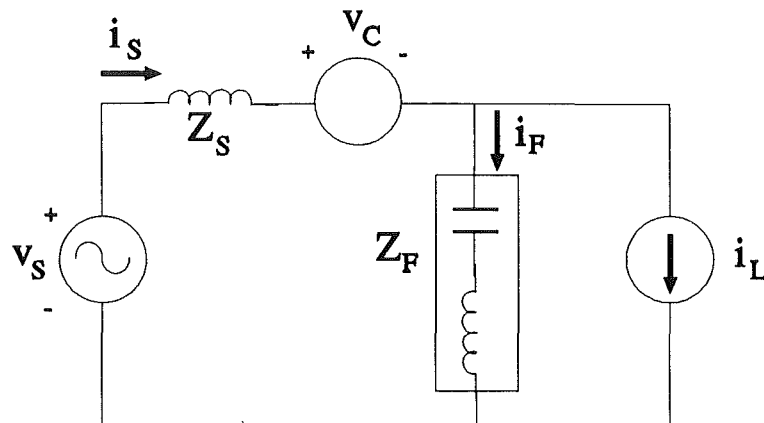


Figure 2.4 Single Phase Model of the Series Active Filter

This controllable voltage source is operated in such a way that it has zero impedance at the fundamental frequency, but appears as an infinite resistance at all the load harmonic frequencies. In practice, because of the bandwidth limitations of the series active filter, a finite maximum resistance appears between the source and load at the harmonic frequencies.

In the ideal case, the load current harmonics are constrained to flow in the passive filter and the voltage across the series active filter is the arithmetic sum of the supply voltage harmonics and the passive filter terminal voltage harmonics. Using the series active filter isolates the shunt passive filter from the supply and the rating of the series active filter is typically in the range of 2-5% of the load VA rating [Bhattacharya et al. 1991].

The use of a shunt passive filter in combination with the series active filter precludes the use of this technique to remove current harmonics from variable frequency generation systems. The shunt active filter discussed below overcomes this limitation.

2.3.2 Shunt Active Filter

The use of a shunt active filter for removal of harmonic currents was first suggested by Sasaki and Machida in 1971 [Sasaki, Machida 1971]. This method of active filtering (Figure 2.5) proposed a technique to eliminate AC current harmonics by using magnetic flux compensation. A representation of the load current is obtained using a current transformer (CT) and the fundamental frequency is filtered out using a series resonant circuit. The resulting load current harmonic component signal is amplified by

a linear amplifier and fed back to the supply via a tertiary winding on the system transformer. Implementation of the amplifier, by operating the power devices in their linear region, restricted the power rating of the compensation system. This compensation system has a limited performance due to the non-ideal signal processing filter used to extract the signal containing the harmonic information. The signal containing the harmonic information is called the compensating current signal, which is then amplified into the compensating current i_c .

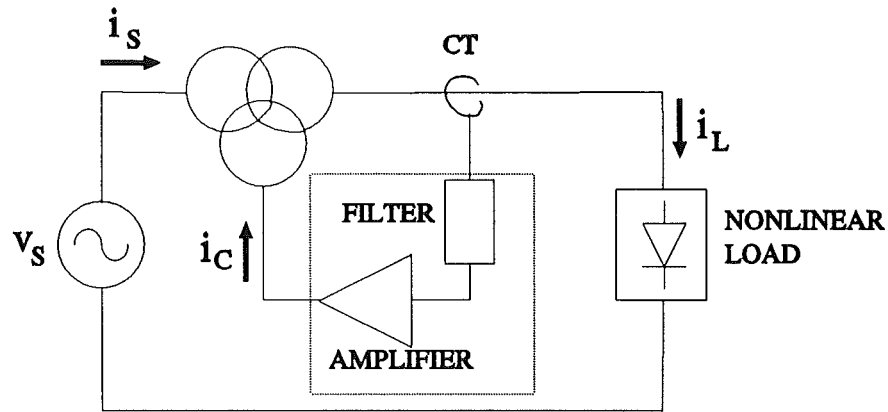


Figure 2.5 Magnetic Flux Compensation Technique to Eliminate Power System Harmonics

To reduce losses, the use of switching power electronic amplifiers in series and shunt active filters was proposed in 1976 [Gyugyi et al. 1976]. Basic concepts and design of an active filter for use in high voltage DC transmission has been suggested by Mohan et al. [Mohan, Peterson, Long, Dreifuerst, Vithayathil 1977]. During the 1980's, advances in the availability of fast switching power electronic devices enabled the implementation of practical active power filters. A 7 kVA experimental active filter, which was described by Akagi et al. [Akagi, Nabae, Atoh 1986], compensated for the current harmonics drawn by a three phase 20 kVA thyristor bridge rectifier. This system verified experimentally that the harmonic supply currents can be eliminated in steady state and under transient conditions.

Since these initial papers on active power filters, many aspects of active filtering have been studied. Active filters have been constructed using voltage source and current source inverters as well as other power amplifier configurations. These types of power amplifiers are discussed in Section 2.3.2.1. The calculation techniques to determine the harmonic current components or compensating current signal are discussed in Section 2.3.2.2, while the control of the power electronic switches to produce the compensating

current is discussed in Section 2.3.2.3.

2.3.2.1 Power Amplifier Configurations

To compensate for the distortion using switching circuits there must be a form of energy storage in a passive element such as an inductor or capacitor [Gyugyi et al. 1976]. The use of a capacitor as the energy storage element is the basis of a voltage source active filter. The control of the energy stored on the capacitor has been investigated [Peng et al. 1990] and the power ratings required for voltage source active filters for different distorted loads has been studied [Lê 1991]. Connecting an additional inverter leg to the neutral conductor and the DC bus of a standard three phase voltage source inverter, it has been shown that this power amplifier configuration (used in an active filter) can reduce harmonic currents in three phase four wire systems [Quinn, Mohan 1992].

Using an inductor for the energy storage device requires a constant level of current flowing in the active filter and these active filters are generally known as current source active filters [Hayashi, Sato, Takahashi 1991]. The use of this energy storage system requires additional signal processing to be performed to determine the switching of the constant inductor current in order to produce the compensating current [Hayafune, Ueshiba, Masada, Ogiwara 1984, Choe, Park 1989].

The use of both capacitor and inductor energy storage devices has been proposed [Malesani, Rossetto, Tenti 1991]. The use of a current source active filter results in fast and accurate control in producing the compensating current, while the capacitor provides an energy storage system which has a low capital cost, is easily implemented and has low losses.

An active filter has been implemented using a modified force-commutated cycloconverter [Madangopal, Cathey 1990]. This scheme extracts the energy required for compensation at the instant it is required, thus eliminating the need for any energy storage device. A disadvantage with this scheme is the implementation of the cycloconverter, which requires a large number of power devices.

2.3.2.2 Compensating Signal Generation

There have been many different methods proposed to generate the compensating current signal. Akagi et al. have proposed the use of the instantaneous reactive power

theory to decompose the three phase current and voltage vectors into an orthogonal two phase representation [Akagi et al. 1986]. The two phase current and voltage vectors are then manipulated, leaving the distortion components of the load current. This is converted back into a three phase representation, thus providing the three compensating current signals.

Enslin et al. proposed a new control philosophy for active power filters using a definition of active and fictitious power [Enslin, Van Harmelen 1990]. The active power is calculated from the cross correlation of supply voltage and current. Fictitious power contains the reactive and harmonic components or uncorrelated power components. Using this control philosophy a thyristor controlled reactive source and dynamic power filter can be operated to remove current distortion from the power system.

Other control techniques which use the frequency components of the load current have been proposed [Hayafune et al. 1984, Williams, Hoft 1991]. These techniques require extensive digital signal processing using a discrete fourier series or fast fourier transform (FFT) to calculate the harmonic information. The disadvantage with these techniques is the time delay between measuring the load signal and providing an updated compensating current signal.

2.3.2.3 Switching Strategy

Pulse width modulation (PWM) generated by a triangular carrier signal has been the standard technique used to convert the compensating current signal into the switching signals for the power devices to produce the compensating current [Akagi et al. 1986, Malesani et al. 1991]. Alternative techniques which include multi-pulse PWM [Hayafune et al. 1984], where harmonic components are decomposed into pulse patterns and then synthesised into a one pulse pattern have been investigated. This synthesised pulse pattern is then transformed into a three level pulse pattern.

Nakajima et al. [Nakajima, Masada, Ogihara 1987] use a method of compensating current generation called component separate PWM. This PWM control scheme uses two converters to produce a direct and quadrature representation of the compensating current.

Other systems use a modifying function to adjust the PWM switching control and improve the generation of the compensating current for their particular active filtering scheme [Doulai, Ledwich 1990, Choe et al. 1989].

2.4 PROPOSED METHOD OF CURRENT DISTORTION COMPENSATION

Since the concept of active filtering was introduced in the early 1970's and the advent of appropriate power electronic devices, significant research has been performed in the area of active filtering. The majority of the effort in this area has been directed at investigating techniques for the derivation of the harmonic components and the switching strategies required to produce the compensating current. The active filter described in this thesis uses a previously developed compensating current generation technique [Henderson 1989] together with a power amplifier switching strategy developed for AC motor speed control [Penny 1986].

A shunt active filter, which can compensate for both harmonic current and phase displacement distortion in the power system is proposed. A block representation of the shunt active filter and signal processing unit (SPU) is detailed in Figure 2.6.

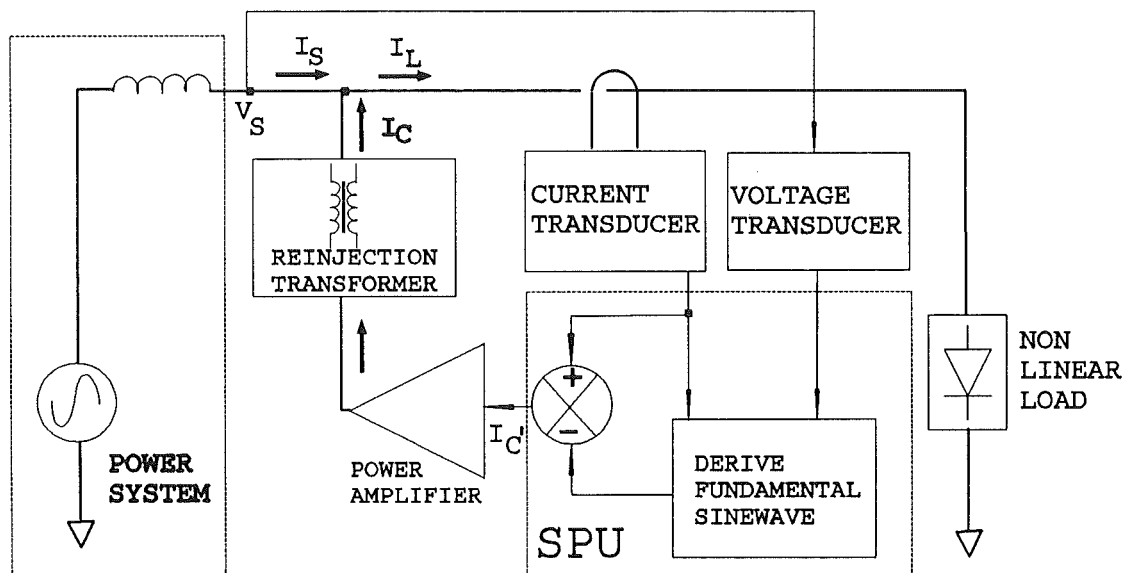


Figure 2.6 Block Representation of Proposed Distortion Compensation System

The non-linear load draws a distorted current from the power system. This load current I_L is sampled by a current transducer and the information passed to the signal processing unit. In the SPU a synthetic sinusoid is derived which is in phase with the fundamental component of the load current (harmonic compensation) or supply voltage (harmonic and displacement compensation). This synthetic sinusoid is then subtracted from the load current signal to produce the compensating current signal, I_C' . This

compensating signal contains the distortion components required to compensate for the supply current distortion caused by the load. The compensating current signal is then amplified by a controlled current, voltage source power amplifier to produce the compensating current. This compensating current flows through a reinjection transformer which interfaces the active filter to the power system. The compensating current I_C on the power system side of the reinjection transformer reduces the harmonic distortion leaving a nearly sinusoidal supply current I_S .

The main feature of this system is that the SPU operates in the time domain and does not require complex signal processing to extract the harmonic frequency components. This technique ensures that the active filter is not referenced to any particular supply frequency and can therefore compensate for any supply frequency up to a limit set by the active filter's frequency response. The compensating current signal is amplified by a controlled current power amplifier which uses a time delay method to generate the switched compensating current. This time delay is simple to implement and produces a band of switching frequencies (spread spectrum), unlike the traditional triangular carrier PWM.

The proposed active filtering system is computer simulated in the next chapter to gain an insight into the operation and performance. A hardware analogue version of the active filter is then discussed, followed by experimental measurements of distortion reduction. An "intelligently" controlled digital active filter that can optimise its operational performance is then presented. Finally two novel applications of active filtering are considered.

CHAPTER 3

MODELLING AND COMPUTER SIMULATION

The use of computer simulation techniques provide a means to gain a better understanding of the possible performance of a power electronic system prior to constructing the hardware. A number of general purpose circuit analysis programs, such as ECAP, SCEPTRE and SPICE2, can be used to simulate power electronic systems [Rajagopalan 1987].

SPICE2 is one of the most popular programs in simulating general electronic systems. SPICE2 can be extended to power electronic circuits by using additional semiconductor power device models. However a disadvantage with using SPICE2 to simulate a power electronic system is that all the circuit elements, including the control circuitry, must be modelled [Rajagopalan 1987]. To accurately determine the system switching detail the time step used in the simulation is decreased. This can result in a possible convergence failure of SPICE2 and a long processing time when high frequency converter systems are simulated for a number of power system cycles.

A special purpose simulator, EMTP, has been developed for modelling the interconnection of a large number of devices, such as those used in large capacity converters [Rajagopalan 1987]. EMTP and the other packages, ECAP and SPECTRE, require large amounts of computer processing and storage memory to operate.

Assuming that the power electronic semiconductor devices are ideal, the computer processing requirements are reduced. The use of ideal switches produces a simulation which does not model the detailed switching transients of the power devices, but produces the overall operational performance of the system. If the detail of switching is required then a program such as SPICE2 could be used. Programs that model power electronic systems with ideal switching devices tend to use a state-space formulation [Rajagopalan 1987].

This chapter describes a computer simulation technique used to investigate the possible performance of the proposed shunt active filter, prior to the construction of hardware. The simulation technique is a state-space method, based on a mathematical formulation that is developed in Section 3.1. The implementation of the mathematical formulation to model the active filter using the computer package MATLAB is described in Section 3.2. Section 3.3 presents the results of the computer simulations of the active filter's performance.

3.1 MATHEMATICAL MODEL

The mathematical model is based on a state-space analysis, where the state variables are inductor flux and capacitor charge. Using the branch formulation developed for modelling thyristor controlled circuits [Arrillaga, Duke 1980] and modifying that formulation to include capacitive branches [Duke, Round, Henderson 1990], the following matrix equations can be written for the capacitive (*c*), resistive (*r*) and inductive (*l*) branches:

$$I_c = C_{cc} \frac{d(K_{cn}^T V_n)}{dt} \quad (3.1)$$

$$R_{rr} I_r = K_{rn}^T V_n \quad (3.2)$$

$$\frac{d(L_{ll} I_l)}{dt} = E_l - R_{ll} I_l + K_{ln}^T V_n \quad (3.3)$$

where

I_c, I_r, I_l	current vectors
V_n	nodal voltage vector
E_l	e.m.f vector of inductive branches
R_{rr}	resistance branches matrix
R_{ll}	resistance matrix of inductive branches
L_{ll}	inductance matrix
C_{cc}	capacitance matrix

and K_{cn}^T , K_{rn}^T and K_{ln}^T are the capacitive, resistive and inductive branch-node incidence matrices respectively. Expressing Kirchhoff's current law in terms of these incidence matrices yields

$$K_{nc} I_c + K_{nr} I_r + K_{nl} I_l = 0 \quad (3.4)$$

It is computationally efficient to subdivide the nodes according to the type of branches connected to them. The subdivision of nodes is:

- nodes with at least one capacitive branch (α)
- nodes with at least one resistive branch, but with no capacitive branch connections (β)
- nodes with only inductive branches (γ)

Thus

$$\begin{aligned} K_{cn}^T &= [K_{c\alpha}^T : K_{c\beta}^T : K_{c\gamma}^T] \\ K_{rn}^T &= [K_{r\alpha}^T : K_{r\beta}^T : K_{r\gamma}^T] \\ K_{ln}^T &= [K_{l\alpha}^T : K_{l\beta}^T : K_{l\gamma}^T] \end{aligned} \quad (3.5)$$

where from the definition of nodes

$$K_{c\beta}^T = K_{c\gamma}^T = K_{r\gamma}^T = 0 \quad (3.6)$$

Rewriting Equ. (3.4) in partitioned form

$$\begin{aligned} \frac{d(Q_{\alpha\alpha})}{dt} &= -(K_{\alpha r} I_r + K_{\alpha l} I_l) \\ \text{where } Q_{\alpha\alpha} &= C_{\alpha\alpha} V_{\alpha} = K_{\alpha c} C_{cc} K_{c\alpha}^T V_{\alpha} \end{aligned} \quad (3.7)$$

and $Q_{\alpha\alpha}$ is the matrix of capacitor charges.

Also:

$$K_{\beta r} I_r = -K_{\beta l} I_l \quad (3.8)$$

$$K_{\gamma l} I_l = 0 \quad (3.9)$$

from which

$$K_{\gamma l} \frac{d(I_l)}{dt} = 0 \quad (3.10)$$

An expression for the voltage vector of β nodes (V_{β}) can be defined as follows:

- (a) premultiply Equ. (3.2) by $K_{\beta r} R_{rr}^{-1}$
- (b) note that $K_{r\gamma}^T = 0$
- (c) substitute Equ. (3.8) in Equ. (3.2)

$$\begin{aligned} V_{\beta} &= -R_{\beta\beta} (K_{\beta l} I_l + K_{\beta r} R_{rr}^{-1} K_{r\alpha}^T V_{\alpha}) \\ \text{where } R_{\beta\beta}^{-1} &= K_{\beta r} R_{rr}^{-1} K_{r\beta}^T \end{aligned} \quad (3.11)$$

Similarly, an expression can be obtained for the voltage vector of γ nodes (V_γ):

- (a) note that the flux linkages $\psi_{ll} = L_{ll}I_l$ and Equ. (3.10)
- (b) premultiplying Equ. (3.3) by $K_{\gamma l}L_{ll}^{-1}$
- (c) partitioning $K_{ln}^T V_n$

$$V_\gamma = -L_{\gamma\gamma}K_{\gamma l}L_{ll}^{-1}(E_l + K_{l\alpha}^T V_\alpha + K_{l\beta}^T V_\beta - R_{ll}I_l) \quad (3.12)$$

where $L_{\gamma\gamma}^{-1} = K_{\gamma l}L_{ll}^{-1}K_{l\gamma}^T$

and inductances are considered to be unchanging with time.

To formulate the mathematical model in state-space refer back to Equ. (3.3) and using Equ. (3.12) to eliminate V_γ

$$\frac{d(\psi_{ll})}{dt} = [U_{ll} - K_{l\gamma}^T L_{\gamma\gamma} K_{\gamma l} L_{ll}^{-1}][E_l + K_{l\alpha}^T V_\alpha + K_{l\beta}^T V_\beta - R_{ll}I_l] \quad (3.13)$$

where U_{ll} is a unit matrix of order l

Using Equ. (3.11) to eliminate V_β

$$\frac{d(\psi_{ll})}{dt} = M_{ll}[E_l + (K_{l\alpha}^T - N_{lr}K_{r\alpha}^T)V_\alpha - \mathfrak{R}_{ll}I_l] \quad (3.14)$$

where $M_{ll} = U_{ll} - K_{l\gamma}^T L_{\gamma\gamma} K_{\gamma l} L_{ll}^{-1}$
 $\mathfrak{R}_{ll} = R_{ll} + K_{l\beta}^T R_{\beta\beta} K_{\beta l}$
 $N_{lr} = K_{l\beta}^T R_{\beta\beta} K_{\beta r} R_{rr}^{-1}$

since from Equ. (3.2)

$$I_r = R_{rr}^{-1}(K_{r\alpha}^T V_\alpha + K_{r\beta}^T V_\beta) \quad (3.15)$$

Equ. (3.7) can be written as

$$\frac{d(Q_{\alpha\alpha})}{dt} = -[K_{\alpha l}L_{ll}^{-1}\psi_{ll} + K_{\alpha r}R_{rr}^{-1}(K_{r\alpha}^T V_\alpha + K_{r\beta}^T V_\beta)] \quad (3.16)$$

Using Equ. (3.11) to eliminate V_β

$$\frac{d(Q_{\alpha\alpha})}{dt} = -(K_{\alpha l} - K_{\alpha r}N_{rl}^T)L_{ll}^{-1}\psi_{ll} - K_{\alpha r}R_{rr}^{-1}M_{rr}K_{r\alpha}^T V_\alpha \quad (3.17)$$

where $M_{rr} = U_{rr} - K_{r\beta}^T R_{\beta\beta} K_{\beta r} R_{rr}^{-1}$
 U_{rr} is a unit matrix of order r
 $N_{rl}^T = R_{rr}^{-1}K_{r\beta}^T R_{\beta\beta} K_{\beta l}$

Defining

$$\begin{aligned} G_{ar} &= K_{ar} R_{rr}^{-1} M_{rr} \\ A_{al} &= K_{al} - K_{ar} N_{rl}^T \end{aligned} \quad (3.18)$$

and substituting $C_{\alpha\alpha}^{-1} Q_{\alpha\alpha}$ for V_α and $L_{ll}^{-1} \psi_{ll}$ for I_l , Equ. (3.14) and (3.17) can be combined into a single matrix equation which is in the general state-space form.

$$\begin{bmatrix} \frac{d(\psi_{ll})}{dt} \\ \frac{d(Q_{\alpha\alpha})}{dt} \end{bmatrix} = \begin{bmatrix} -M_{ll} R_{ll}^{-1} & M_{ll} A_{la}^T C_{\alpha\alpha}^{-1} \\ -A_{al} L_{ll}^{-1} & -G_{ar} K_{ra}^T C_{\alpha\alpha}^{-1} \end{bmatrix} \begin{bmatrix} \psi_{ll} \\ Q_{\alpha\alpha} \end{bmatrix} + \begin{bmatrix} M_{ll} \\ 0 \end{bmatrix} [E_l] \quad (3.19)$$

By using the flux, charge and interconnection relationships it is possible to determine the currents and voltages at various nodes and branches in the model.

To implement this mathematical formulation the state-space equation (Equ. (3.19)) has to be solved. The state-space equation is converted into a discrete representation by the simulation software. The state vectors are then calculated for a defined step length. If a device has switched during this time step the input connection and component matrices are modified and the discrete simulation is rerun.

To start the simulation the state-space technique requires a set of initial conditions which can be set to zero. To achieve a steady state result a large amount of computer processing may be required, so the choice of initial conditions is important. The simulation can be run and the initial conditions adjusted until a steady state result is achieved. To model the active filter the interconnection of the semiconductor devices and discrete components must be determined in order to provide the connection matrices for the formulation. The active filter simulation model is discussed in the next section.

3.2 ACTIVE FILTER MODEL

The shunt active filter is modelled by the circuit shown in Figure 3.1. The circuit is divided into four main sections, the power system, the reinjection transformer, the power amplifier and the load.

The power system is modelled by a sinusoidal voltage source, V_{ac} , at fundamental frequency with a series impedance, R_s and L_s . Values of R_s and L_s are made small to simulate a strong power system with a sinusoidal supply voltage as this is typical of a

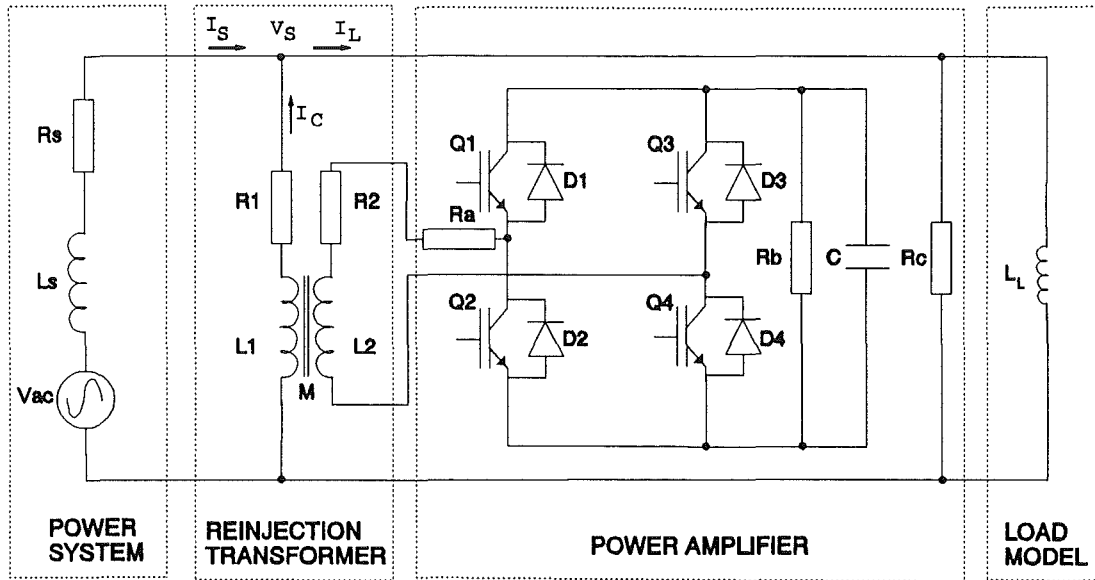


Figure 3.1 Computer Model of the Active Filter

national power system. Therefore the voltage V_s , at the point of reinjection, is nearly the same as V_{ac} . The reinjection transformer is modelled as a mutual coupling between two inductive branches, has a turns ratio of two and a leakage inductance of 20 mH. The capacitor, C , is used as the energy storage device in the power amplifier. Resistor R_a represents the sum of the power transistors "ON" resistance and the bus capacitor's (C) equivalent series resistance. The switching losses in the transistors and the power consumed by the voltage clamping circuitry are represented by resistor R_b , while resistor R_c models the power consumed by the control circuitry. Each of the transistors $Q1$ to $Q4$ and the free-wheeling diodes $D1$ to $D4$ are modelled as ideal switches.

To simulate the active filter a load model must be connected to the power system. The nonlinear load could be modelled using the inductive, capacitive and resistive branches. This implementation of the load would increase the programming and computational time of the active filter simulation. An alternative technique is to model the load with an extremely large inductor, L_L since the current in such an inductor changes insignificantly during one switching interval. At the beginning of the switching interval the initial condition of the inductor's flux is set to a level equal to that required to produce the load current at that instant in time. By setting a current value for the inductor the simulation program does not have to be changed for each different load type. Only a data file containing load current and time information has to be supplied to carry out the simulation. This information can be provided by previous simulations (even produced by other simulation packages) or captured from an oscilloscope.

Since the transistor and free-wheeling diodes are modelled as ideal switches, the active filter computer model assumes that the on state of both the transistor and its free-wheeling diode are the same. Thus only one model is necessary to model either the transistor or its free-wheeling diode. Using this assumption, only two model configurations are required to simulate the active filter. These two configurations are shown in Figure 3.2.

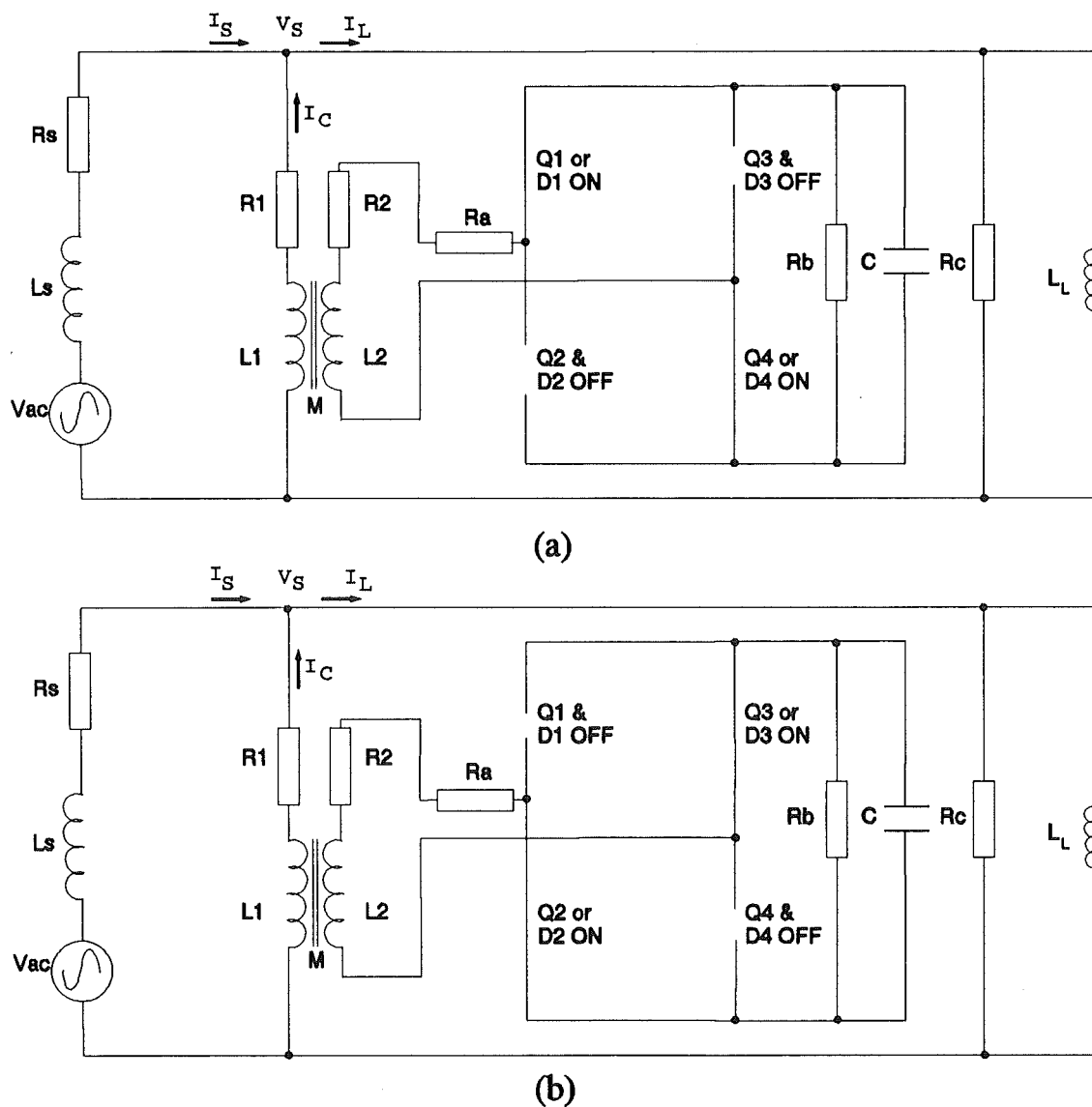


Figure 3.2 Two Model Configurations used for Simulating the Active Filter

(a) Q_1, Q_4 or D_1, D_4 ON (b) Q_2, Q_3 or D_2, D_3 ON

To control the current flowing in the reinjection transformer diagonally opposite pairs of transistors are switched on or the current is allowed to free-wheel in diagonally opposite pairs of diodes. The first model, Figure 3.2(a), is used when Q1 and Q4 or D1 and D4 are on, while the second model, Figure 3.2(b), is used when the other pair Q2 and Q3 or D2 and D3 are on.

To force the current in the power amplifier to follow the compensating current signal (Section 2.3.2), a switching strategy developed by Penny [Penny 1986] is used. With reference to the transistor switching diagram (Figure 3.3), the topological model changes (transistor switching instants) are determined in the following way: Assuming the power amplifier output current is greater than the compensating current signal (Point A), the simulation, using the appropriate circuit model, is allowed to run until the power amplifier output current is less than the compensating current signal (Point B). Linear interpolation is then used to determine the exact crossing instant (Point C). The simulation is restarted from this time and allowed to run for a set time ($t \mu s$). This time delays the transistor switching instant until Point D and determines the average switching frequency ($f_{av} \approx 1/4t$) of the power amplifier. At Point D the circuit topology is changed and the simulation runs until the next crossing point (Point E) can be determined. Restarting from Point E the simulation runs for a further $t \mu s$ until it reaches Point F. This pattern of simulation, followed by linear interpolation, further simulation and model changing continues, producing the appropriate compensated supply current.

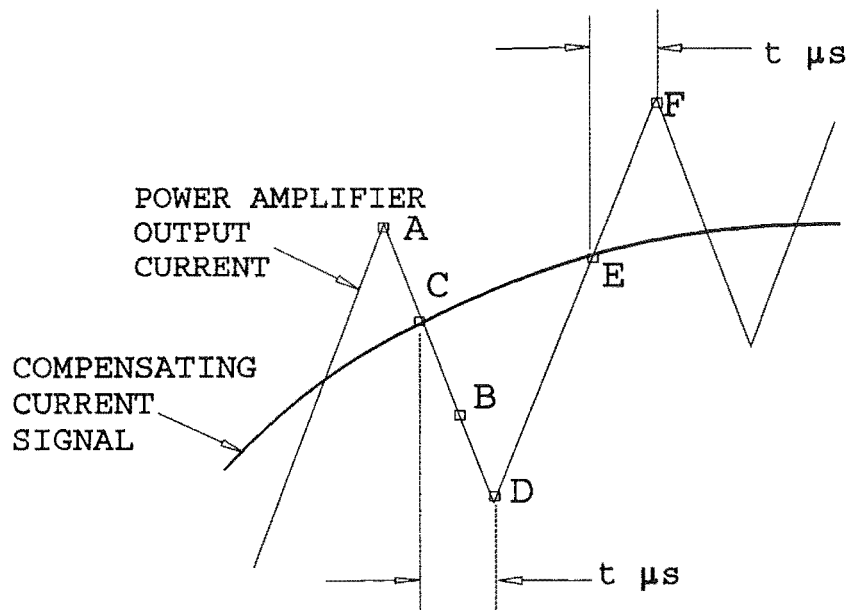


Figure 3.3 Time Delayed Switching Strategy for the Controlled Current Inverter

This switching strategy does not produce a fixed switching frequency. It produces a band of switching frequencies which is determined by the required compensating current signal. The switching frequencies can not be prespecified and are asynchronous in nature.

3.2.1 Implementation of the Computer Model

Traditionally, the software required for the implementation of computer simulations has been written using general purpose computer languages such as Pascal, Fortran and C. The use of these languages has meant that basic data handling and graphical routines had to be written before any modelling could be considered. However, this is now changing with the advent of computer packages such as MATLAB [Moler, Little, Bangert 1987]. MATLAB was originally designed to perform general matrix manipulations and solve matrix equations, but it has now evolved into a powerful simulation and analysis software package for the solution of scientific and engineering calculations. The basic file handling, graphical output and matrix handling routines are already contained within MATLAB. To simulate a power electronic system only a state-space formulation and the control tasks have to be implemented. MATLAB provides an ideal environment for state-space analysis and simulation of power electronic circuits. Therefore results can be produced from computer simulations in a shorter time than was previously possible.

The simulation of the active filter using the state-space formulation (Equ. (3.19)) has been implemented using MATLAB as the programming environment. MATLAB converts the continuous time domain state-space formulation into the discrete time domain form. The state variables can be measured throughout the simulation enabling data to be stored for later processing and for immediate computation of losses and performance. At the completion of a simulation run MATLAB provides the plotting routines for the screen and hardcopy output, as well as functions such as Fast Fourier Transforms (FFT) to calculate the harmonic spectra.

3.3 COMPUTER SIMULATION OF THE ACTIVE FILTER'S PERFORMANCE

The simulation program is initially implemented in MATLAB running on an IBM PC-compatible. To complete an active filter simulation for one 50 Hz cycle, operating

at an average switching frequency of 25 kHz, required a computational time of 4 hours. When a SUN SPARC workstation became available the simulation of the active filter for one 50 Hz cycle could be completed with a reduced time of 15 minutes. Since the computational ability of the SUN SPARC workstation is faster than the PC, the transient performance of the active filtering system could be easily simulated for a number of fundamental cycles.

This section presents the results of the computer simulation in steady state and transient operation of the active filter. Section 3.3.1 presents the steady state, performance while Section 3.3.2 presents the transient performance. These results are validated in Chapter 5 against the experimental performance results of a hardware single phase active filter.

3.3.1 Steady State Operation

For the steady state case, a combination of non-linear and linear loads is used. The power supply is a single phase 240 V 50 Hz, system with the load consisting of a base resistive load of $2.2 A_{RMS}$ and a single phase bridge rectifier, capacitor and resistive load drawing $2.1 A_{RMS}$. The reinjection transformer has a turns ratio of two to one and the DC bus capacitance is $1880 \mu F$. For this simulation the time delay (t , Figure 3.3) is set to $10 \mu s$, which gives an average switching frequency of 25 kHz. The results, produced by the simulation, of the active filter compensating for this distorted load are presented in Figure 3.4.

Figure 3.4(a) illustrates the distorted load current I_L (Figure 3.1) and the compensated supply current I_s which has been converted into a nearly sinusoidal waveform. The compensating current, on the power amplifier side of the reinjection transformer, with high switching frequencies imposed on it is shown in Figure 3.4(b). The DC bus voltage in Figure 3.4(c) starts at $260 V_{DC}$ and finishes after one fundamental period at $260 V_{DC}$, showing that the simulation is in a steady state.

The variation of the capacitor bus voltage in Figure 3.4(c) illustrates the bidirectional power flow through the power amplifier. Compensating for the distortion produces losses in the active filtering system, therefore real power must be supplied to the power amplifier. This occurs when the free-wheeling diodes conduct current resulting in the voltage on the bus capacitor rising. Thus energy is being stored on the bus capacitor. As the instantaneous compensating current diverges from zero, the power transistors are conducting and forcing current into the supply and the bus voltage falls.

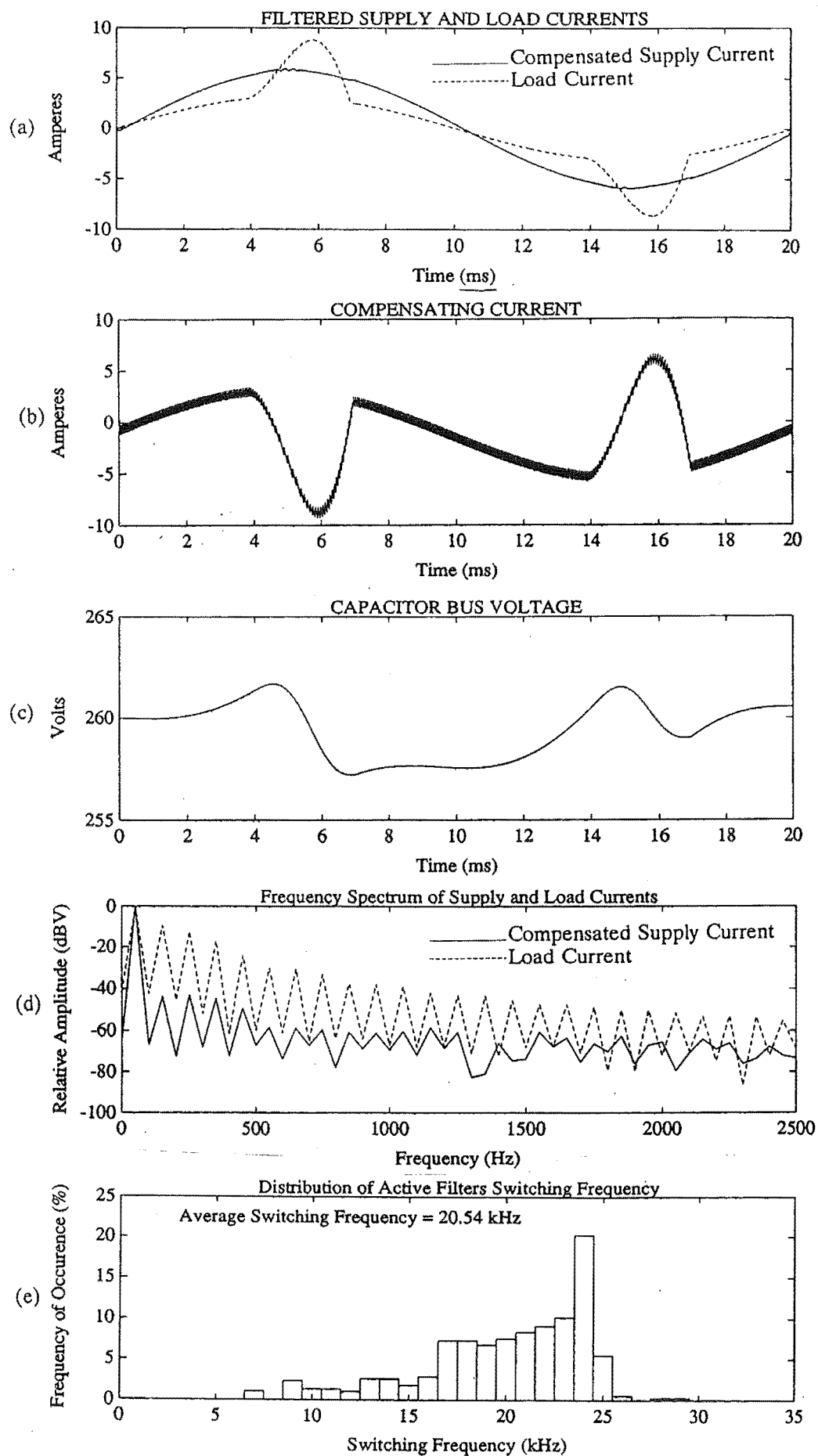


Figure 3.4 Results of Steady State Simulation

By controlling the real power flow into the active filter the voltage on the bus capacitor can be altered. Implementation of the control of real power flow is discussed in more detail in Section 4.1.1.2.

The frequency spectra of the computed compensated supply current I_s (Figure 3.1) and load current is shown in Figure 3.4(d). The third harmonic of the compensated supply current has fallen to a level 45 dBV below the fundamental (0.56% of the fundamental). All the other harmonics, up to 1500 Hz, show a reduction in amplitude and these spectra give an indication of the ideal performance that could be expected from the active filter.

The time delay switching strategy produces a band of switching frequencies which is determined by the compensating current waveform produced by the power amplifier. Low frequency switching components exist in the compensating current during the peak of the bridge rectifier load current pulse as shown in Figure 3.4(b). An advantage of computer simulation techniques is that exact switching frequencies of the transistors can be obtained. Figure 3.4(e) shows the distribution of switching frequencies for this particular load and time delay of 10 μ s. The predominant switching frequency is 24 kHz, although on occasions the switching frequency does fall as low as 7 kHz and rise as high as 29 kHz. The actual time averaged switching frequency is 20.5 kHz.

3.3.2 Transient Performance

With a larger number of high performance computing machines available it is becoming possible to simulate high frequency switching circuits for a number of power system fundamental cycles. The transient operation of the active filter can last for a number of fundamental cycles. This section details the transient performance of the active filter with integral control of the synthetic sinusoid magnitude controller (Section 2.4 and Section 4.1.1). Computer simulation and actual performance measurements of a more sophisticated bus voltage controller are discussed in Section 6.5.

To investigate the transient response of the active filter the bridge rectifier load described in Section 3.3.1 was subjected to a step increase in load current from 2.1 A_{RMS} to 4.2 A_{RMS} . The transient response of the computer simulated active filter is presented in Figure 3.5. The step increase is applied to the load after two cycles of steady state operation of the active filter (Figure 3.5(a)). This step increase in load current causes a step change in the compensating current (Figure 3.5(b)). To produce the compensating current for this step increase the energy initially comes from the bus capacitor and

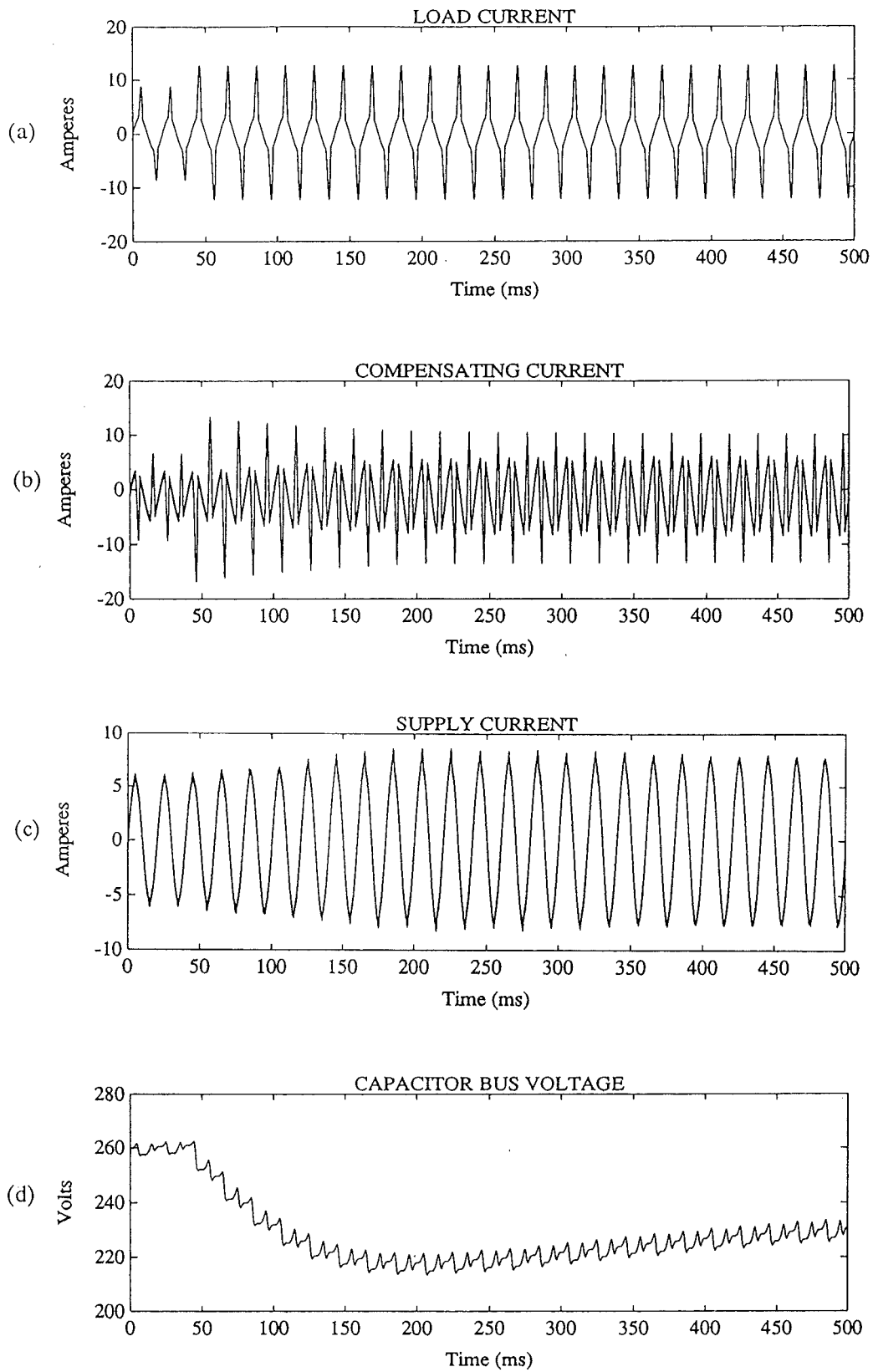


Figure 3.5 Computed Transient Response of the Active Filter

therefore the bus voltage falls (Figure 3.5(d)). An integral controller slowly ramps up the magnitude of the synthetic sinusoid and after three integral time constants (300 ms) the compensated supply current (Figure 3.5(c)) has reached its new steady state operating level.

Peaks appear in the compensated supply current as the power amplifier is unable to produce a compensating current that can follow the compensating current signal due to a low voltage level on the bus capacitor. These peaks are just noticeable in the compensated supply current waveform between 120 and 300 ms. As the bus voltage rises to its new steady state operating level the active filter is able to provide full compensating current and these peaks disappear. The effects of a low bus voltage are fully discussed in Section 4.1.1.2.

3.4 SUMMARY

This chapter has derived a state-space formulation which is used computer simulate the operation of the proposed shunt active filter. The mathematical state-space formulation uses three predefined branch types to simulate a power electronic circuit using ideal power devices. The state vectors are the inductor fluxes and capacitor charges. Two models of the active filter are required for the simulation, assuming the transistors and diodes are ideal devices. This simulation technique was implemented by the MATLAB software package. To model various non linear loads an inductive branch with a large value was used. By setting the level of flux in this inductor at small time intervals, the required load current can be made to flow in the inductor. This technique eliminates the need to model each different type of load.

The switching strategy, using a fixed time delay, was detailed and the asynchronous nature of switching shown. This asynchronous switching produces a band of switching frequencies. Results for steady state operation are presented and they show that the distortion in the load current can be effectively removed from the supply current.

A preliminary investigation of the transient performance is discussed and the use of computer simulation as a tool in determining the characteristics of different controllers for transient operation of the active filter is further considered in Chapter 6.

CHAPTER 4

ANALOGUE ACTIVE FILTER

This chapter deals with the development of the hardware to implement the proposed active filter described in Chapter 2. Henderson carried out preliminary investigations and he developed a demonstration single phase analogue active filter [Henderson 1989]. The active filter has been further developed to provide both harmonic and phase angle displacement compensation for single and three phase systems. The hardware required to perform active filtering in a single phase power system is described in Section 4.1. A three phase unit has been constructed from three separate single phase active filters and this is described in Section 4.2. The performance of the single and three phase analogue active filters is presented in Chapter 5.

4.1 SINGLE PHASE HARDWARE DESCRIPTION

The active filter, as shown by Figure 4.1, has two distinct parts, the signal processing unit (SPU) and the power amplifier. The SPU determines the required compensation signal, while the power amplifier increases this compensating current signal to a level suitable for reinjection into the power system. Details of the SPU hardware and a description of the power amplifier are presented in the next two sections.

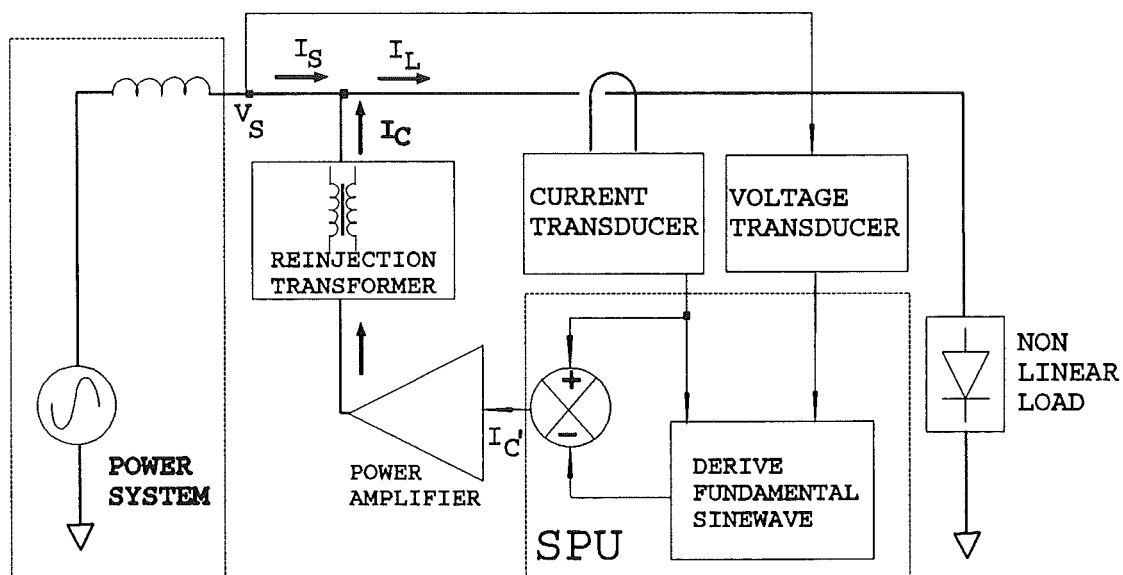


Figure 4.1 Block Representation of Active Filtering System

4.1.1 Signal Processing

The SPU (see Figure 4.2) and has two main functions. Firstly the SPU obtains the phase displacement information from either the load current fundamental or the supply voltage fundamental and then generates a synthetic sinusoid. Secondly a magnitude control circuit in the SPU controls the amplitude of the synthetic sinusoid. These two functions, which produce a compensating current signal by subtracting a synthetic sinusoid with the required phase displacement and magnitude from the load current signal, are discussed below.

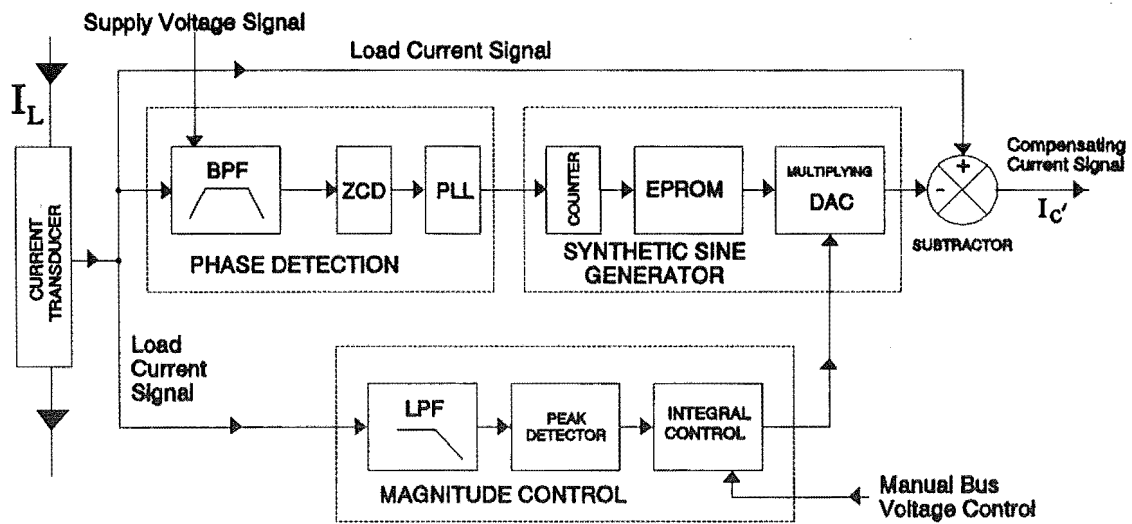


Figure 4.2 Signal Processing Unit (SPU) of the Analogue Active Filter

4.1.1.1 Compensating Current Signal Generation

The load current, I_L , is monitored by a current transducer (Figure 4.2). The load current signal produced by this transducer is then used by the phase detection, magnitude control and compensating current signal generation circuitry.

The phase detection subsystem positions the synthetic sinusoid generation in phase with the fundamental component of the load current or the supply voltage. If the sinusoid is in phase with the supply voltage the active filter system is able to provide compensation for both harmonic and displacement distortion. When the sinusoid is in phase with the fundamental of the load current only harmonic compensation is possible as no displacement information is contained in this signal.

The bandpass filter (BPF) extracts the fundamental phase information from the input signal and is designed to have a 180 degree phase lag at the fundamental frequency, so that no phase shift occurs in the fundamental of the load current signal. The zero crossings of the fundamental frequency are extracted by a zero crossing detector (ZCD). A phase locked loop (PLL) uses these zero crossings to track any changes in frequency of the supply.

The synthetic sinusoid generation subsystem produces a sinusoid with the magnitude of the fundamental component of load current and in phase with the load current or supply voltage fundamental. Using the output of the PLL, a counter increments an address location in the eight bit EPROM. A synthetic sinusoid is stored in a look-up table format in the EPROM. Only one half of the sinusoid (1024 points) is stored in the EPROM. The counter clocks out 1024 points for the sinusoid from the EPROM and the output is converted into an analogue form by a multiplying digital to analogue converter (DAC). For the next 1024 points the output of the DAC is inverted, thus a synthetic sinusoid has been generated with a 9 bit, 2048 point representation. The analogue synthetic sinusoid has a THD of 0.16% with all the harmonic components 66 dBV below the fundamental. The amplitude of the synthetic sinusoid is adjusted by a signal generated from the magnitude control circuitry. Operation of the magnitude control circuitry is discussed in the following section. The synthetic sinusoid is then subtracted from the load current signal to produce the compensating current signal, I_{C1} .

Operation of the SPU is illustrated by Figure 4.3. For a single phase bridge rectifier with capacitive and resistive load current (Figure 4.3(a)), a synthetic sinusoid (Figure 4.3(b)) is generated from the load current signal. After subtracting this synthetic sinusoid from the load current signal the compensating current signal shown in Figure 4.3(c) is produced.

4.1.1.2 Magnitude Control

The magnitude control strategy is based on detecting the magnitude of the fundamental component of load current as illustrated in Figure 4.2. A low pass filter is used to extract the fundamental component of the load current. The amplitude of the fundamental is then determined by a peak detector which is then compared to the value being produced by the DAC. An error signal is produced which is used by an integral controller to set the magnitude of the synthetic sinusoid.

Ideally, the job of the magnitude control circuit is to produce a sinusoid which has

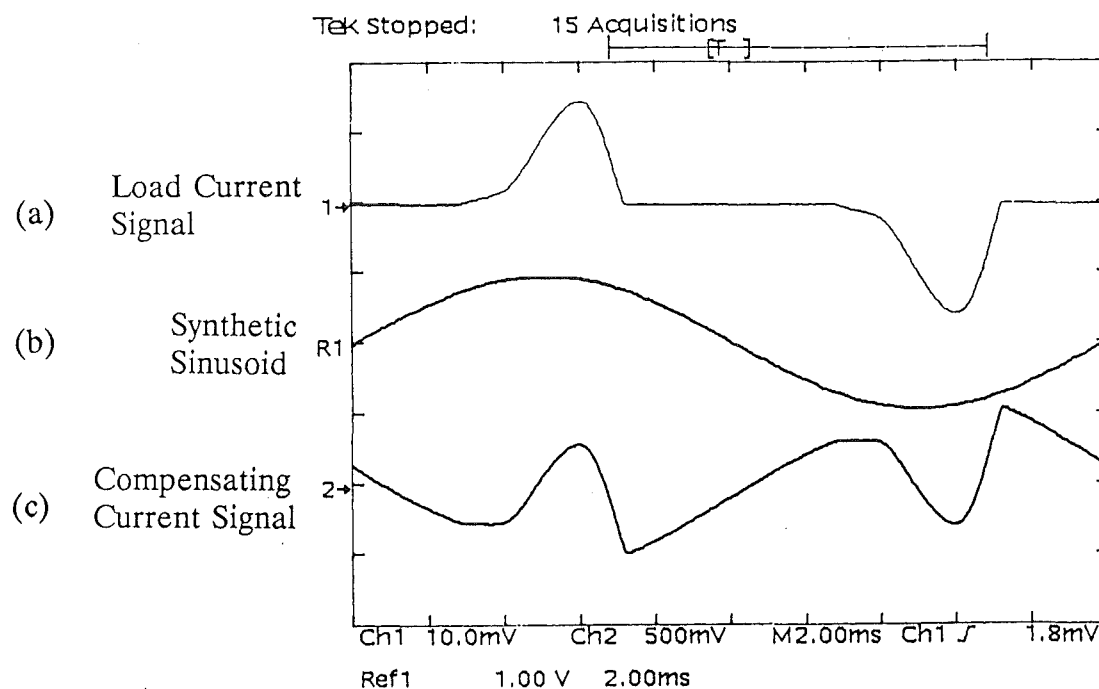


Figure 4.3 Generation of Compensating Current Signal from the (a) load current and (b) synthetic sinusoid, resulting in the (c) compensating current signal

the same amplitude as the fundamental component of the load current. Subtracting this ideal sinusoid from the load current signal would leave only the harmonic distortion components (assuming only harmonic distortion existed in the load current). Amplifying and reinjecting this distortion would cancel the current distortion drawn by the load, leaving the supply current with only the fundamental component.

To reinject the amplified harmonic distortion to achieve cancellation requires real power to be consumed to overcome the active filter losses. Some of these losses are the conduction and switching losses of the semiconductor devices in the power amplifier and resistive losses in the transformer and capacitors. By increasing the magnitude of the synthetic sinusoid, additional fundamental current (real power) flows into the active filter. If more real power enters the active filter than is consumed by the active filter the additional energy is stored on the bus capacitor (Figure 3.1) and is indicated by a rise in the DC bus voltage level.

To successfully reinject current, sufficient voltage must exist on the bus capacitor to overcome the instantaneous supply voltage. If insufficient voltage exists on the capacitor then full compensation is not possible and the supply current would contain a high level of distortion. The effect of the bus voltage on the compensated supply current is shown in Figure 4.4. The uncompensated supply current (Figure 4.4(a)) is due to a

combination load of a bridge rectifier circuit in parallel with a resistive circuit. When the active filter is not compensating the DC bus voltage is 165 V_{DC} and is produced by rectification of the supply voltage ($240\text{ V}_{\text{RMS}}$) on the secondary side of the two to one step down reinjection transformer. The compensated supply current for a bus voltage of 180 V_{DC} is presented in Figure 4.4(b). The peak of the bridge rectifier circuit current is still present. By increasing the amplitude of the synthetic sinusoid, such that the bus voltage is now 220 V_{DC} it is possible to have a nearly sinusoidal supply current (Figure 4.4(c)). Therefore the voltage level on the bus capacitors is important in providing an adequate level of compensation. The minimum DC bus voltage level which is able to provide adequate compensation is dependent on the type of load and the amount of distortion current.

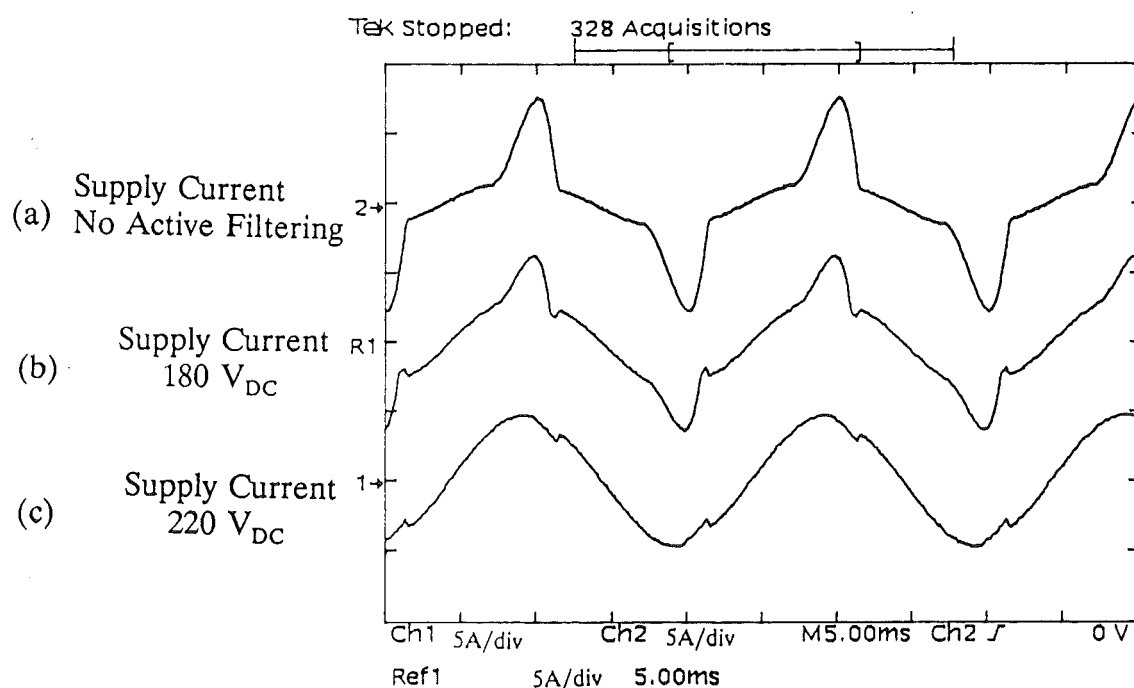


Figure 4.4 Effect of Bus Voltage on Compensation Ability of the Active Filter

A limitation of the magnitude controller is that the same output level, representing the amplitude of the fundamental load current component, is produced regardless if phase displacement compensation is required. If phase displacement compensation is not being provided, the magnitude controller would produce an excess level of real power flow into the active filter. Therefore the synthetic sinusoid magnitude is adjusted manually to control the bus voltage for this and other applications. Manual control is also useful to investigate the performance of the active filter over wide ranges of operating conditions.

A bus voltage controller has been implemented with the same integral control

configuration as used in the magnitude control circuitry. The actual voltage on the bus capacitor is measured and compared to a required bus voltage value. The error between these two signals is used by the integral controller to adjust the amplitude of the synthetic sinusoid. A time constant of 100 ms is used in the integral controller to suppress the effect of switching interference on the operation of the magnitude of the synthetic sinusoid. However, the use of this 100 ms time constant for the bus voltage control system made the response of the active filter very slow to load changes. A bus voltage controller with a faster response is implemented in the digitally controlled active filter and is described in Section 6.5.1.

4.1.2 Power Amplifier

The power amplifier for the single phase active filter is based on an H bridge arrangement of power transistors. This arrangement of power devices and the switching control circuits is shown in Figure 4.5.

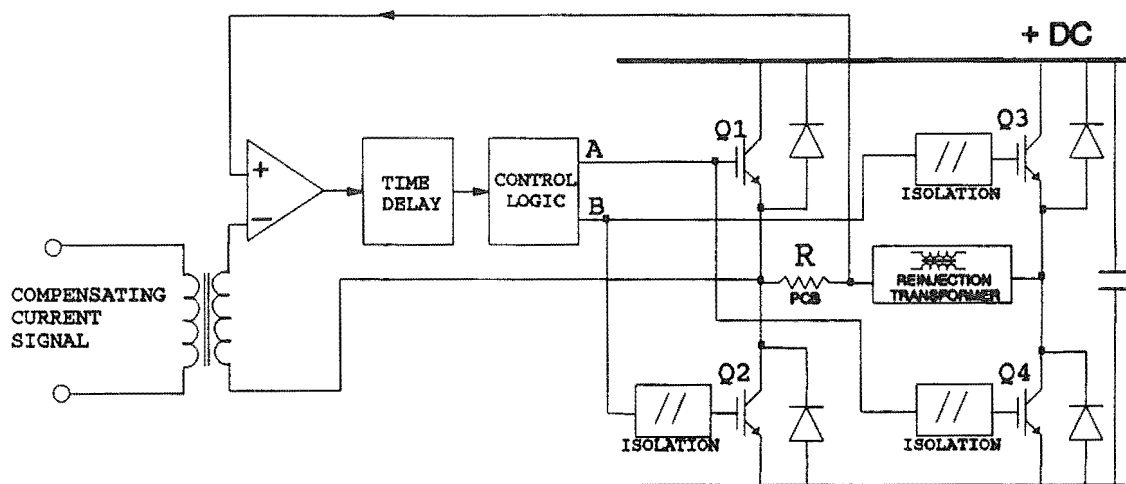


Figure 4.5 Power Amplifier Configuration

The amplifier uses four Insulated Gate Bipolar Transistor (IGBT) power transistors with the rating of 500 V and 10 A. The average switching frequency of the active filter is adjusted by a time delay circuit. Initially an average switching frequency of 25 kHz (time delay of 10 μ s) is used for the performance measurements. Isolation is required for the gate drives and is provided by opto-couplers and separate power supplies. The total amplifier is rated to provide up to 2 kVA of distortion power. The implementation of the time delay switching strategy is discussed followed by information on the reinjection transformer.

4.1.2.1 Switching Strategy

The power amplifier can be described as a controlled current voltage source inverter. The controlled current switching strategy was developed by Penny [Penny 1986] and was described in detail in Section 3.2. This switching strategy uses a current sense resistor (R_{PCB} in Figure 4.5), which is referenced to a high side transistor (Q1), and a time delay to produce the required compensating current. The current sense resistor is able to accurately determine the direction and actual level of compensation current flowing in the reinjection transformer. The amplifier current is then compared to the compensating current signal and the output of the comparator (Figure 4.5) provides information on whether to increase or decrease the current through the reinjection transformer by switching diagonally opposite pairs of transistors.

Figure 4.6 illustrates the hardware implementation of the time delay and comparator. The charging of the capacitor C , through resistor R , is used to produce the time delay. This circuit has the characteristic of being very robust against interference produced by the switching circuits and is simple to implement.

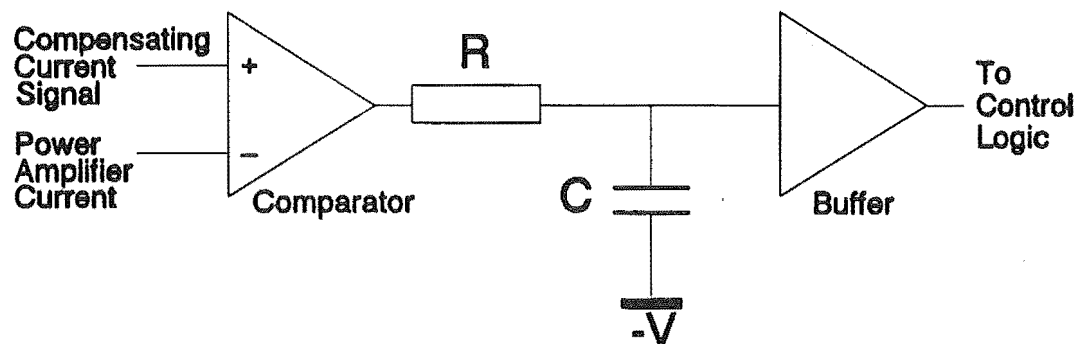


Figure 4.6 Hardware Implementation of the Time Delay Circuit

The control logic circuitry (Figure 4.5) uses the output of the time delay to make a decision on which pair of transistors (A or B) to switch on to make the current rise or fall through the reinjection transformer.

The ground reference point for the switching control circuitry is referenced to the emitter of Q1. This ground point floats up and down with the switching of Q1 and Q2. The SPU circuitry providing the compensating current signal is earthed so a signal transformer is used to isolate the SPU and the power amplifier's control circuitry while still accurately transmitting the compensating current signal.

4.1.2.2 Reinjection Transformer

A reinjection transformer (Figure 4.5 and Figure 4.1) is used to interface the power amplifier of the active filter to the power system. The power amplifier requires some inductance in series with itself and the power supply to limit the rate of rise of current [Enslin et al. 1990]. The reinjection transformer is designed to provide sufficient leakage inductance to limit the rate of rise of the reinjected current to minimise the high frequency current ripple on the compensating current.

A reinjection transformer is used in the prototype to model the operation of the active filter in higher voltage power systems. The present semiconductor technology does not provide the voltage ratings to operate directly off high voltage systems, therefore a step down transformer must be used as an interface. For example, in New Zealand the active filter could be required to operate off a 11 kV distribution system. The hardware prototype of the active filter operates from a 240 V_{AC} power source with a reinjection transformer having a step down ratio of two to one and a leakage inductance of 20 mH.

The reinjection transformer could be replaced with an inductor when the active filtering system is operated from a distribution network with a voltage less than the power semiconductor devices rating.

4.2 THREE PHASE ACTIVE FILTERING SYSTEM

The three phase active filter consists of three independent single phase filters connected as shown in Figure 4.7.

Each single phase active filter independently removes distortion from one of the phases. These active filters perform the task of monitoring each phase's load current, producing the required compensating current and injecting it back into the appropriate phase via a reinjection transformer connected between that phase and neutral.

Since the neutral conductor carries the combination of the phase's harmonic distortion in a three phase network [Arrillaga et al. 1985], by converting the individual phase supply currents into sinusoidal currents, any current distortion would automatically be removed from the neutral. If the load was unbalanced, then a residual neutral current would flow even if individual phase current harmonic distortion was completely compensated for. By interconnecting the DC bus capacitors it is possible to transfer current from one phase to another. Therefore it is possible to take current from a phase that is most heavily loaded and transfer it to the lightly loaded phase. Using this

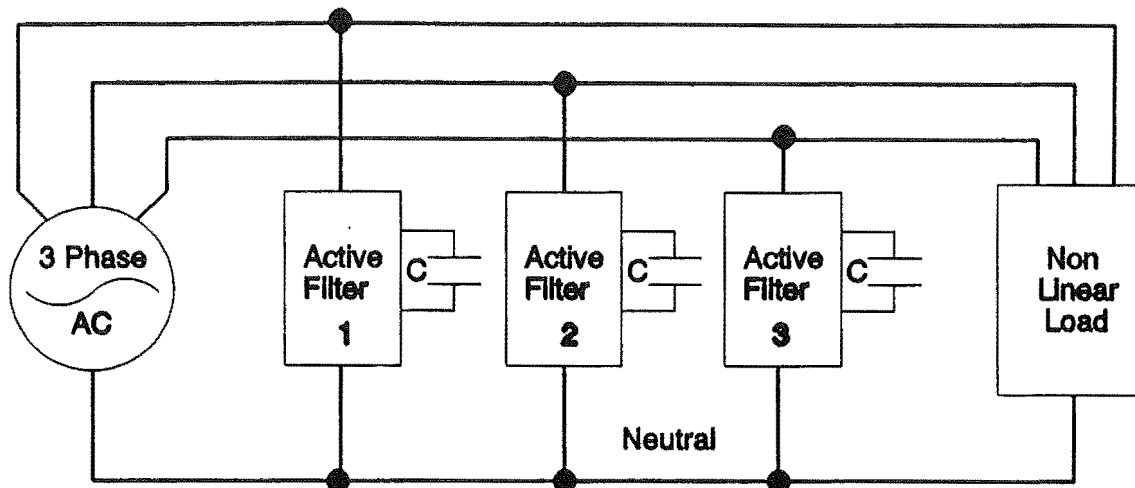


Figure 4.7 Connection of the Three Phase Active Filter

technique it is possible to balance the phase currents and reduce the neutral current. The performance of the three phase active filter to compensate for balanced and unbalanced harmonic loads is presented in Section 5.2.

4.3 SUMMARY

This chapter has presented the hardware design of the single phase analogue active filter. The signal processing unit derives a synthetic sinusoid from the phase and magnitude information of the load current. When the synthetic sinusoid is generated in phase with the fundamental supply voltage signal, the active filtering system can provide both harmonic and phase displacement compensation. The sinusoid is subtracted from the load current signal to produce the compensating current signal. This technique uses a time domain approach which is simple to implement.

The magnitude control of the synthetic sinusoid is initially performed by monitoring the fundamental level of the load current. By adjusting the magnitude of the synthetic sinusoid the flow of real power into the active filter can be controlled. The real power is necessary to overcome the losses of the active filter and is stored on a bank of capacitors, with the voltage level indicating the level of stored energy. A controller using this voltage level can control the magnitude of the synthetic sinusoid.

The power amplifier uses a controlled current and time based switching strategy to produce the compensating current. A reinjection transformer is used as an interface between the active filter and the power system to provide a voltage interface and to limit the rate of rise of compensating current.

A three phase active filter could be constructed by connecting three single phase active filters together. This would enable the reduction of neutral current due to unbalanced harmonic loads.

CHAPTER 5

PERFORMANCE OF THE ANALOGUE ACTIVE FILTER

This chapter deals with the experimental performance of the single and three phase analogue active filters. The steady state performance of the single phase active filter is discussed first and this is followed by a discussion of the steady state operation of the three phase active filter. The transient behaviour of both the single and three phase active filters is discussed in Section 5.3. The single phase active filter's ability to remove supply current distortion and to operate efficiently under various operating conditions is discussed in Section 5.4.

5.1 SINGLE PHASE STEADY STATE PERFORMANCE

5.1.1 Harmonic Current Compensation

The ability of the active filter to remove harmonic distortion from the supply current is investigated in this section. A typical distortive single phase load (Figure 5.1) operating from a 240 V_{RMS} supply is used to illustrate the active filters ability to remove current distortion.

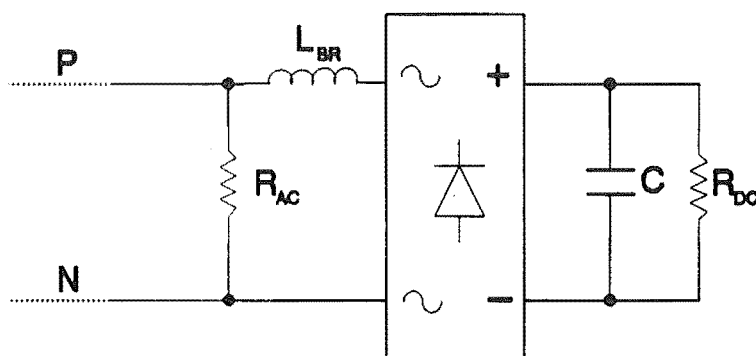


Figure 5.1 Single Phase Harmonic Load

The load consists of a single phase bridge rectifier with a capacitor (C) and resistive (R_{DC}) load. A small amount of inductance (L_{BR}) is in series with the bridge rectifier to simulate the leakage inductance of a transformer or line filter. In parallel with the bridge rectifier is a resistance (R_{AC}) to simulate a real power load such as heating or lighting. The single phase bridge rectifier circuit is found in most personal computers and with the combined resistive load, simulates a typical commercial building

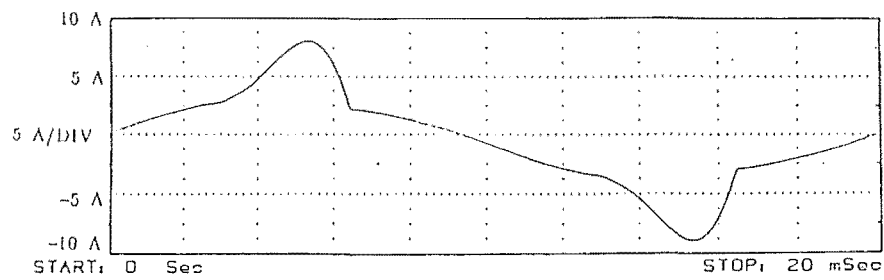
load. This load current is shown in Figure 5.2(a). The resistive load (R_{AC}) draws a sinusoidal current, while the bridge rectifier draws a current pulse as the capacitor is recharged at the peak of the supply voltage.

The THD, taking into account frequencies up to 1050 Hz, for this particular combined load is 42.1%. The compensating current produced by the active filter is shown in Figure 5.2(b). Low frequency switching components are noticeable on the compensating current waveform and show the variability of the switching frequency produced by the time delay switching strategy. For all of these examples the time delay is set to 10 μ s, which results in an average switching frequency of 25 kHz. The compensated supply current, shown in Figure 5.2(c), is now nearly sinusoidal and the THD has been reduced to 2.6%.

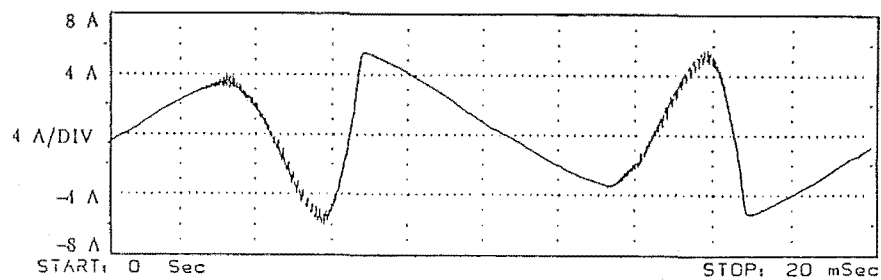
Figures 5.2(d) and (e) show the measured spectra of the load current and compensated supply current respectively. From a comparison of these spectra, it can be seen that with compensation the third harmonic (150 Hz) has fallen 23 dBV and the fifth harmonic (250 Hz) has fallen 27 dBV. The third harmonic of the compensated supply current is now 35 dBV below the fundamental (1.78% of the fundamental).

Examining the compensated supply current reveals that notches appear at the time the rectifier turns off. These notches occur because the response of the amplifier is limited by the leakage inductance of the reinjection transformer and cannot accurately track the discontinuity caused by the turn off of the bridge rectifier load.

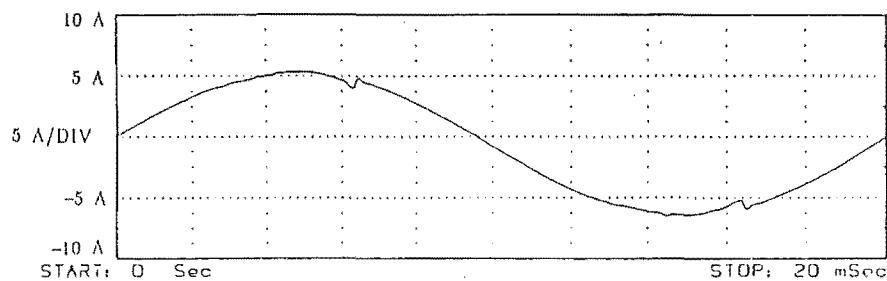
A comparison between the computer simulation results (Figure 3.4) and the actual active filter performance (Figure 5.2) can be made since the load used in the simulation is identical to the load shown in Figure 5.1. Near the peak of the compensated supply current in the experimental results a number of small ripples occur. These ripples are due to the fast rate of change of the compensating current signal producing low switching frequencies. Notches are also apparent in the computed compensated supply current, but because of the scale of the waveform, they are not so obvious. The amplitude of the compensated supply current's third harmonic component in the computer simulation is 0.56% of the fundamental compared with 1.78% for the experimental measurements. The computer simulation is an ideal case, therefore the actual performance is expected to be slightly worse, which it is. The simulation results closely agree with the actual experimental measurements, both in respect to harmonic current reduction and waveform shape, to be able to use computer simulation as a tool, to predict the active filter's performance for different load types and system conditions.



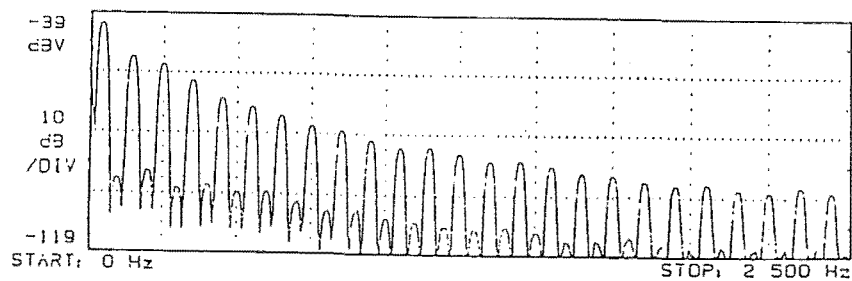
(a) Load current



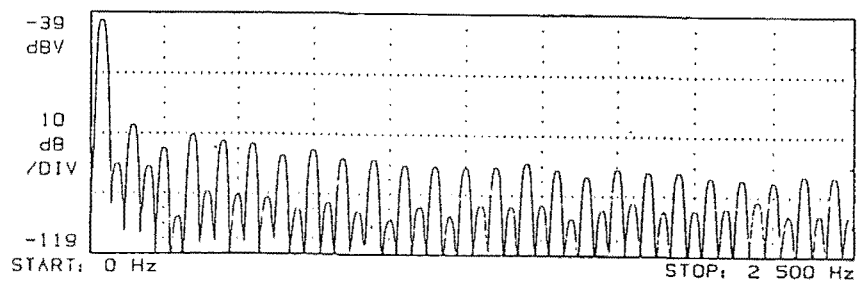
(b) Compensating current



(c) Compensated supply current



(d) Load current spectrum



(e) Compensated supply current spectrum

Figure 5.2 Steady State Operation of the Active Filter for a Harmonic Load

5.1.2 Distortion Compensation

The ability of the active filter to compensate for both harmonic and displacement (reactive power) distortion is investigated in this section. A load similar to that described in the previous section is used, but with an additional inductive load (L_{AC}) connected in parallel with the resistive load R_{AC} (Figure 5.3). Variation of L_{AC} provides a changeable level of fundamental displacement in the load current.

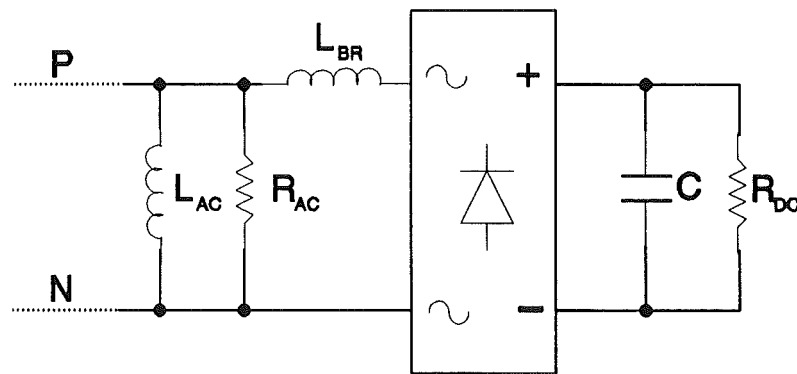


Figure 5.3 Single Phase Harmonic and Displacement Load

A typical load current drawn by this load shown in Figure 5.4(a) and has a measured THD of 24.8%. By synchronising the synthetic sinusoid in the SPU with the fundamental component of the load current it is possible to compensate only for the harmonic distortion. The compensated supply current I_s , and supply voltage V_s , are shown in Figure 5.4(b) for the case where only harmonic compensation is being carried out. The supply current THD has been reduced to 1.53% and the supply current is still phase displaced 55° from the supply voltage.

It is possible to correct for both the harmonic and displacement distortion by synchronising the synthetic sinusoid generated in the SPU to the fundamental component of the supply voltage. The compensating current produced to provide complete distortion compensation is shown in Figure 5.4(c) and the compensated supply current I_s , and supply voltage are shown in Figure 5.4(d). In addition to the reduction in supply current THD from 24.8% to 4.3%, the supply current has been phased shifted by 55° and is now in phase with the supply voltage. The actual phase displacement between the supply voltage and supply fundamental current is now less than one degree. As a result of compensating for the harmonic and phase displacement distortion the RMS level of supply current has also been reduced.

The reduction in the harmonic distortion is also illustrated in the comparison of

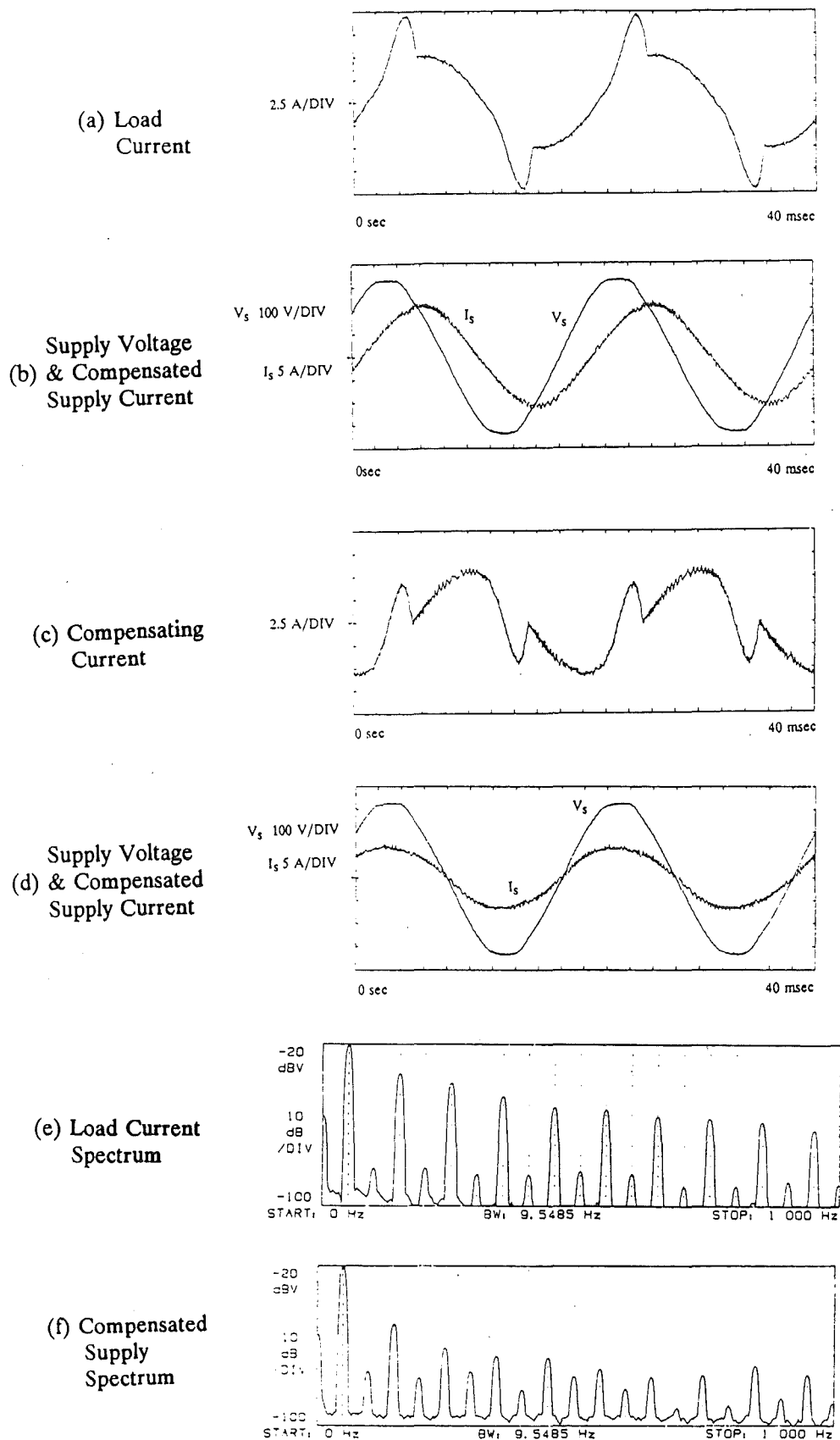


Figure 5.4 Steady State Operation of the Active Filter to a Distorted Load

load and supply current spectra (Figures 5.4(e) and (f)) for total compensation. The third harmonic (150 Hz) has been reduced by 15 dBV and is now 28 dBV below the fundamental (3.98% of the fundamental), while the fifth harmonic (250 Hz) has been reduced by 22 dBV and is now 40 dBV below the fundamental (1.0% of the fundamental).

5.2 THREE PHASE STEADY STATE OPERATION

5.2.1 Performance

Operation of three single phase active filters working together as a three phase active filter unit is demonstrated in this section for two different loads. The first load is a three phase bridge rectifier with capacitive and resistive load. The second is a three phase bridge rectifier with inductive and resistive load. The three phase active filter is operated with each single phase active filter independently producing the compensating current for each phase. The bus voltage on each active filter is adjusted independently so that all three are identical.

Initially a lightly loaded three phase bridge rectifier with capacitive and resistive load, drawing a DC current of 3 A and operating on a 415 V_{RMS} line to line power supply, is used to assess performance (Figure 5.5). The phase current drawn from this load has a THD of 53.6% (Figure 5.6(a)). When the three phase active filter is operating the compensated supply current (Figure 5.6(b)) is nearly sinusoidal and the THD is reduced to 2.5%.

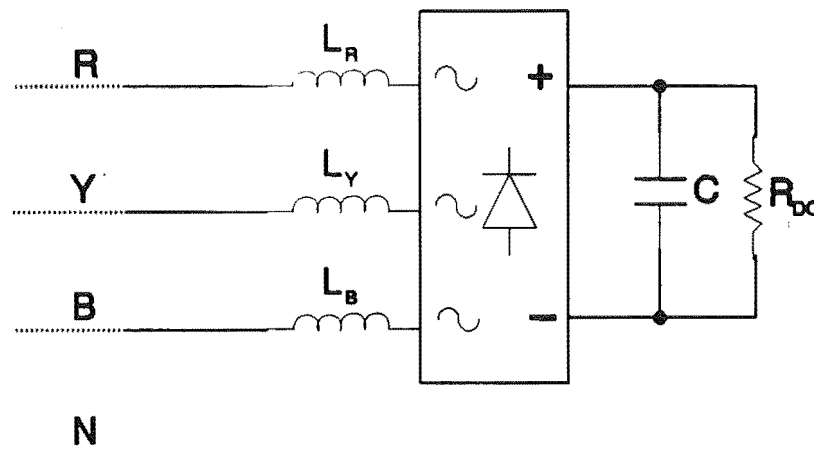
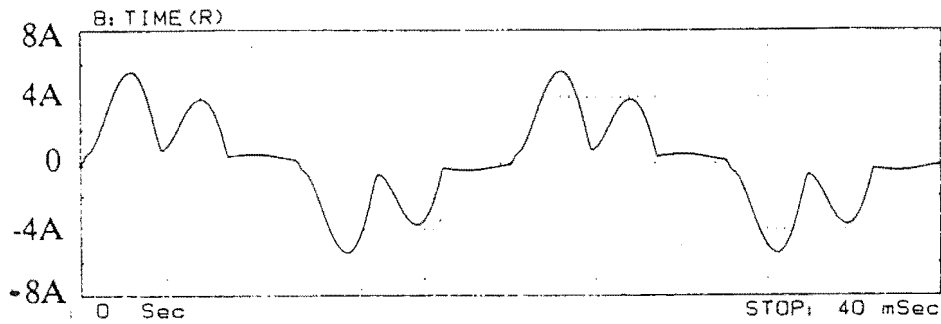
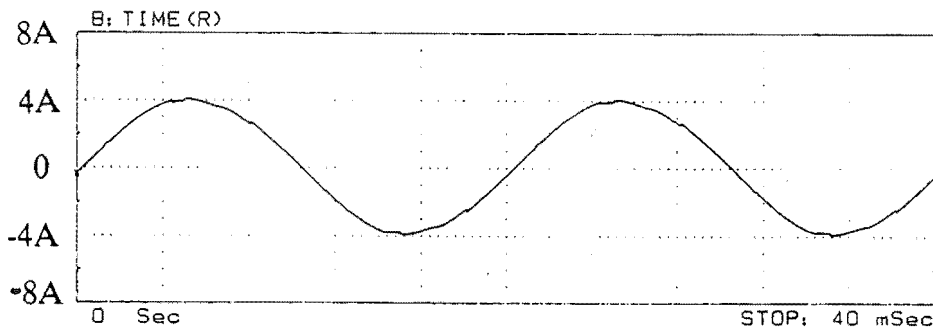


Figure 5.5 Three Phase Bridge Rectifier with Capacitive and Resistive Load



(a) Load Current



(b) Compensated Supply Current

Figure 5.6 Steady State Results for a Three Phase Active Filter Compensating for a Bridge Rectifier with Capacitive and Resistive Load

Compensation for a three phase bridge rectifier with inductive and resistive load (Figure 5.7) is also used to assess performance. The supply voltage is 200 V_{RMS} line to line and the DC load current is 10.8 A. Each active filter is operated with an average switching frequency of 25 kHz and a DC bus voltage of 230 V_{DC}. Figures 5.8(a) and (b) illustrate the load and compensated supply currents respectively. The load current is 7.6 A_{RMS} and has a THD of 14.4%, while the compensated supply current is nearly sinusoidal with a reduced THD of 1.33%. Magnitude of the supply current has now increased to 9.4 A_{RMS} since the active filter requires additional real power to operate.

Figure 5.8(c) shows the phase to neutral voltage of the power supply while Figure 5.8(d) illustrates the compensating current produced by the active filter. The spectra of the load is shown in Figure 5.8(e) and the dominant components compared to the fundamental are the 5th (250 Hz) and 7th (350 Hz) harmonics. The 5th harmonic is only 17.8 dBV below the fundamental (12.9% of the fundamental) while the 7th harmonic is 24.6 dBV below the fundamental (5.9% of the fundamental). The spectra of the compensated supply current in Figure 5.8(f) shows that all the harmonic components up to 950 Hz have been reduced. The 5th and 7th current harmonics are now 45.6 dBV and

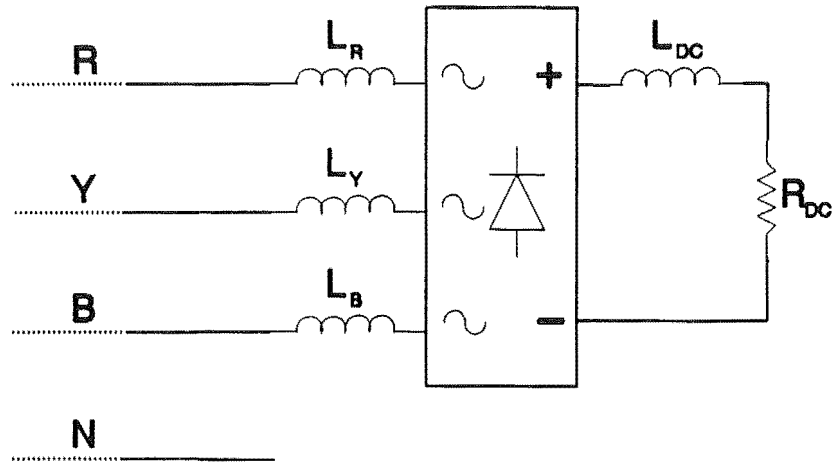


Figure 5.7 Three Phase Bridge Rectifier with Inductive and Resistive Load

47.4 dBV below the fundamental (0.52% and 0.43% of the fundamental) respectively. The fundamental magnitude has increased from the load current to compensated supply current spectra by 1.92 dBV or 24.8%. This is the additional fundamental current consumed by the active filter as real power.

5.2.2 Phase Balancing

By using three separate single phase active filter units connected in a three phase active filter configuration, the individual control of supply current drawn from each phase can be maintained. By connecting each of the individual active filters DC bus capacitors together (Figure 5.9) it is possible to pass energy from one phase to another. This section briefly looks at the possibility of performing phase balancing with this configuration. The aim of phase balancing is to force the supply current in each phase to have the same RMS value. With a three phase unbalanced linear load the imbalance in phase currents appears as a neutral current. By balancing each phase, by shifting current from one phase to another or by making the loads identical, it is possible to eliminate that neutral current.

An unbalanced harmonic load (Figure 5.10) consisting of a constant three phase bridge rectifier with inductor and resistor and an additional three phase resistor load bank ($R_X R_Y R_B$) is used. The harmonic load is provided by the bridge rectifier circuit, which draws balanced phase currents, while the unbalance in line currents is achieved by varying the resistive load in each phase of the resistor bank. Typical three phase load and neutral currents are presented in Figure 5.11.

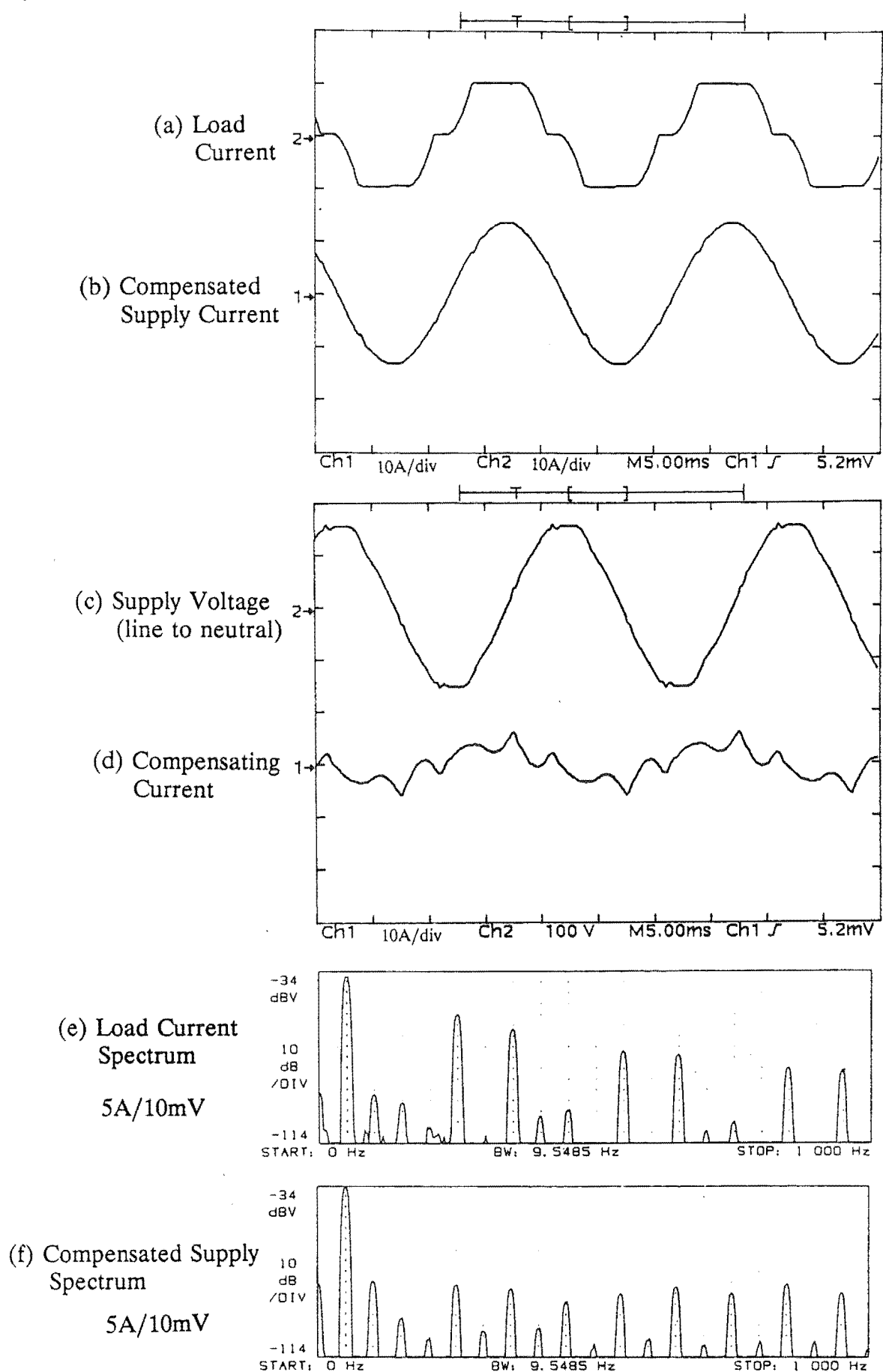


Figure 5.8 Active Filter Compensating for Three Phase Bridge Rectifier with Inductive and Resistive Load

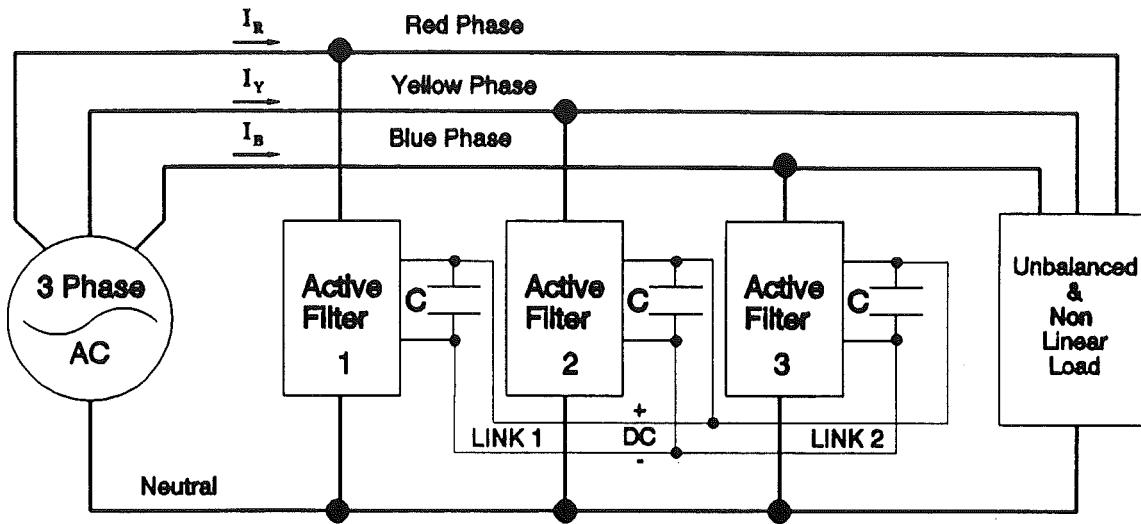


Figure 5.9 Connection of the Three Phase Active Filter to provide Phase Balancing

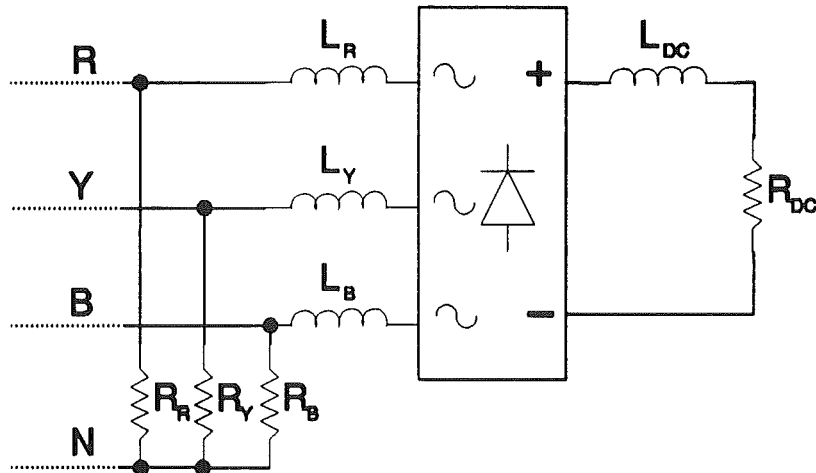


Figure 5.10 Load to Provide Unbalanced and Harmonic Currents

Each phase has a different load combination and total RMS value of current flowing. The harmonic load draws $6.2 A_{RMS}$ from each phase, while the resistive bank draws from red, yellow and blue phases $3.0 A_{RMS}$, $1.8 A_{RMS}$ and $0 A_{RMS}$ respectively. Therefore the unbalance in the load is only caused by the three phase resistor load and the current flowing in the neutral ($2.6 A_{RMS}$) is sinusoidal.

The supply currents RMS and THD values for non active filtering and active filtering are listed in Table 5.1 with the compensated supply and neutral current waveforms shown in Figure 5.12.

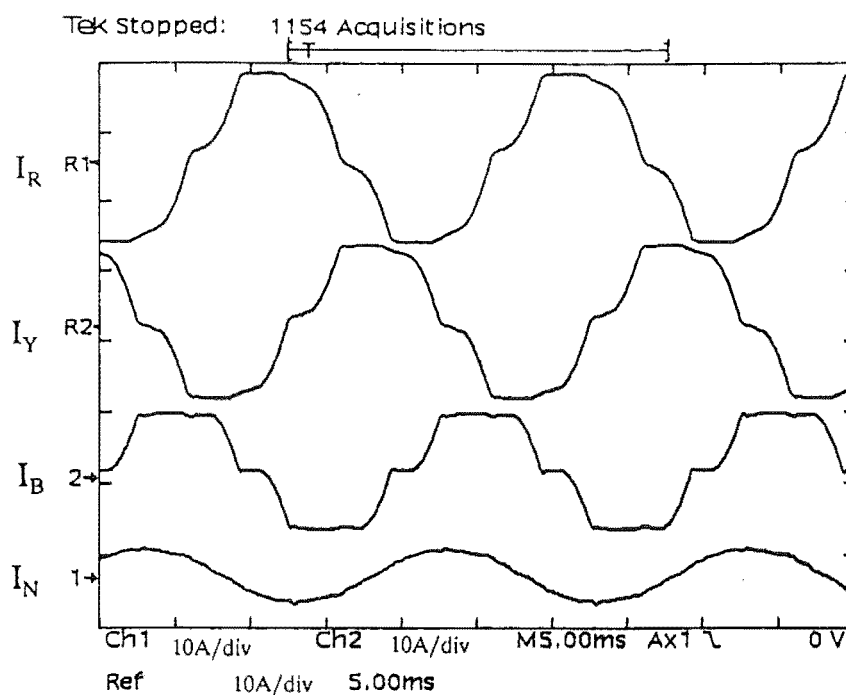


Figure 5.11 Supply Current for an Unbalanced, Harmonic Load before Active Filtering

TABLE 5.1 Comparison of Supply Current Values for Phase Balancing

SUPPLY CURRENT PHASE	NO ACTIVE FILTERING		ACTIVE FILTERING	
	I_{RMS}	THD (%)	I_{RMS}	THD (%)
RED (I_R)	9.2	10.9	8.6	10.8
YELLOW (I_Y)	8.0	12.0	8.6	8.4
BLUE (I_B)	6.2	16.4	8.6	4.2
NEUTRAL	2.6	5.1	1.6	146.0

The supply current I_B is now more sinusoidal and the magnitude has increased from $6.2 A_{RMS}$ to $8.6 A_{RMS}$. The largest load current (I_R) before active filtering, has a reduced magnitude, but still has nearly the same level of THD (10.8%). I_Y THD has reduced from 12.0 to 8.4%, while the magnitude has increased from 8 to $8.6 A_{RMS}$. The current flowing in the neutral conductor has been reduced by 38.5%, from $2.6 A_{RMS}$ to $1.6 A_{RMS}$. Phase balancing has almost eliminated the fundamental component from the neutral, leaving the resultant harmonic components. Therefore the harmonic components are larger than the fundamental which results in a high value of THD for the neutral

current. This high value of THD for the neutral current is caused by the active filtering system not fully compensating for the distortion, especially in the red phase, leaving the residue harmonic components to flow in the neutral. The three phase active filter is unable to compensate for the harmonic load current of the red phase because the synthetic sinusoid magnitude of each active filter is adjusted to balance the RMS supply currents. The synthetic sinusoid magnitudes of the three active filter units result in a DC bus voltage which is unable to provide adequate compensating current to reduce the RMS current level and remove the harmonic distortion.

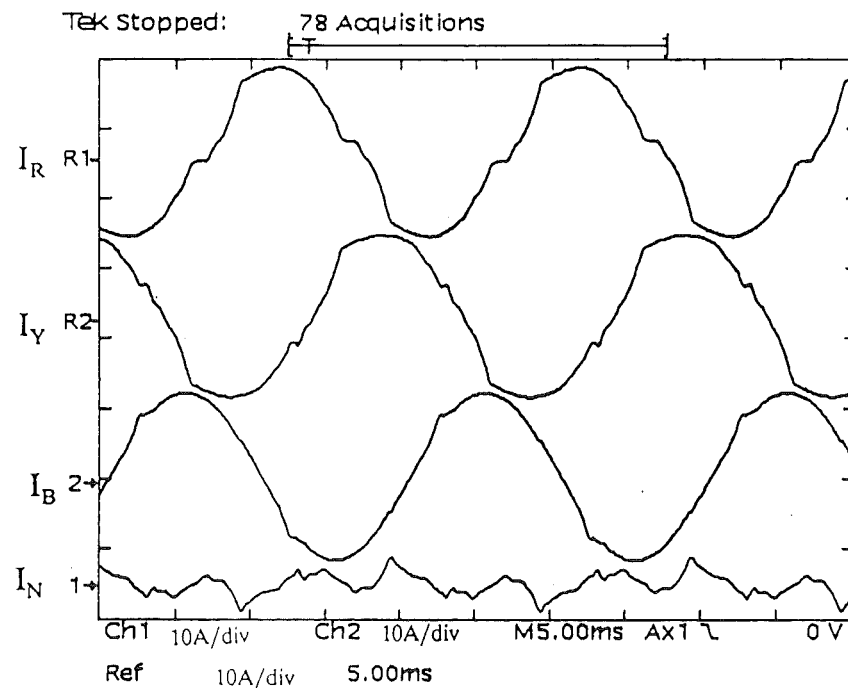


Figure 5.12 Supply Current for Active Filtering with an Unbalanced, Harmonic Load

The transfer of current between phases, or load balancing, can be seen in the flow of current from one set of DC bus capacitors to another. Figure 5.13 shows the DC bus voltage at a level of $154 V_{DC}$ and the flow of current in the two DC bus voltage links (Figure 5.9). DC current, as well as even harmonic components, flow in these links and the harmonic component with the largest magnitude is 100 Hz. Even harmonics components are present in the voltage ripple on the DC bus capacitors. This ripple on the bus capacitors then causes even harmonic components to be imposed on top of the DC link currents.

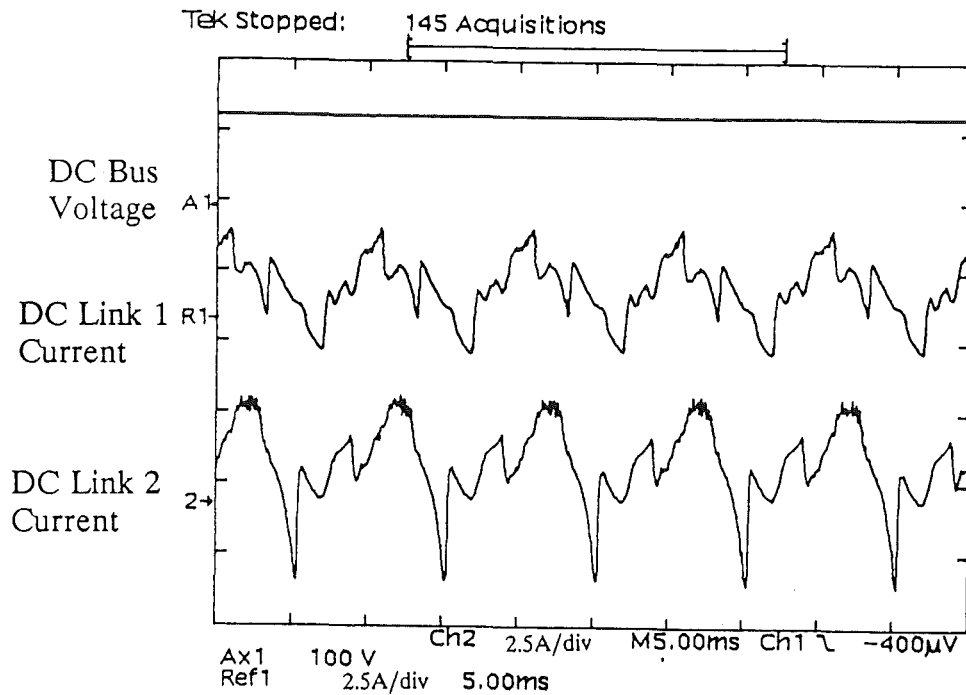


Figure 5.13 DC Link Currents due to Phase Balancing

5.3 TRANSIENT PERFORMANCE

5.3.1 Single Phase

The transient performance of the single phase active filter, using the magnitude controller described in Section 4.1.1.2 is considered in this section. A single phase bridge rectifier with capacitive and resistive load and a base resistive load (as described in Section 3.3.1) is used to produce a distorted load.

To investigate the transient response of the active filter, the rectifier load is modified such that the load current is subjected to a step increase from $2.1 A_{RMS}$ to $4.2 A_{RMS}$ (Figure 5.14(a)). At the instant the step increase in load current is applied, the compensating current (Figure 5.14(b)) experienced a step change because the output of the magnitude controller can not respond quickly enough to the load current change. The energy for this step increase in compensating current initially comes from the bus capacitors and thus the DC bus voltage (Figure 5.14(d)) falls. The fundamental component of the load current produced by the magnitude controller now slowly ramps up to the new value. At approximately two time constants (time constant is 100 ms) after the step change in load has occurred, the compensating and compensated supply currents have reached their new steady state levels. The bus voltage will however be still slowly ramping up to a new bus voltage level set by the excess flow of real power into the active

filter.

The experimental performance results for a step increase in load current can be compared to the transient performance of the active filter in the computer simulation in Section 3.3.2. Initial load type and step increase are identical for the measured performance and computer simulation. The experimental compensating current (Figure 5.14(b)) shows the initial peaks due to insufficient bus voltage (Section 4.1.1.2) and then settles to a fixed level just as the computer simulation does in Figure 3.5. Voltage on the bus capacitors for the actual and computer simulation results both fall at the same rate and slowly start to increase 150 ms after the load change occurred.

Agreement between the experimental and computed results for this particular transient load change has been good. Both the steady state and transient response experimental results validate the computer modelling and simulation technique in Chapter 3. The computer simulation technique could now be used with reasonable accuracy to predict operation of the active filter for different load configurations.

5.3.2 Three Phase

The three phase active filter system has been designed to operate either with manual control of the magnitude of the synthetic sinusoid or with a bus voltage control system. Using manual magnitude control the amplitude of the synthetic sinusoid generated in each phase can be controlled independently. This is a useful technique to balance the three phase currents. The bus voltage controller is based on the integral controller described in Section 4.1.1.2 and in the three phase active filter it has a time constant of 100 ms.

The transient response of the three phase active filter, while compensating for a three phase bridge rectifier with inductive and resistive load as described in Section 5.2.1, is now considered. The DC side of the rectifier load is initially drawing 7 A_{DC} and a step increase in load current results in the DC current being increased to 11 A_{DC}. Response of the bus voltage controller to this load change and the subsequent drop in bus voltage can be observed in Figure 5.15(a). The bus voltage controller initially takes 450 ms to start to increase the voltage on the bus capacitors. An underdamped response is provided by the controller and it takes over 8 s to reach the value of bus voltage (235 V) prior to the load change. Over this time span, the supply current is difficult to observe as many fundamental periods occur and the digital storage oscilloscope produces aliasing on the output (Figure 5.15(b)). Full compensation of the supply current does not occur until the

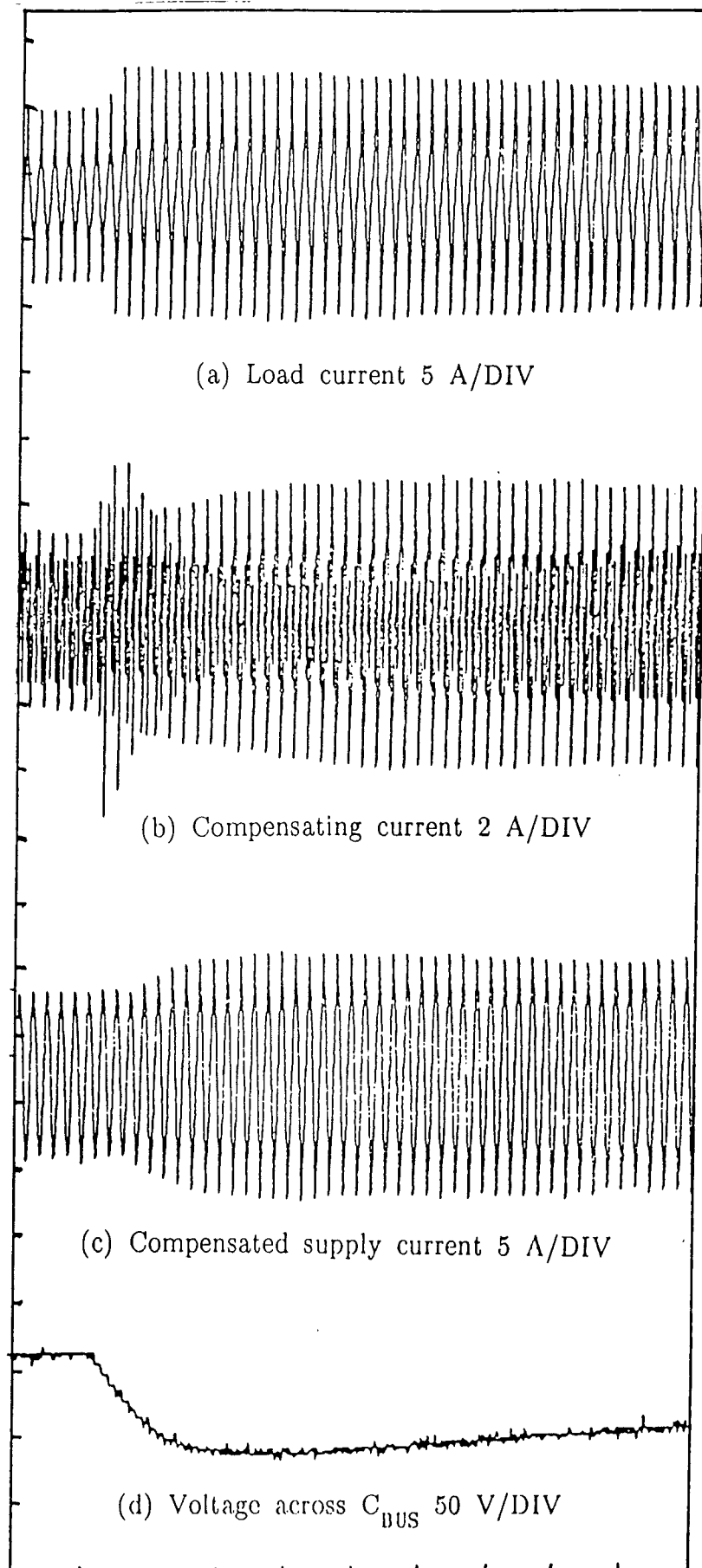


Figure 5.14 Single Phase Active Filter's Transient Response to a Step Increase in Harmonic Load (Time Scale 100ms/div)

bus voltage returns to a level sufficient for reinjection (Section 4.1.1.2). The minimum voltage for adequate compensation for this three phase load is 150 V_{DC} and the controller takes 950 ms to achieve this level after the load has changed.

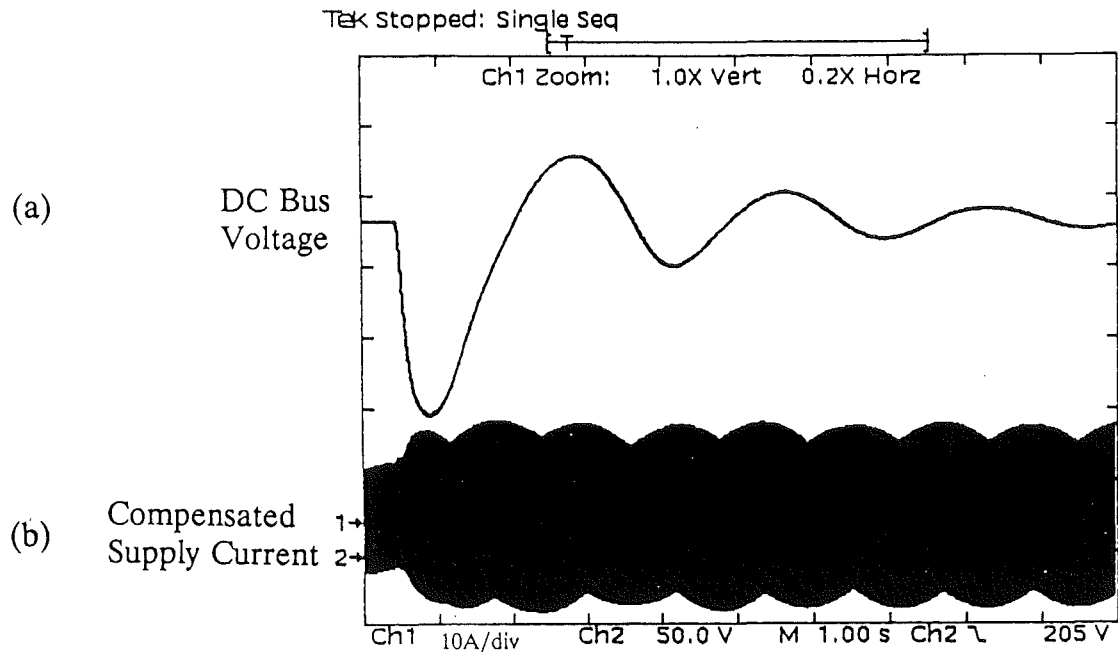


Figure 5.15 Transient Response for the Three Phase Active Filter for a step increase in Load Current using a Bus Voltage Controller

From these results it can be seen that the integral based controller's performance is most unsatisfactory. The use of an improved bus voltage controller is investigated further in Section 6.5.1.

5.4 OPERATIONAL PERFORMANCE OF THE SINGLE PHASE ACTIVE FILTER

The performance of the single phase active filter can be judged by its ability to reduce the harmonic and displacement content of the supply current for a non-linear load. The objective of active filtering is to reduce the THD, and on occasions the displacement, of the supply current. Supply current THD can be altered by changing the operating conditions of the active filter. These conditions are controlled by the switching time delay (average switching frequency) and the DC bus voltage. Altering the average switching frequency and DC bus voltage also has an effect on the operating efficiency of the active filter.

The operating efficiency of the active filter is based on the real power flow in the total system and is determined from the fundamental current that is in phase with the supply voltage. Assuming that the load and active filter is supplied from a strong AC system, the real power is the product of the voltage and in phase fundamental current component ($V_I \cos \theta$). The efficiency (ζ) of the compensation system can be defined by Equ. (5.1) where ΔP is the power consumed by the active filter.

$$\zeta = \frac{P_{\text{LOAD CURRENT}}}{P_{\text{COMPENSATED SUPPLY CURRENT}}} = \frac{P_L}{P_L + \Delta P} \quad (5.1)$$

The DC bus voltage has an effect on the switching frequency profiles for a fixed switching time delay. Figure 5.16 shows the spectrum of the compensating current on the inverter side of the reinjection transformer. By increasing the DC bus voltage from 190 to 350 V_{DC}, with a fixed time delay of 15 μ s, Figures 5.16(a) and (b) show a decrease in the lower frequency components and a slight increase in the higher frequency components. The low frequency components (2-10 kHz) at a bus voltage of 190 V_{DC} have been shifted above 10 kHz when the bus voltage is increased to 350 V_{DC}. This is explained by considering the rate of rise of current through the reinjection transformer. The voltage ($V_{DC}(t) - v(t)$) to leakage inductance (L_{leakage}) ratio as given in Equ. (5.2) governs this rate of rise of compensating current [Enslin et al. 1990]. When the bus voltage is increased and the supply voltage is constant, this effectively increases the rate of rise of current and causes the switching frequency band to shift to a higher frequency. This allows the active filter to produce a compensating current which can more closely follow faster changing waveforms.

$$\frac{dI_C}{dt} = \frac{V_{DC}(t) - v(t)}{L_{\text{leakage}}} \quad (5.2)$$

where $v(t)$ is the supply voltage
 $V_{DC}(t)$ is the bus capacitor voltage

The performance of a single phase analogue active filter compensating for a combined rectifier and resistive load (Figure 5.1) is illustrated by Figure 5.17.

Figure 5.17(a) shows the measured efficiency of the active filter with different average switching frequencies and DC bus voltages. The efficiency of the active filter improves with low bus voltages because the rate of rise of current has decreased. The switching frequency profile now contains a greater proportion of lower frequency components. Hence the switching losses decrease because the power amplifier is

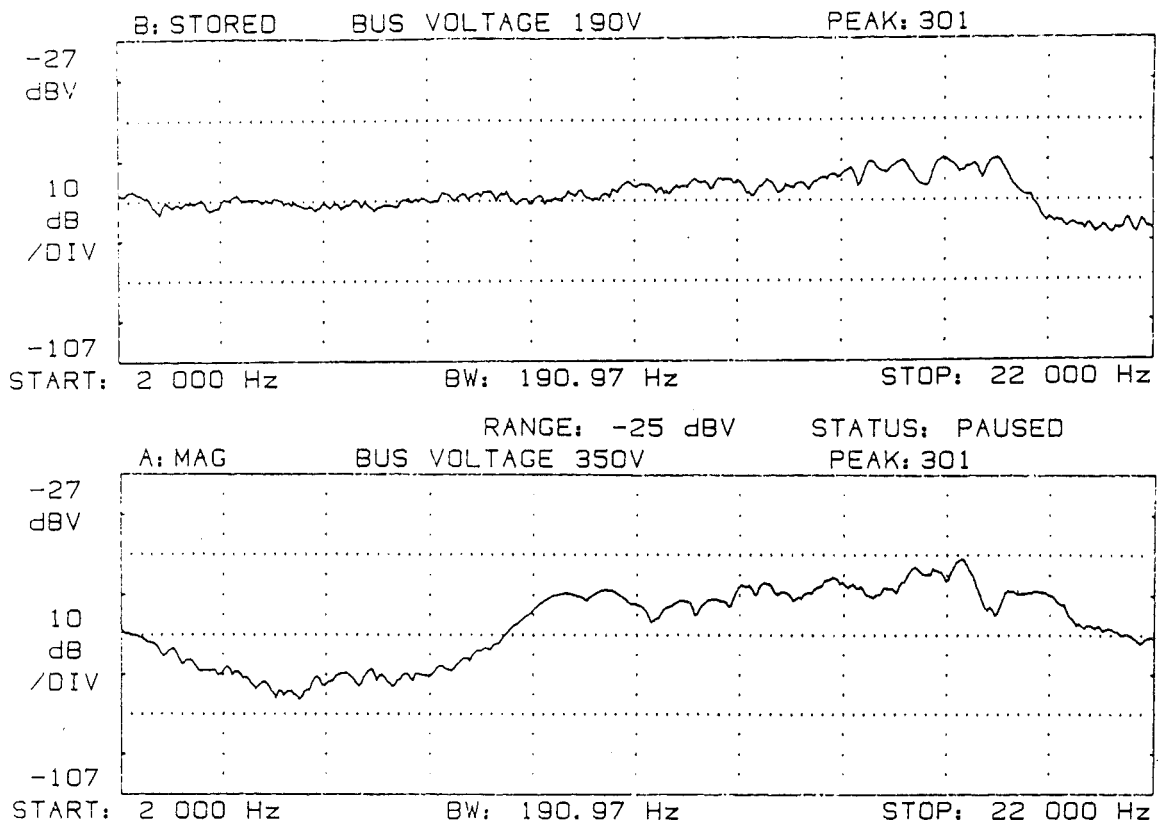


Figure 5.16 Switching Frequency Profiles for a DC Bus Voltage Increase from 190 V_{DC} to 350 V_{DC}

switching at a lower average frequency and a lower bus voltage is applied across the semiconductor devices. As the bus voltage is increased, with the same switching time delay, the semiconductor switching losses increase significantly and the efficiency decreases. At low frequencies (less than 5 kHz) the current excursions around the required compensating current are increased and the conduction losses of the system become dominant. At high switching frequencies (greater than 20 kHz) the switching losses of the system become more dominant and thus the efficiency tends to fall. The most efficient average switching frequency for this particular non-linear load is in the range 17 - 20 kHz. To establish an appropriate bus voltage operating level the THD performance of the active filter must also be considered.

The measured level of supply current THD at various bus voltages and average switching frequencies is shown in Figure 5.17(b). At low bus voltages the THD performance is poor because the DC bus has insufficient stored energy to reinject enough compensating current for complete harmonic cancellation. By increasing the bus voltage the system can better compensate for the harmonic distortion, however, the incremental increase in THD at higher bus voltages is small. The other factor that can alter the THD

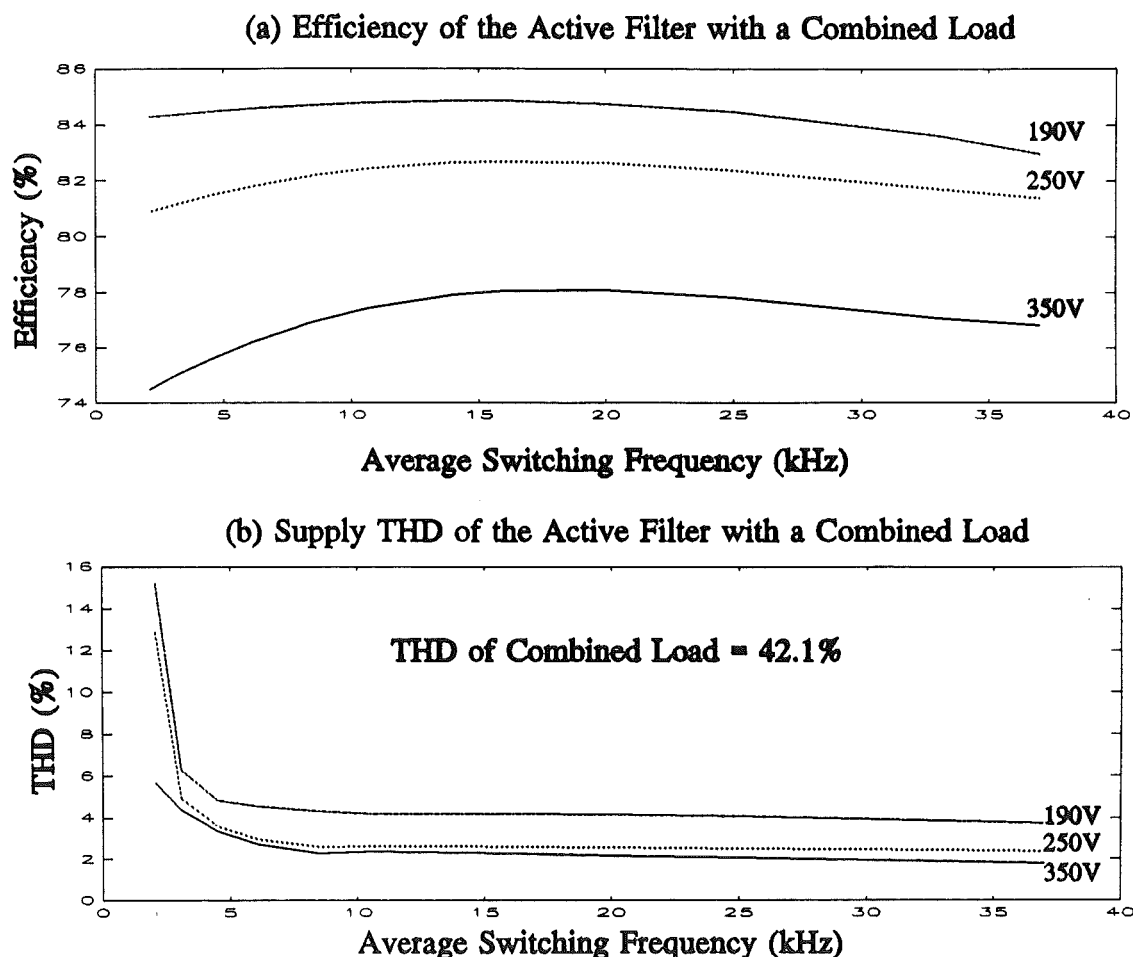


Figure 5.17 Performance of the Single Phase Active Filter

performance is the average switching frequency. At low switching frequencies (less than 7 kHz) the THD is up to three times larger than that which can be achieved at higher frequencies. The reason for this trend is that at low frequencies the compensating current does not closely follow the compensating current signal and thus the harmonic compensation is less than ideal. As the frequency increases the amplifier output current can follow the required compensating current signal more closely and thus the harmonic content can be further reduced.

Another consideration is the audible noise the power amplifier produces. Ideally the average switching frequency should be chosen to be outside the audible range of humans. Thus an optimum operating region for the active filter can be selected by choosing an average switching frequency of at least 20 kHz and a bus voltage of 230 V_{DC}. This would produce a level of 2.6% THD in the supply current, a reduction from 42.1%,

and the system would be operating with an efficiency of 83.6%.

By changing the average switching frequency and DC bus voltage of the power amplifier, an optimum operating point, which achieves low supply current distortion at a high level of efficiency, can be reached. With different types of loads, this optimum operating point changes as the efficiency and supply current THD are dependent on the amount of distortion contained in the load current. Since typical commercial loads can vary over time, an intelligent, digitally based controller, which could monitor the active filter efficiency and reduction in supply current THD and alter the operating point of the active filter to achieve optimal performance, is proposed.

5.5 SUMMARY

This chapter has dealt with the performance evaluation of the active filter and has compared its actual performance to that predicted by the computer modelling. Verification of the computer modelling has been performed for the single phase active filter for both steady state and transient operation. The comparison between the computer simulation and actual experimental results show that they are in agreement and sufficiently reliable to allow the computer simulation to predict the of operation of the active filter for different load types.

The use of the single phase active filter as a device to compensate for both harmonic and displacement distortion has been shown. In the analogue active filter the displacement correction always shifts the compensated supply current back to unity power factor. With a flexible digital controller the amount of displacement correction could be adjusted in a range from non displacement compensation to providing unity power factor.

The operation of a three phase active filter was presented and its ability to compensate for two types of harmonic loads is detailed. By using three single phase active filters to construct a three phase active filter each phase can be controlled independently. This control of each supply current is demonstrated by balancing the supply currents of an unbalanced harmonic load.

The ability of the single and three phase active filters to provide compensation during a load change was demonstrated. Use of an analogue controller with integral control limited the rate at which compensation could be provided after a transient had occurred. A large integral time constant produced a slow response by the analogue controller. The use of a faster controller is investigated in Section 6.5.1.

Finally the operating characteristics of the single phase active filter were demonstrated. By manipulating the bus voltage and average switching frequency (switching time delay) of the active filter, it is possible to change the reduction in the supply current's THD and operational efficiency of the overall filtering system. It has been proposed that by using an intelligent, digitally based controller it would be possible to operate the active filter in such a way as to achieve a low value of supply current distortion while maintaining a high level of operational efficiency.

CHAPTER 6

DIGITAL CONTROLLER FOR THE ACTIVE FILTER

In the previous chapter it was shown that the supply current THD and efficiency of the active filter can be affected by changing two operating conditions, DC bus voltage and average switching frequency. By adjusting these two conditions the active filter can be operated to maintain the lowest supply current THD for the greatest operating efficiency. The actual optimum operating point of the active filter is dependent on the type of load being compensated for. In an industrial/commercial environment, where the composition of the load is not exactly known, a system which can control the operating point of the active filter is required.

This control could be implemented in analogue hardware, however a digital controller has more advantages. Digital controllers tend to be flexible, able to implement more complex control algorithms such as adaptive control, store information and monitor the system's performance [Astrom, Wittenmark 1984]. A digitally based controller is implemented in the active filter in order to perform automatic optimisation.

6.1 REQUIREMENTS OF A DIGITAL CONTROLLER

The main requirement of the digital controller is to compute the compensating current signal to the same accuracy as the SPU of the analogue active filter and to generate this signal in real time (calculations completed before the next input arrives). In addition, it must automatically determine new operating points for various types of loads. To achieve these various objectives the following main tasks are required from the digital controller:

- measurement of the load current
- tracking the fundamental frequency of the power system
- control of the DC bus voltage
- control of the average switching frequency
- determining the fundamental supply and load power factor
- calculating of the compensating current
- calculating the operational efficiency
- calculating the THD of supply voltage, supply and load currents
- calculating the RMS values of supply voltage, supply, load and compensating currents.

The frequency components of the supply voltage, supply and load currents are

required to calculate the THD and the efficiency of the system. A Fast Fourier Transform (FFT) is able to extract frequency information, however this process requires a large amount of computer processing [Brigham 1974]. To be able to operate in real time a fast digital controller is therefore required. Calculation of the analogue active filter's compensating current signal is performed in the time domain therefore the delay between measuring the load current and generating that compensating current signal must be kept to a minimum. The digital controller must be fast enough to minimise the delay in processing the compensating signal to maintain the system under real time control.

Microprocessors have been around for 20 years and now a special class of microprocessors called Digital Signal Processors (DSPs) are available which offer very fast execution times [Bose 1992a, Lin, Frantz, Simar 1987]. DSPs contain specialised functions such as dedicated hardware multipliers, extensive pipelining of instructions, special digital processing instructions and fast instruction cycle times [Papamichalis 1990].

The current range of DSPs can be broken into two main categories, those based on integer arithmetic and those based on floating-point arithmetic. Traditionally integer based arithmetic is used in applications where high speed is important as it is easily implemented in hardware. Previously in applications where floating-point arithmetic is required, implementation is provided by software routines due to the large expense and chip area required to implement floating-point arithmetic in hardware. A problem with integer arithmetic is that the programmer must contend with round off error and lack of precision. Floating-point arithmetic can now be easily implemented in hardware and is able to provide the programmer with a convenient method of performing high speed computations, while still maintaining accuracy and precision [Papamichalis 1990].

Another consideration in choosing a digital controller is the ease of programming. Programming can be very time consuming if the code has to be written using assembly language. This time can be reduced if a high level language is used. However, the implementation of an algorithm in a high level language normally leads to slow execution due to inefficiencies in producing the compiled code [Astrom et al. 1984, Simar, Davis 1988].

A TMS320C30 DSP from Texas Instruments is used as the processor in the digital controller for the active filter because it is a floating point based DSP with very fast execution times and a large amount of expansion capability [Texas Instruments 1991]. A high level C language compiler, which is able to make a good C program almost as efficient as the equivalent assembly language program, is available for the TMS320C30

[Simar et al. 1988]. This reduces software development time and yet still provides real time control of the system.

6.2 HARDWARE DESCRIPTION

This section describes the hardware implementation of the digital controller for the active filter. The TMS320C30 DSP is implemented on a commercial IBM compatible PC based interface card. The DSP system consists of the TMS320C30 plus 32 k by 32 bit static RAM, access to all of the input/output and peripheral interfaces and an interface to the PC for hardware and software development. The interconnection of the TMS320C30 to the signals required for active filtering is shown in Figure 6.1.

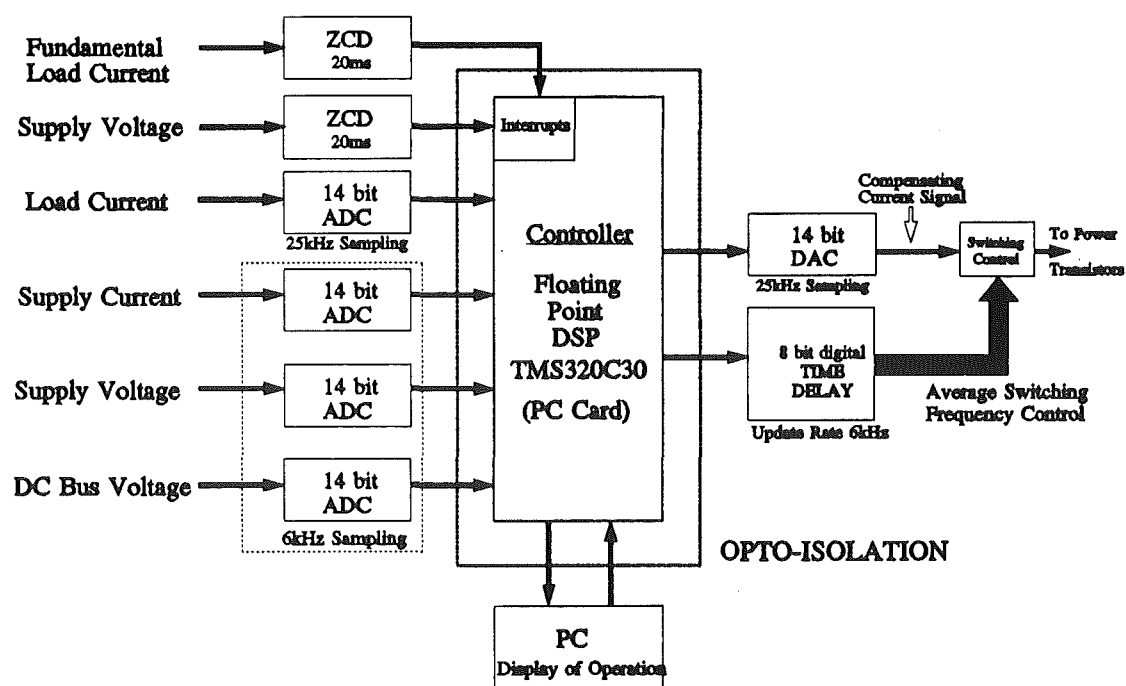


Figure 6.1 External Connection of the Active Filter to the TMS320C30 Digital Controller

The initial requirement of the digital controller is to implement the signal processing functions of the analogue active filter. The primary task is to measure the load current, subtract a fundamental sinusoid and output the resulting compensating current signal to the switching control circuit. An Analogue to Digital Converter (ADC) with a resolution of 14 bits is used to measure the load current (Figure 6.2). A 14 bit converter gives the system a large dynamic range, the ability to measure low level signals with the same accuracy as high level signals.

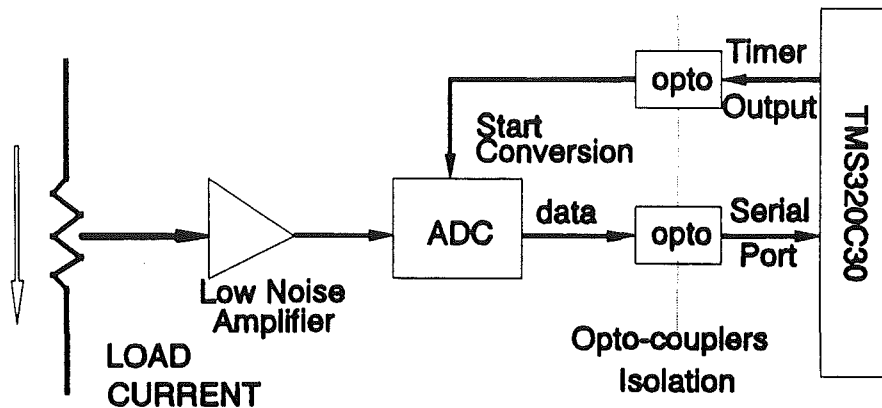


Figure 6.2 Load Current's Measurement System

The sample rate for the load current ADC system was determined so that the delay between the input sample and the output of the computed result is less than one degree of phase delay of the fundamental frequency. For a supply frequency of 50 Hz this results in a maximum time between samples of $55.6\mu\text{s}$ or a sample rate greater than 18 kHz. An ideal sampling rate of 25.6 kHz is used so that 512 samples would be recorded during each fundamental period. Collecting 512 samples ensures that an efficient FFT algorithm can be used to determine the harmonic components and to reduce spectral leakage [Arrillaga et al. 1985, Brigham 1974].

The fundamental frequency of the supply (power system) is never constant and to track the shifts in frequency a sample rate multiplier is implemented. A sample rate multiplier detects the supply voltage zero crossing and alters the sample rate so that exactly 512 samples are collected in the next fundamental period. The sample rate is produced by an internal timer and is adjusted by software every fundamental period if a shift in frequency is detected.

The supply current, supply voltage and DC bus voltage ADC's (Figures 6.1 and 6.3) and the time delay output (Figure 6.4) are sampled at a lower rate of 6.4 kHz. This corresponds to 128 samples per fundamental period, which is derived by dividing the sample rate of the load current ADC by four. This lower sample rate is used because the system only requires the frequency spectra and RMS information from these signals. A sample rate of 6.4 kHz enables the FFT to calculate up to the 50th harmonic component. Using a lower sample rate also allows the TMS320C30 more time for the calculation of other control functions. The supply current, supply voltage and DC bus voltage are measured using 14 bit serial ADC's. These inputs are memory mapped into the TMS320C30 because only two serial ports exist on the TMS320C30. Therefore each of

these serial signals has to be converted to a parallel format and then transferred to the expansion data bus.

Supply voltage and current are measured to provide information on the total power factor, displacement angle and THD levels. The fundamental component of the supply current is used in conjunction with the fundamental of the load current to determine the operational efficiency of the digitally controlled active filter. Measurement of the DC bus voltage is used by the bus voltage controller to adjust the magnitude of the synthetic sinusoid to control the real power flow into the active filter.

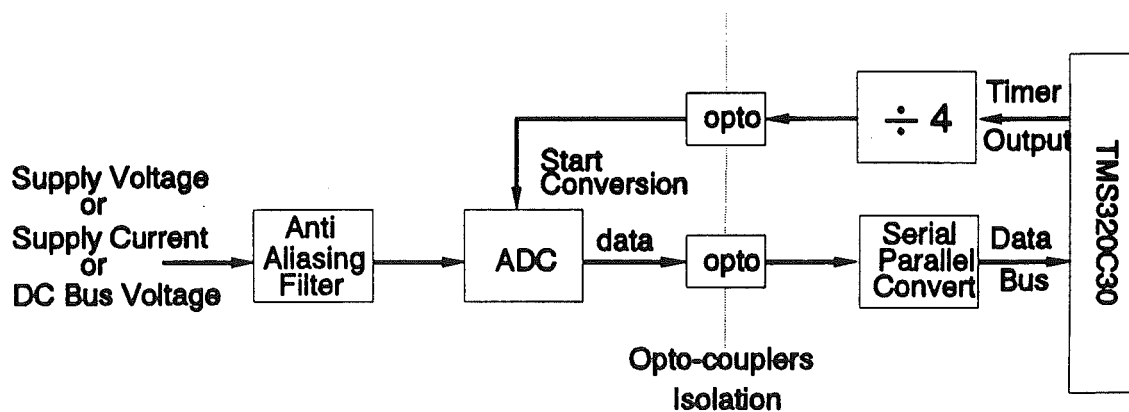


Figure 6.3 Lower Sampling Rate Analogue to Digital Converters

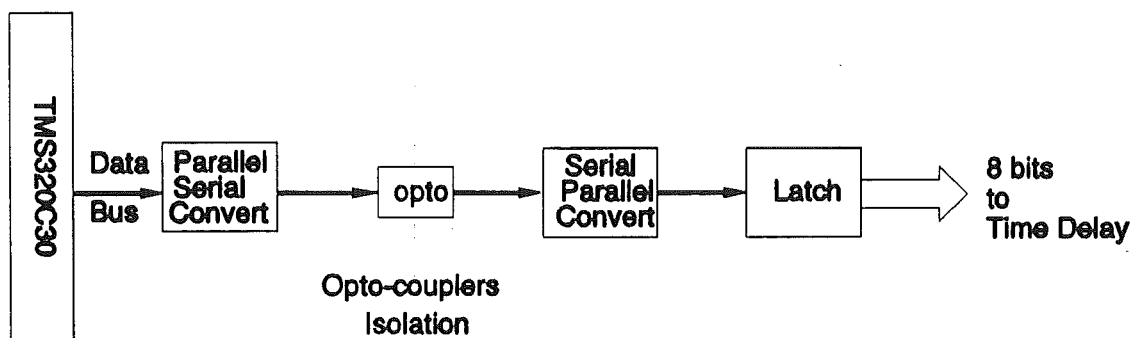


Figure 6.4 Low Sample Rate Digital Output for Time Delay Circuit

The digital time delay output (Figure 6.4) adjusts the average switching frequency of the active filter. Figure 6.5 illustrates the digital version of the adjustable time delay. An edge detector determines when the actual current (compensating current) in the reinjection transformer has exceeded the required current level given by the compensating current signal. A counter is started and when the counter output has the

same value as the set delay (8 bit value) the new switching state is stored in a latch. The new switching state is transmitted to the switching control circuit. With an eight bit value and an oscillator frequency of 2 MHz a variable time delay between $3\ \mu\text{s}$ and $128\ \mu\text{s}$ can be achieved. This corresponds to an average switching frequency range from 2 kHz to 80 kHz. Implementing a digitally controlled time delay requires a greater level of complexity compared to the implementation of the analogue fixed time delay described in Section 4.1.2.1.

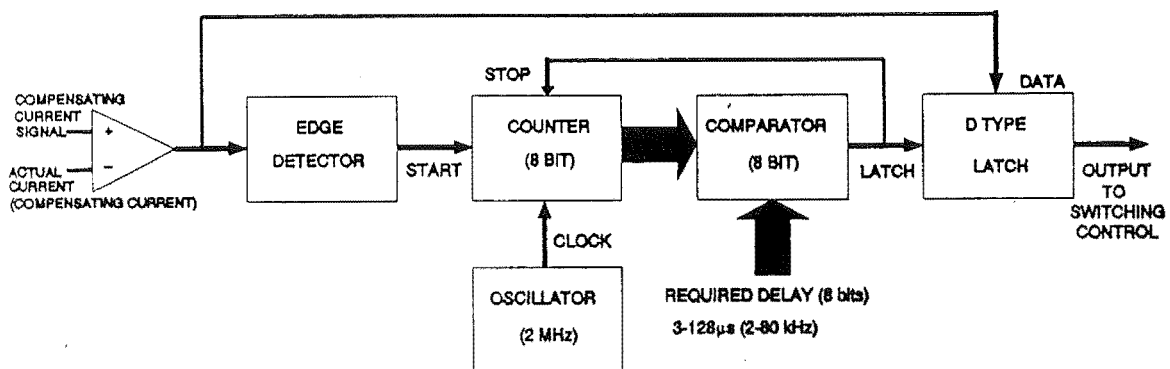


Figure 6.5 Digitally Controlled Time Delay

The fundamental load current's period is determined by band-pass filtering the load current, monitoring the zero crossings with a zero crossing detector (ZCD) and sending an interrupt to the TMS320C30 (Figure 6.1). This enables the digital controller to determine the fundamental power factor (displacement angle) from the fundamental load current's relationship with the supply voltage.

The various signals that are measured and generated by the digital controller exist at different levels of potential. To transfer signal information between devices, such as the ADCs, TMS320C30 and Digital to Analogue Converters (DACs), isolation between devices is important. These different levels of potential exist because in a digital system the ideal location for the ADCs and DACs is at the source or output of the signal. For example, the load current ADC measures the load current directly at the supply potential (Figure 6.2), while the DC bus voltage ADC is referenced to the zero voltage side of the power amplifier bus capacitors. Isolation is provided by opto-isolation devices (opto-couplers) for all the input and output signals to the TMS320C30 with the data being transmitted across this isolation barrier in a serial format. Using a serial data format minimises the number of opto-couplers required to transfer the information. The load current ADC and compensation current DAC are connected via opto-couplers to the serial port of the TMS320C30.

The power amplifier is of similar construction to the analogue controlled power

amplifier described in Section 4.1.2. The output of the time delay is split into two signals, each to control the diagonally opposite pairs of IGBT transistors in the H bridge arrangement. The rating of the IGBT transistors used in the digitally controlled active filter is increased to 1200 V, 25 A modules to utilise the full capability of the reinjection transformer.

The TMS320C30 card has a connection to an IBM compatible PC (Figure 6.1). The PC enables the operator to manually control the operation of the active filter and to operate the active filter in an automatic data collection or a self optimising mode. The PC based system allows the active filter's performance data (THD values, total power factor, efficiency) and operational status (average switching frequency, bus voltage, fault status) to be displayed on the PC with automatic recording of that performance data. In addition, it provides a platform for the software development for the TMS320C30 based active filter controller.

6.3 SOFTWARE DESCRIPTION

This section discusses the software implementation of the digital controller. The software to control the active filter can be divided into two types, interrupt and non interrupt functions. The interrupt functions process events such as measuring the load current, which must be processed as soon as possible after the event in order for the controller to remain in real time control. The non interrupt functions are background tasks, such as the calculation of efficiency, which are processed when the TMS320C30 has some free time. The majority of the software was written in the high level language C to decrease the time involved in programming. The main interrupt function was initially written and compiled in C and the resulting assembly code was then hand optimised to increase the execution speed.

6.3.1 Interrupt Functions

The real time control routines are all interrupt driven and occur at different rates as detailed by Figure 6.6. The most critical interrupt (Interrupt 1 Figure 6.6) is the generation of the compensating current. This interrupt occurs more frequently than any other interrupt and is given the highest priority since its functionality affects the performance of the active filter and the control routines. If this interrupt occurs while the TMS320C30 is executing a low priority interrupt, the TMS320C30 will give the

processing time to the compensating current interrupt.

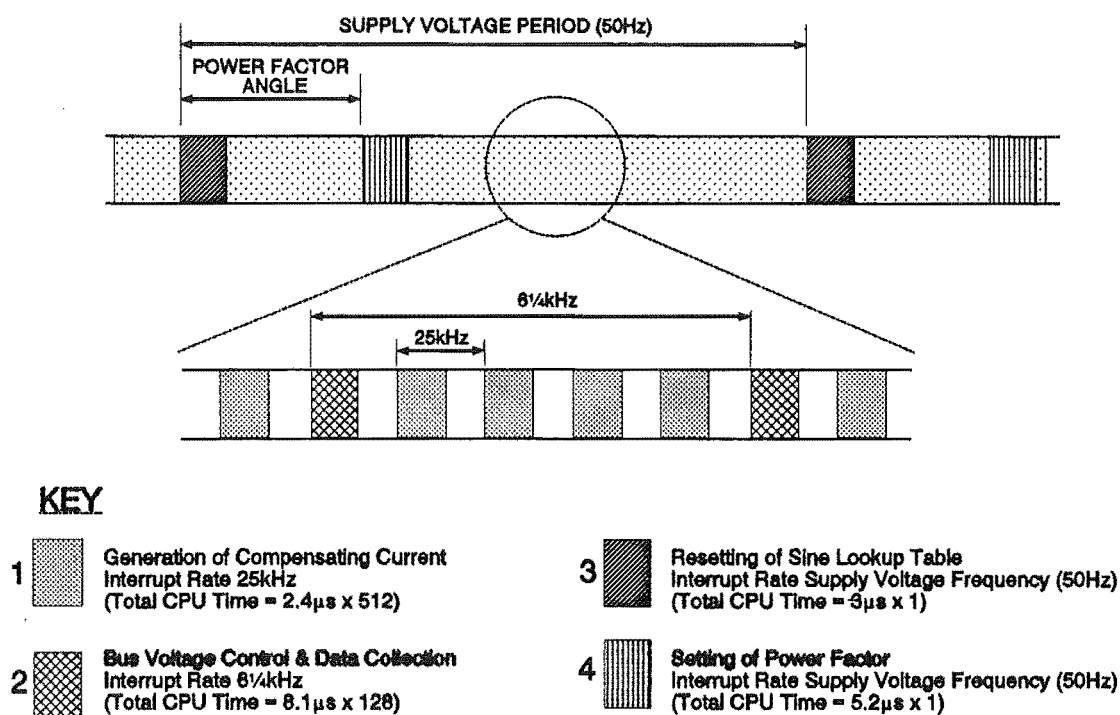


Figure 6.6 Interrupt Timing of TMS320C30

To generate the compensating current the timer which determines the sample rate sends a signal to the load current ADC to start the conversion process. The data is then loaded by the ADC into the serial port register of the TMS320C30. Once the load current sample is loaded, the TMS320C30 then sets an internal interrupt indicating the serial port data is ready. A software interrupt routine is executed and the load current sample is read by the software. A synthetic sinusoid is then subtracted from the load current to produce the compensating current signal. This synthetic sinusoid is stored in a look-up table. A table pointer variable keeps track of the position of the sinusoid in the look-up table. Depending on whether the active filter is performing any displacement compensation the look-up table position can be modified. The value of the sinusoid at that table position is extracted and multiplied by a magnitude value. This magnitude value is generated by the user (manual adjustment mode) or by the bus voltage controller (Section 6.5.1). The generated sinusoid is then subtracted from the load current value resulting in the compensating current signal. This compensating current sample is written to the output of the serial port. When the next sample from the load current ADC is being transferred into the TMS320C30 the compensating current signal will be sent out to the DAC. At the end of the interrupt routine the pointer value to the

table position is incremented by one. This is the most frequent interrupt as it occurs at a rate of 25.4 kHz and consumes 6.1% of the TMS320C30 processing time every fundamental period.

The next most frequent interrupt (Interrupt 2 Figure 6.6) occurs at a rate of 6.4 kHz. This interrupt executes a function which implements a proportional-integral (PI) bus voltage controller and is discussed in more detail in Section 6.5.1. The interrupt procedure is initiated by an external interrupt, indicating that the output of the DC bus voltage ADC has been converted from the serial to parallel format. The interrupt routine reads in the DC bus voltage value, compares it to the set DC bus voltage level and produces an error signal. A new level of magnitude for the fundamental sinusoid is calculated from the gain, error and integral values. The integral value is then updated using the error signal and the sampling rate.

During interrupt 2 (Figure 6.6) data is collected for the calculation of efficiency, THD and RMS values. The supply current, supply voltage and load current values are read from the appropriate ADCs and converted from offset binary and two's complement representation into the TMS320C30 floating-point format. This information is then stored in three separate data blocks for later processing. After the data collection has been performed, a value is written to the digital time delay to set the average switching frequency.

The final two interrupts both operate at the low rate of once every fundamental period. Interrupt 3 (Figure 6.6) is synchronised with the supply voltage fundamental. This interrupt adjusts the sample rate of the system and resets the pointer to the sine look-up table position. Both these operations keep the active filter synchronised to the supply fundamental. The sample rate multiplier operates by determining the number of samples measured between exiting the last interrupt 3 and entering the present interrupt 3 function. If the number of samples is less than 512 then the sample rate is increased in proportion to the difference and with a number of samples greater than 512 the sample rate is decreased accordingly. A small amount of hysteresis is added to stop the system from continually shifting around 512 samples for small changes in frequency. The accuracy of the sample rate multiplier is limited by the resolution of the internal timer. The TMS320C30's internal timer has a resolution of 120 ns which enables the time between samples to be shifted in steps of 120 ns. If the time between samples is increased by 120 ns and 512 samples are placed in one fundamental period, the sample rate multiplier can track changes of 0.15 Hz for a 50 Hz fundamental frequency.

Interrupt 4 (Figure 6.6) records the displacement power factor of the load current

by calculating the number of samples measured (number of times interrupt 1 has occurred) since the supply voltage interrupt (Interrupt 3). Knowing the time between samples allows the system to calculate the actual number of degrees of phase shift between the fundamental supply voltage and current. This routine also sets the displacement power factor correction angle. Via the PC, the user enters a required displacement power factor to be achieved. The sine look-up table pointer is then offset by this value. The system allows the user to adjust the power factor to any value from 90 degrees leading to 90 degrees lagging. Depending on the energy requirements for compensation, the system may not be able to fully compensate for the distortion due to a low DC bus voltage (Section 4.1.1.2).

6.3.2 Non Interrupt Functions

The main operations outside the interrupt functions are the calculation of efficiency and THD. The supply voltage, supply current and load current information is passed to the FFT routine once 128 samples have been collected. A 128 point real radix-2 FFT optimised for the TMS320C30 is implemented to calculate the frequency components [Tessarolo 1991]. The three FFT's are calculated within 18 ms over two fundamental cycles. The THD of the inputs are calculated using Equ. (1.1) from the magnitude result of each FFT. The efficiency is obtained by dividing the fundamental load current's magnitude by the fundamental of the supply current's magnitude and taking into account the displacement factor between them (according to Equ. (5.1)).

Signals measured from any real source are likely to contain both systematic and random variations [Arrillaga et al. 1985]. To smooth out any variations in the measured efficiency, THD and RMS results an averaging function is implemented. The previous five values of each of the measurements are stored in a rotating array and the average is updated after every measurement. The average information of all the signals is then passed back to the PC for display and to the automatic optimal control function which implements the optimisation algorithms described in Chapter 7.

Two other functions performed by the digital controller are the routines to control the starting and stopping of the active filter and any decoding of fault information. The start and stop routines can be initiated by the operator's instructions. The fault routine monitors the output of the hardware fault detection unit. The hardware fault detection unit automatically stops the active filter if a fault such as overvoltage or overcurrent is detected. This function is implemented in hardware to provide the system with the fastest

possible response. The software detects which fault has occurred and informs the operator on the PC of the particular fault. These non critical functions including the automatic control function consume the remaining free time of the TMS320C30.

6.4 STEADY STATE PERFORMANCE

The performance of the digitally controlled active filter is determined by how well the system can reduce the harmonics of the load current. The load current, shown in Figure 6.7(a), is produced by a bridge rectifier, capacitor and resistor drawing $7.5 A_{RMS}$ in parallel with a resistive load of $5.3 A_{RMS}$. The load current has a THD of 36.9%, measured up to 1050 Hz, and the peak current is $24.8 A_{RMS}$. When the active filter is operating the supply current is turned into a nearly sinusoidal current with a THD of 5.3% (Figure 6.7(b)). The overall RMS current level of the supply has been reduced to $12.4 A_{RMS}$ and the peak current is now only $18.2 A_{RMS}$. Figures 6.7(c) and (d) show the supply voltage ($240 V_{RMS}$) and the compensating current respectively. The measured compensating current is $5.4 A_{RMS}$ on the supply side of the reinjection transformer.

The spectra of the load and supply currents are detailed in Figures 6.7(e) and (f) respectively, with the third harmonic of the load current only 9.0 dBV below the fundamental (35% of the fundamental). The supply current third harmonic is reduced to 27.9 dBV below the fundamental (4% of the fundamental).

These results were taken with the DC bus voltage set at 242 V and an average switching frequency of 22 kHz. The operating efficiency of the active filter was 94.8% and the power factor (distortion and displacement components) increased from 0.922 to 0.992.

6.5 TRANSIENT PERFORMANCE

The transient performance of the digitally controlled active filter is determined by how well the system maintains the compensation of the supply current during a load change. Compensation ability is primarily dependent on the amount of energy stored in the bus capacitor of the active filter. When a sudden load current increase occurs, the active filter has to supply the additional harmonic components and these extra harmonic components are created from the energy stored in the DC bus capacitor. Since the real power flow into the active filter does not rise instantly in response to the falling energy level, the voltage on the DC bus capacitors falls. If the voltage falls too far then the

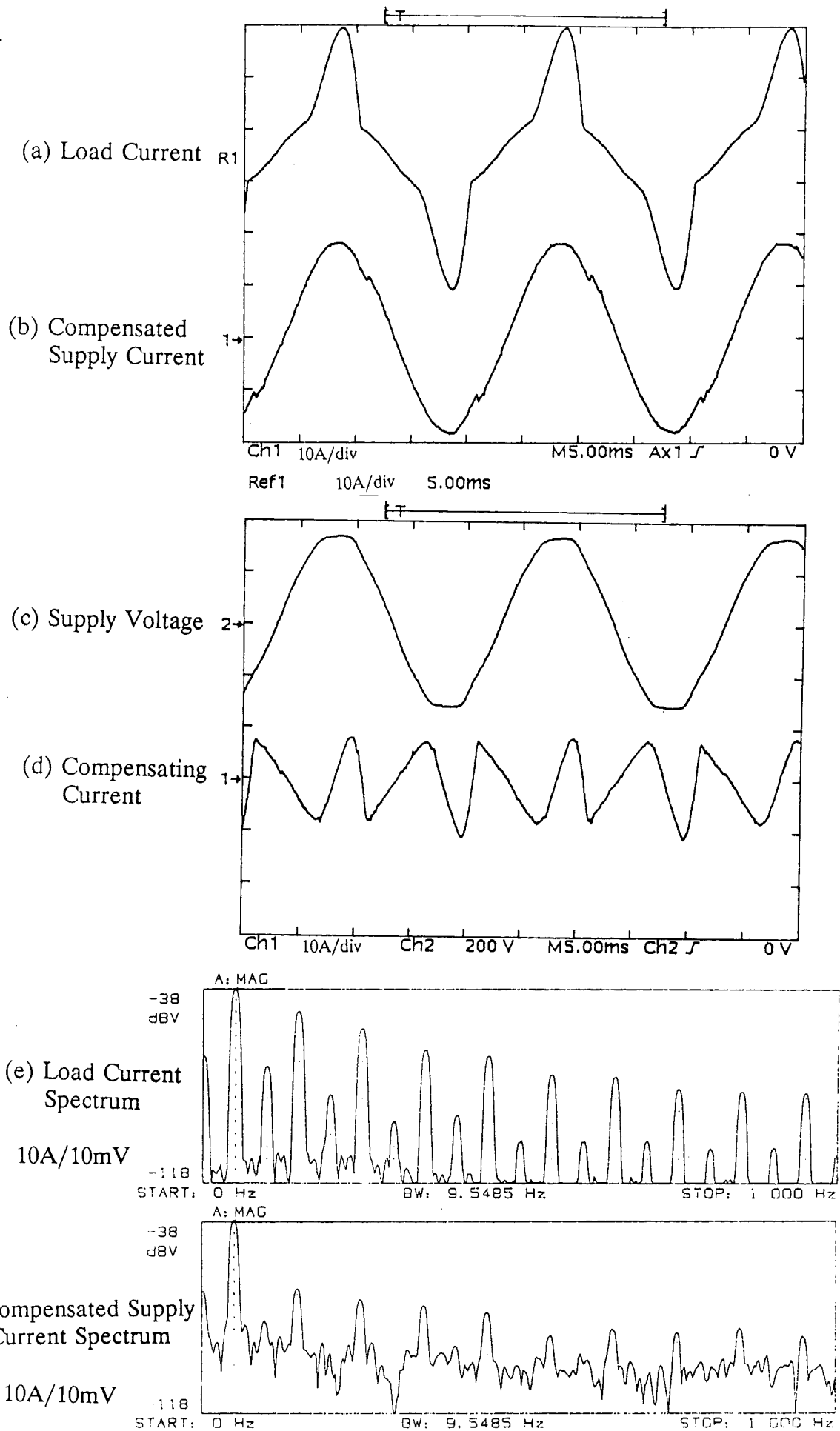


Figure 6.7 Operational Performance of the Digitally Controlled Active Filter

active filter cannot fully compensate since the voltage on the DC bus capacitors is not sufficient to inject current against the instantaneous supply voltage (Section 4.1.1.2). Therefore full compensation is not possible until the voltage (energy stored) on the DC bus capacitors increases.

6.5.1 Bus Voltage Control

To provide complete compensation, the system requires a fast controller to monitor the voltage level on the bus capacitors and to adjust the real power flow (magnitude of reference sinusoid) into the active filter to maintain a set voltage.

A proportional plus integral (PI) controller is used to adjust the real power flow since it is not as sensitive to noise corrupting the bus voltage signal as a proportional plus integral plus derivative (PID) controller. The derivative term in the PID controller can accentuate the noise on the bus voltage signal causing glitching in the output of the controller [Astrom et al. 1984]. Figure 6.8 details the implementation of the PI controller in the active filter system.

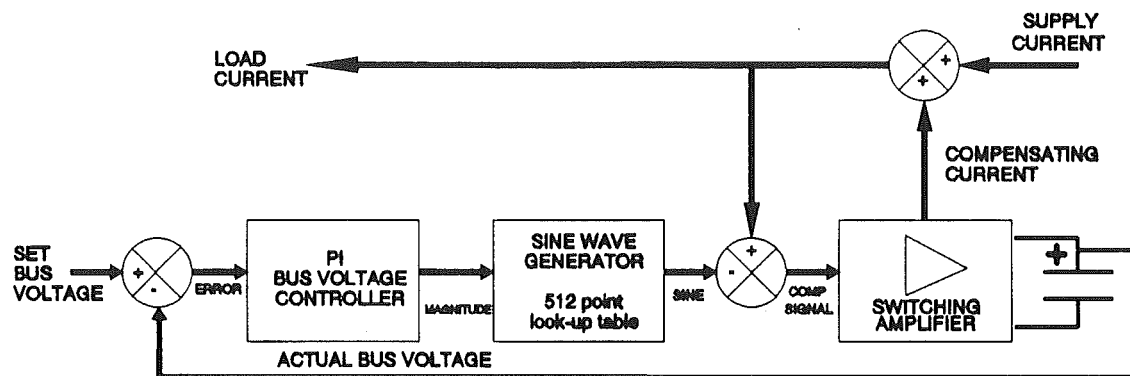


Figure 6.8 Implementation of PI Bus Voltage Controller

The voltage on the DC bus voltage capacitors is monitored and an error signal is produced from the difference between the actual bus voltage and the set bus voltage value. Using the error signal the PI controller outputs a magnitude level which is then used to produce the reference sinusoid and compensating current signal. The compensating current signal is converted by the power amplifier into the compensating current which is injected into the supply, making the supply current nearly sinusoidal. The voltage on the capacitors is controlled by the magnitude of the synthetic sinusoid, which in turn controls the real power flow into the active filter.

The PI controller is implemented in the digital domain using the following form [Astrom et al. 1984]:

$$u(kh) = K_c e(kh) + i(kh) \quad (6.1)$$

$$e(kh) = y_r - y(kh) \quad (6.2)$$

$$i(kh+h) = i(kh) + e(kh) \frac{h}{T_i} \quad (6.3)$$

where h = sampling period
 y_r = set point
 y = measured output
 k = integer sample number

The output of the controller (u) in Equ. (6.1) uses the error signal e , the difference between the set reference bus voltage and measured bus voltage (Equ. (6.2)) and the integral value i . The integral equation (Equ. (6.3)) calculates the next value from the previous integral value and a portion of the error signal which is dependent on the integral time constant T_i . From Equ. (6.1) and Equ. (6.3) there are two adjustable parameters, the gain K_c and the integral time constant T_i . These parameters control the response of the PI controller. To determine the gain and time constant, the Ziegler-Nichols closed loop tuning rules were implemented. The Ziegler-Nichols tuning method is widely known for determining good settings of PID and PI controllers for a wide range of common processes [Hang, Astrom, Ho 1991]. The method involves increasing the gain until the system is on the verge of instability. This gain value is called the ultimate gain K_u , and the period of oscillation is called the ultimate period T_u [Gatland 1992]. The proportional gain K_c and integral time constant T_i are then determined for a PI controller from Table 6.1 [Hang et al. 1991, Astrom et al. 1984].

TABLE 6.1 Ziegler-Nichols Tuning Formula

CONTROLLER	P	PI	PID
Proportional Gain	$K_c = 0.5K_u$	$K_c = 0.45K_u$	$K_c = 0.6K_u$
Integral Time		$T_i = 0.85T_u$	$T_i = 0.5T_u$
Derivative Time			$T_d = 0.125T_u$

The gain in the bus voltage controller was increased until the system went unstable at a proportional gain of 5 ($K_p = 5$). At this level of gain the ultimate period was measured at 20 ms. From the rules in Table 6.1 the gain K_c was set to 2.25 and the integral time constant T_i at 17 ms. These tuning rules are only a first approximation, so the final tuning has to be done manually [Astrom et al. 1984].

To manually adjust the PI controller, the gain K_c is kept constant and the integral time constant T_i adjusted. The active filter's performance is compared for different values of time constant by monitoring the system's response to a step change in load current. The load current consists of a base resistive load of 2.3 A_{RMS} and a bridge rectifier, capacitive and resistive load of 2.7 A_{RMS}. The step increase in load current is produced by the bridge rectifier component of the load being increased to 5.9 A_{RMS}. Figure 6.9 shows the bus voltage and supply current for a load increase from 5.0 A_{RMS} to 8.2 A_{RMS} for various values of T_i . Figure 6.9(a) shows the case where T_i is 17 ms. The bus voltage had reached the reference level of 242 V in 70 ms, while the supply current became sinusoidal within 50 ms. In Figure 6.9(b) T_i was set to 10 ms, the bus voltage now reaches the reference of 242 V in 40 ms with some overshoot and the supply current is sinusoidal within 30 ms. Figure 6.9(c) shows the case where T_i is 5 ms, the bus voltage reaches the reference in 20 ms, but overshoots and oscillates for 120 ms, while the supply current is sinusoidal within 10 ms.

It can be seen from the results shown in Figure 6.9 that a lower T_i will make the system respond more quickly. However, another test to consider is the startup transient of the system. Figures 6.10(a) and (b) show the startup transients for time constants of 10 ms and 5 ms respectively. For a 10 ms time constant the overshoot in bus voltage is only 10 V and the bus voltage stabilises within 100 ms, however with a time constant of 5 ms the overshoot is now 50 V and the system takes longer (greater than 200 ms) to stabilise.

Throughout these tests, the gain remained fixed at 2.25 (set by the gain given in Table 6.1), while the time constant was adjusted for the step and startup tests. Increasing the gain could result in the system becoming unstable. Considering the startup and step load change response of the active filter system a gain of 2.25 and an integral time constant of 10 ms was chosen as the parameters of the PI controller.

A potential problem can exist due to the connection of the compensating current in the control loop (Figure 6.8). If the magnitude of the synthetic sinusoid being generated is being continuously varied by the PI controller the supply current can be contaminated by sub-harmonics. These sub-harmonics may cause problems in the case

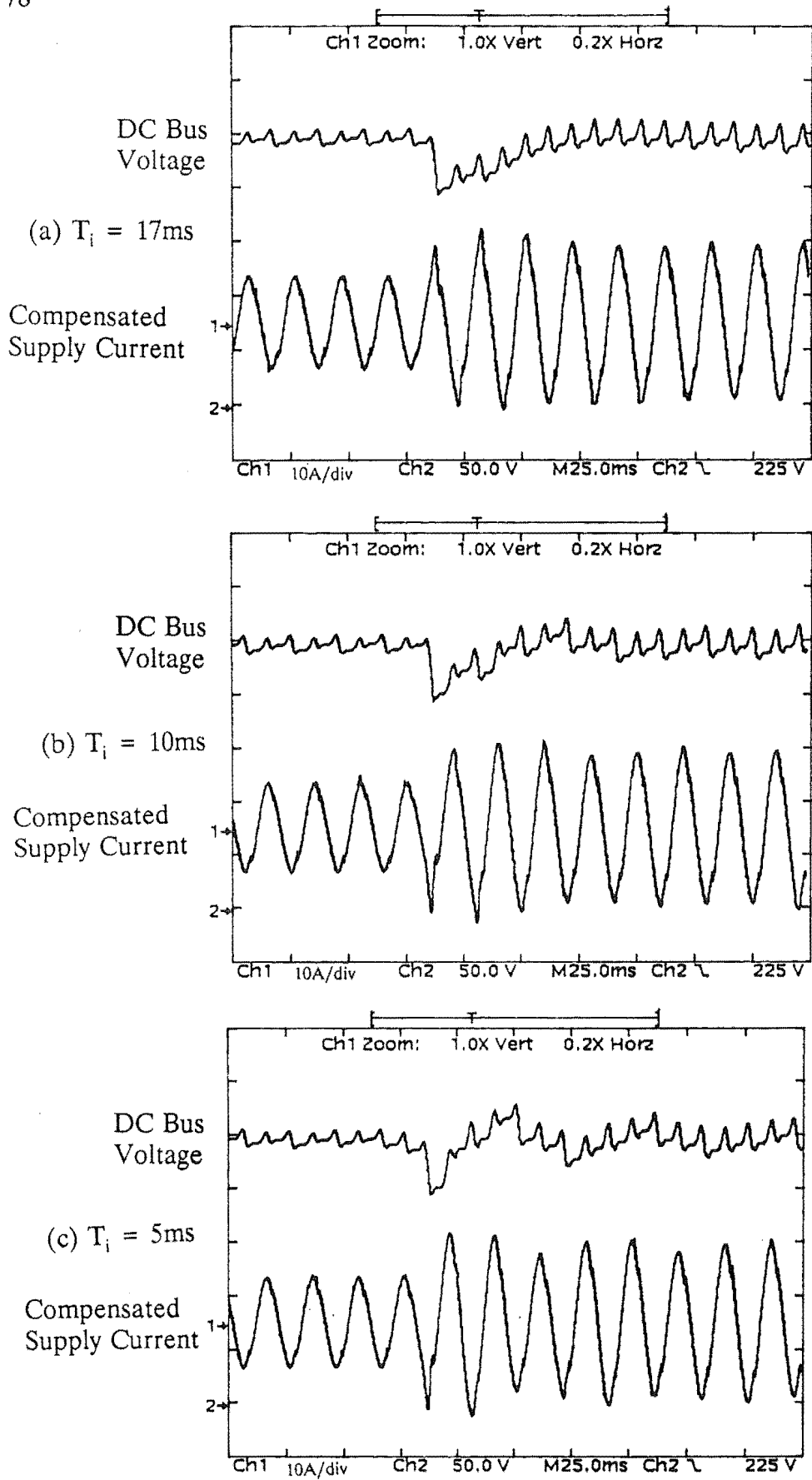


Figure 6.9 PI Controller Response to Different Integral Time Constants

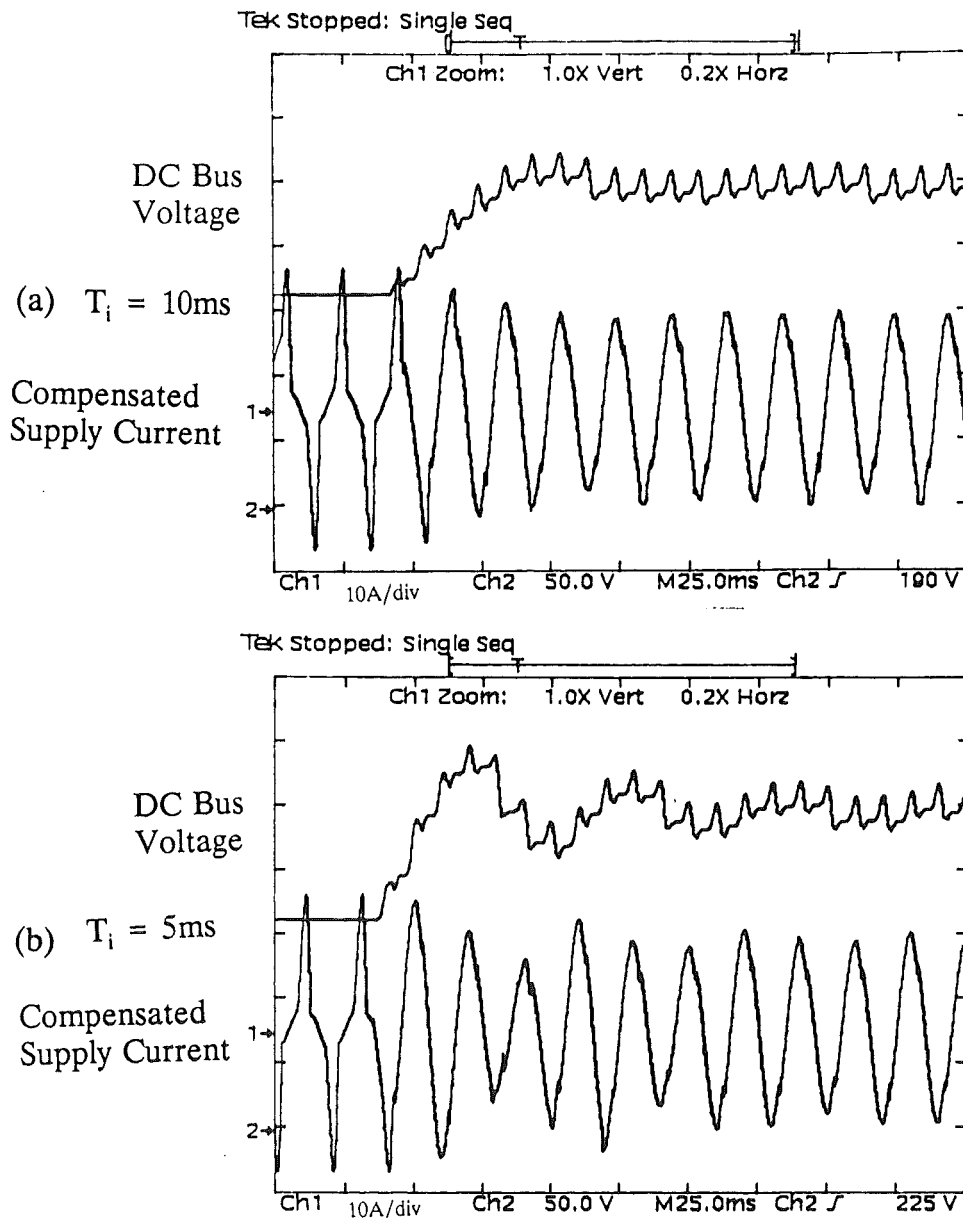
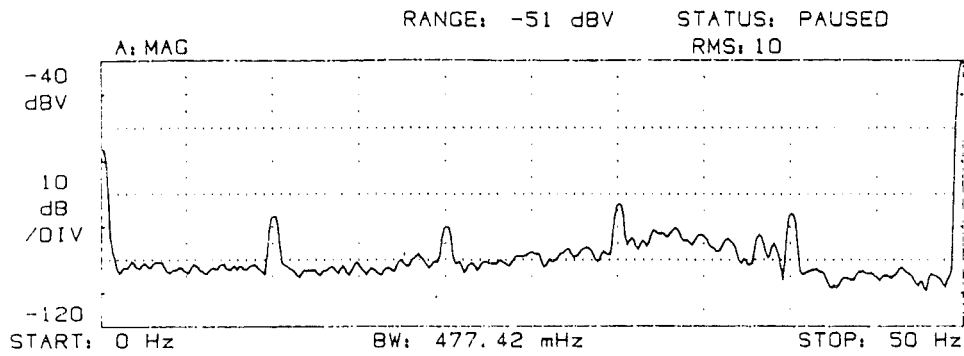
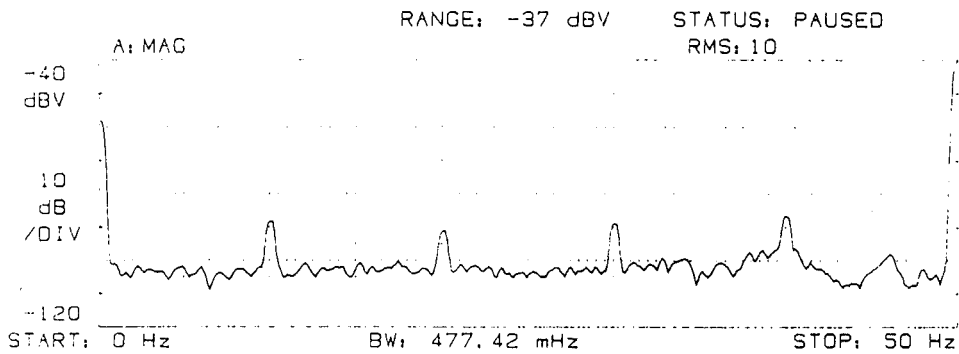


Figure 6.10 Startup Transient of PI Controller

of a weak power system where the supply current is sufficiently large to effect the supply voltage. Sub-harmonics on the supply voltage may be seen in lighting load as flickering [Shepherd, Hulley 1987]. Figures 6.11(a) and (b) show the difference in sub-harmonics for time constants of 5 ms and 17 ms. For a time constant of 5 ms the total magnitude of sub-harmonics compared to the fundamental is 1.04% compared to 0.78% for 17 ms. Thus by increasing the time constant the production of sub-harmonics is reduced. If sub-harmonics are a problem a solution could be to use a larger time constant, T_i and add an additional term into the bus voltage control loop to speed up the response of the active filter to load changes.

(a) Supply Current Subharmonics for $T_i = 5\text{ms}$ (b) Supply Current Subharmonics for $T_i = 17\text{ms}$ **Figure 6.11** Sub-harmonics due to PI Controller

6.5.2 Feed-Forward Control

To speed up the control loop for a disturbance such as a load change, the implementation of a feed-forward controller can be considered [Astrom et al. 1984]. The addition of feed-forward control to compensate for load changes can be added between the load current and the input to the sine wave generator as shown in Figure 6.12.

The proposed feed-forward controller measures the load current, detects the change in load current and then modifies the magnitude of the synthetic sinusoid until the slower PI controller is able to fully control the sinusoid magnitude. Figure 6.13 shows in detail the components of the feed-forward controller.

A differentiator is used to detect any load changes. The threshold detector output, o_t , only responds to load changes above a threshold level T_h (initially set to 10% of the maximum load current). An integrator, which is connected to the output of the threshold, integrates the threshold value multiplied by an exponential decay. The effect of the

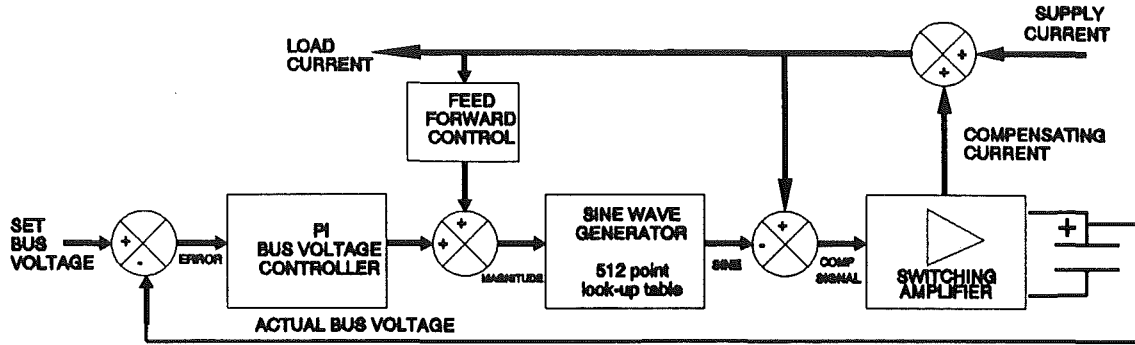


Figure 6.12 Addition of Feed-Forward to Bus Voltage Controller

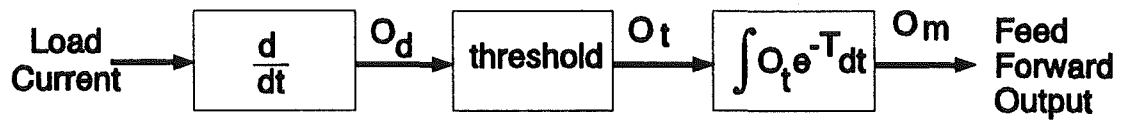


Figure 6.13 Feed-Forward Controller

exponential is for the output of the feed-forward controller o_m , to decay away at a known rate once a steady state has been reached.

The differentiator is implemented as a three tap finite impulse response (FIR) filter [Oppenheim, Schaffer 1989]. Figure 6.14 illustrates the output of the differentiator for a two tap FIR (dashed) and three tap FIR (dotted) filter for a typical single phase distorted load current. Both filters detect the sharp falling edge on the bridge rectifier current when it is in a steady state. Therefore the threshold level T_h , would need to be set to a level greater than the FIR output for the largest load current. The three tap differentiator has the advantage of rejecting the lower frequency components of the load current compared to the two tap differentiator.

The rate at which the feed-forward output decays is set by how fast the PI controller can respond. In Section 6.5.1 the 17 ms time constant of the PI controller responded in 60 ms. Figure 6.15 shows the experimental output of the feed-forward controller due to a step change in load current. Using a decay time of 10 ms the feed-forward output decays away within four to five supply cycles, which is less than the response time of the PI controller.

The operation of the feed-forward controller is simulated using the computer modelling technique as described in Chapter 3. The PI controller parameters in the simulation are set to a gain of 2.25 and a time constant of 17 ms. Figure 6.16 illustrates the bus voltage response due to a step increase in load current using a PI controller and

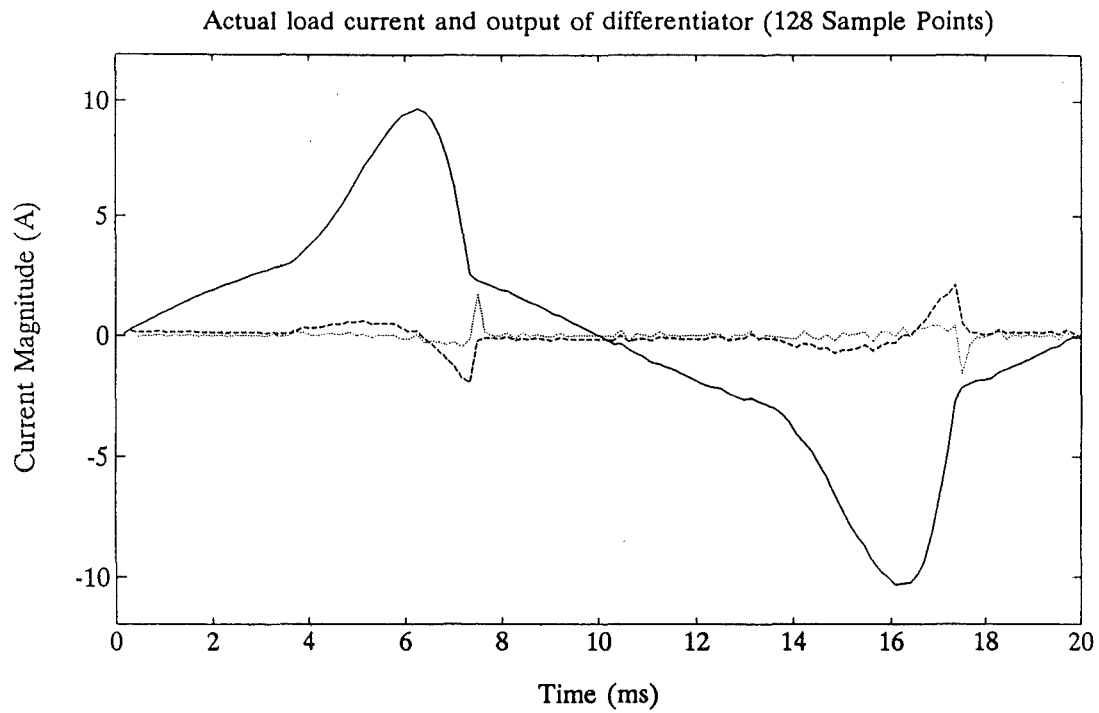


Figure 6.14 Output of Differentiator

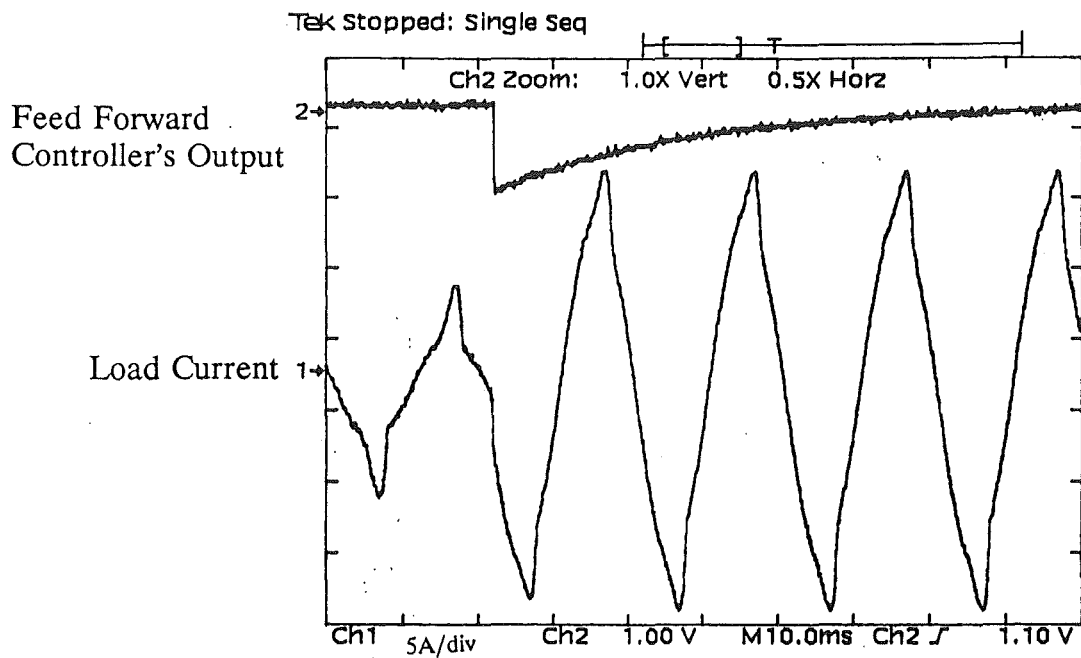


Figure 6.15 Experimental Output of Feed-Forward Controller Due to Step Load Change

PI and feed-forward control (PI+FF). The steady state bus voltage is 240 V_{DC} , the load consisted of a single phase bridge rectifier, capacitor and resistor drawing 13 A_{RMS} and the step increase in load current is 50%.

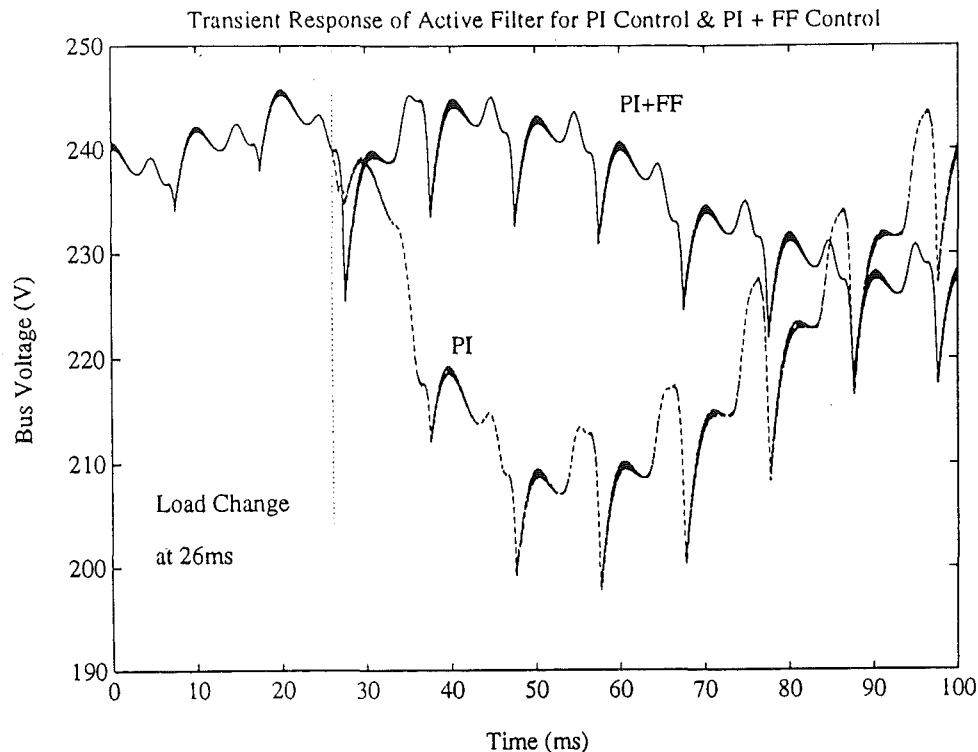


Figure 6.16 Response of Bus Voltage to Feed-Forward & PI and PI Controllers

To maintain compensation with this particular type of load, the bus voltage must be greater than 220 V_{DC} (Section 4.1.1.2). Using the PI controller, once the step increase in load occurs at 26 ms, the bus voltage falls to 205 V_{DC} , then starts to rise again after 40 ms once the integrator term becomes effective. In the case of the PI and feed-forward controller, as soon as the step load increase occurs there is a sudden drop in bus voltage since the system can not instantaneously respond to a load change. The feed-forward controller is however able to maintain the level of bus voltage soon after the initial load change. As the influence of the feed-forward controller decays away the PI portion of the controller becomes more dominant. At no time during the step load change does the bus voltage fall below 220 V_{DC} , thus the active filtering system can maintain full compensation during a 50% step increase in load.

The disadvantage with this implementation of the feed-forward and PI controller is having to use a differentiator to detect the load change. Differentiators can be affected by noise contamination which may cause the system to react when no load change exists. In trying to implement the feed-forward in the digitally controlled active filter it was

discovered that the input to the load current ADC is affected by random amounts of switching noise. This caused the system to operate incorrectly with a feed-forward and PI controller. However, with a robust input signal stage and bandlimited differentiator this contamination of noise could be eliminated and the feed-forward and PI controller made to operate correctly in the digitally controlled active filter.

In the present digitally controlled active filter the control of the bus voltage uses a PI controller which provides a response within two fundamental cycles for a step load change. To improve the response of the active filter to step load changes, the implementation of the PI and feed-forward controller would be worthwhile in future prototypes.

6.6 SUMMARY

This chapter presented the design of a digital controller that will be used to automatically determine an optimum operating point for the active filter. The digital controller is based on a high speed digital signal processor. The digitally controlled active filter uses four 14 bit analogue to digital converters, one 14 bit digital to analogue converter and one 8 bit serial output to control the operation of the active filter. The software is based on interrupt routines in order to maintain the operation of the active filter in real time. Three FFT's are implemented to extract harmonic and efficiency information regarding the operating characteristic of the active filter.

The steady state performance of the digitally controlled active filter was shown to be similar to that of the analogue controlled active filter described in Chapter 5. The transient performance of the active filter using a PI bus voltage controller was demonstrated. The tuning of the PI controller was discussed, resulting in a gain of 2.25 and an integral time constant of 10 ms. This PI controller can respond to step load current changes within two fundamental cycles. A feed-forward modification to the PI controller is proposed and simulated results show an improvement can be made to the active filter's transient response.

CHAPTER 7

OPTIMISATION OF ENERGY SAVINGS

The active filtering system is able to remove harmonic and displacement distortion from the supply current. Such an active filter has commercial benefits for large industrial/commercial installations since electricity charges are calculated by measuring the apparent power (S , kVA) and the amount of real power (P , kW) consumed. For higher levels of current distortion (harmonic and phase displacement) drawn from the supply, for the same real power rating, a higher cost is charged for the energy consumed. If a consumer used the proposed active filter to remove distortion from the supply current, savings in the cost of electricity could be expected to be made as the apparent power consumed would be reduced.

The distortion however can not be removed without the consumption of real power. Therefore a trade-off situation exists between lowering the apparent power demand and the increased real power consumption. Different types and levels of load produce different active filter performance characteristics depending on the level and type of distortion present. By manipulating the power amplifier operating conditions (bus voltage and average switching frequency) of the active filter it is possible to control the system losses and quality of compensation.

By implementing the active filter with a DSP digital controller it is possible to use the computational power to calculate the possible energy savings and make "intelligent" decisions on how to operate the active filter under different conditions. The digitally controlled active filter is able to provide automatic optimisation of the energy savings of the system.

The cost of drawing distortion from the supply and the possible savings by active filtering are derived in Section 7.1. The effect of an energy cost ratio, which is the ratio of charge for real power to the charge for apparent power, on the possible savings is shown. Section 7.2 details the possible savings for active filtering and demonstrates the use of a direct optimisation algorithm to determine the point of maximum savings. Results of the optimisation search for the maximum savings point during steady state and transient conditions are shown in Section 7.3. The ability of the active filter to provide fundamental power factor correction is incorporated into the savings optimisation search in Section 7.4.

7.1 COST FUNCTION

To be able to optimise the performance of the active filter, a relationship between the various operating conditions must exist. Figure 7.1 illustrates the relationship between the bus voltage and average switching frequency in terms of the active filter's efficiency and ability to reduce the supply current THD. The single phase distortive load consists of a bridge rectifier, capacitor and resistor combination drawing a load current of $7.2 A_{RMS}$ with a THD of 78.0%. This particular single phase bridge rectifier combination is the load used to obtain the results presented in Sections 7.1, 7.2 and 7.3.

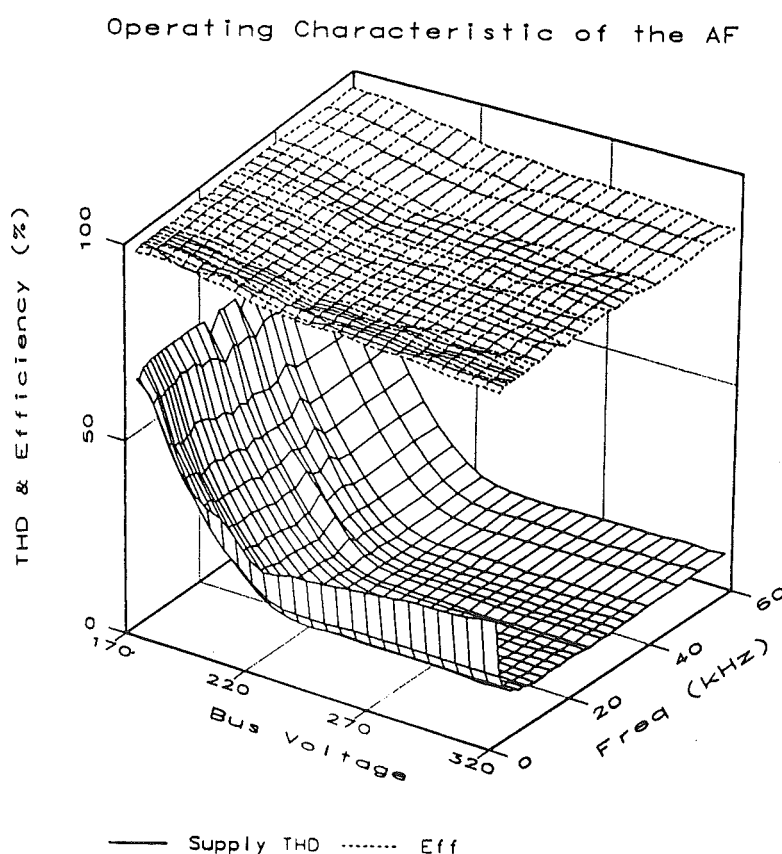


Figure 7.1 Operating Characteristic of the Active Filter

As illustrated by Figure 7.1, increasing the bus voltage and the average switching frequency further reduces the supply current THD, however the efficiency of active filtering decreases. It should be possible to optimise the operating conditions of bus voltage and average switching frequency with the aim to minimise the supply current THD while maximising the efficiency. This idea can be implemented by a penalty function as defined in Equ. (7.1) [Converse 1970, Beightler, Phillips, Wilde 1979].

$$\text{Max. : } L(X) = f(X) + \lambda g(X) \quad (7.1)$$

X

Using Equ. (7.1), $f(X)$ can be defined as the surface of efficiency for the two dimensional vector X of bus voltage and switching frequency and $g(X)$ as the surface of supply current THD. To be able to maximise a penalty surface $L(X)$, which is produced from the efficiency and supply current THD surfaces, a penalty constant of λ must be determined. This weighting constant λ , penalises the surface $L(X)$ depending on the level of supply THD. A disadvantage with this penalty function method for optimising the active filter's operation is that it is difficult to produce a suitable weighting constant. If the weighting constant is too large then the penalty function is biased more to reducing the level of supply current THD than to maximising the efficiency.

An alternative approach is to derive a cost function which describes the operation of the active filter in terms of the actual financial cost of electricity consumption.

7.1.1 Derivation of the Cost Function

It is possible to develop a function which is based on the monetary costs of electricity consumption of the load and supply by active filtering. Using these two costs a savings calculation, defined as the difference between the charge for the energy consumed before and after the process of active filtering, can be determined. The optimisation system can then use this savings function to determine the most economic operating point. To determine the cost before and after active filtering the definitions of power flow are considered. Figure 7.2 defines the power flow for the two cases of no active filtering (a) and active filtering (b).

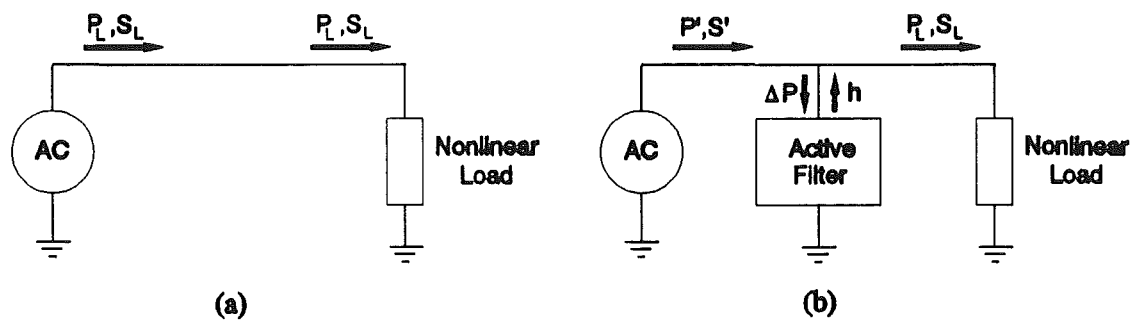


Figure 7.2 Definition of Power Flow (a) No Active Filtering (b) Active Filtering

To determine the cost functions, the definition of power factor and the real to apparent power cost ratio must be defined. Power factor is defined in Equ. (7.2) as the ratio of real power to apparent power consumed.

$$\text{pf} = \frac{P}{S} = \frac{\text{real power}}{\text{apparent power}} \quad (7.2)$$

In order to determine the cost function, the actual charge for electricity consumed must be considered. The energy cost ratio (R_c) is defined in Equ. (7.3) as the ratio of the charge for real power ($\text{Chg}(P)$) to the charge for apparent power ($\text{Chg}(S)$) at some common time rate.

$$R_c = \frac{\text{Chg}(P)}{\text{Chg}(S)} \quad (7.3)$$

Electrical energy consumed in New Zealand is charged depending on the type of consumer. For domestic and small businesses, the charge is based only on the real power (P) consumed per hour (kWh). Large industrial/commercial consumer charges are based on the real power and the peak demand apparent power consumed. For a constant load this peak demand apparent power (S) can be converted into an hourly rate (kVAh). For the current New Zealand charging structure, real power is typically worth approximately five times that of apparent power, giving $R_c = 5$ [Southpower 1991].

For the case where no active filtering is taking place, the cost to the industrial/commercial consumer for a load (P_L, S_L) is defined by the cost function C_{NAF} (Equ. (7.4)), where $\text{pf}_{\text{NAF}} = P_L/S_L$.

$$\begin{aligned} C_{\text{NAF}} &= P_L \text{Chg}(P) + S_L \text{Chg}(S) \\ &= P_L \text{Chg}(P) \left(1 + \frac{1}{R_c \text{pf}_{\text{NAF}}} \right) \end{aligned} \quad (7.4)$$

The extra power (ΔP) the active filter consumes depends on the actual amount of compensation it is providing and the operational efficiency (ζ) of the filter. From the definition of efficiency (Equ. (5.1)), this extra power is given by Equ. (7.5).

$$\Delta P = P_L \left(\frac{1-\zeta}{\zeta} \right) \quad (7.5)$$

When the active filtering is included, with the same nonlinear load, the kVA level at the point of supply has now changed to S' and the real power consumption from the system has increased to P' , resulting in a new cost function C_{AF} (Equ. (7.6)), where $pf_{AF} = P'/S'$.

$$\begin{aligned}
 C_{AF} &= P' \text{Chg}(P) + S' \text{Chg}(S) \\
 &= (P_L + \Delta P) \text{Chg}(P) + \frac{(P_L + \Delta P)}{R_c pf_{AF}} \text{Chg}(P) \\
 &= P_L \text{Chg}(P) \left(1 + \left(\frac{1-\zeta}{\zeta} \right) + \frac{1}{R_c pf_{AF}} + \left(\frac{1-\zeta}{\zeta} \right) \right)
 \end{aligned} \tag{7.6}$$

The savings (SAV) made from active filtering are defined as the difference between the cost of no active filtering (C_{NAF}) and the cost of active filtering (C_{AF}) as given in Equ. (7.7).

$$\begin{aligned}
 SAV &= C_{NAF} - C_{AF} \\
 &= P_L \text{Chg}(P) \left(\frac{1}{R_c pf_{NAF}} - \frac{1}{R_c pf_{AF}} - \left(\frac{1-\zeta}{\zeta} \right) \left(1 + \frac{1}{R_c pf_{AF}} \right) \right)
 \end{aligned} \tag{7.7}$$

By expressing the savings made relative to the cost of operating the load without active filtering (Equ. (7.8)), it is possible to remove the dependency on the real power consumed by the load (P_L) and the charge for that power ($\text{Chg}(P)$).

$$SAV_R = \frac{\frac{1}{R_c pf_{NAF}} - \frac{1}{R_c pf_{AF}} - \left(\frac{1-\zeta}{\zeta} \right) \left(1 + \frac{1}{R_c pf_{AF}} \right)}{1 + \frac{1}{R_c pf_{NAF}}} \times 100 \text{ (\%)} \tag{7.8}$$

In the special case where the supply voltage is sinusoidal, the power factor can be defined in terms of the displacement ($\cos\theta$) and distortion (μ) factors as in Equ. (7.9) [Arrillaga et al. 1985, Duke, Round 1990].

$$\begin{aligned}
 pf &= \mu \cos\theta \\
 \text{where } \mu &= \frac{I_{FUND}}{I_{RMS}} = \frac{1}{\sqrt{1 + THD^2}}
 \end{aligned} \tag{7.9}$$

The percentage savings can now be expressed in terms of current THD and fundamental phase displacement as in Equ. (7.10).

$$SAV_R = \frac{\frac{\sqrt{1 + THD_{NAF}^2}}{R_c \cos \theta_{NAF}} - \frac{\sqrt{1 + THD_{AF}^2}}{R_c \cos \theta_{AF}} - \left(\frac{1 - \zeta}{\zeta} \right) \left(1 + \frac{\sqrt{1 + THD_{AF}^2}}{R_c \cos \theta_{AF}} \right)}{1 + \frac{\sqrt{1 + THD_{NAF}^2}}{R_c \cos \theta_{NAF}}} \times 100 (\%) \quad (7.10)$$

From Equ. (7.8) and (7.10) the energy savings can be calculated from the efficiency, energy cost ratio, total power factor, current THD and phase displacement angle of the load and the supply. Using the efficiency and THD information in Figure 7.1 and a cost ratio of five (present New Zealand ratio) the possible savings for a single phase bridge rectifier load are given in Figure 7.3.

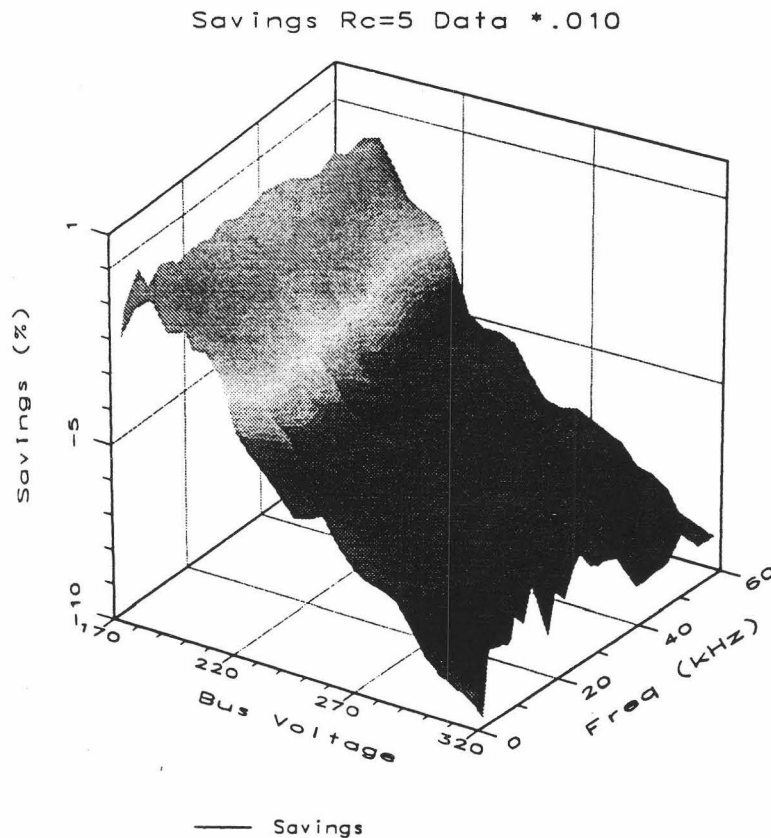


Figure 7.3 Energy Savings Gained by Active Filtering

The maximum savings point in Figure 7.3 has a value of 0.2% at a bus voltage of 189 V and an average switching frequency of 5 kHz. At this maximum point the supply current THD is 41.2%, compared to the load current THD of 78.0%, and the active filtering system has an operating efficiency of 97.3%. The supply current THD reduction is not significant due to the high value of the energy cost ratio. A larger energy cost ratio occurs when the real power is worth more than the equivalent apparent power. With the operation of the active filter with this high cost ratio, an increase in real power consumption (lower efficiency) has a greater reduction in savings than the increase due to the reduction in the distortion component. The influence of the energy cost ratio on the possible savings available from active filtering is investigated in the next section.

7.1.2 Energy Cost Ratio

Since the energy cost ratio affects the cost of energy to the consumer it has a profound influence over the level of savings achievable by active filtering. By changing the energy cost ratio, an additional cost can be added to penalise the consumer for distortion power consumed. The distortion (harmonic and/or displacement) only affects the apparent power and not the real power components, the minimum cost for drawing a distorted load occurs when only kWh are charged for. The maximum cost to the consumer, on the otherhand, is when kVAh is the only charge for electricity consumed. Figure 7.4(a) shows the additional cost to the consumer drawing a distorted load for different charging schemes. As shown there is no additional charge for distortion when only real power (kWh) is charged for. However if only kVAh is charged for, the additional cost of distortion rises quite quickly as THD increases.

Included in Figure 7.4(a) is the additional cost of distortion for charging schemes when the energy cost ratio is five (R5) and one (R1). There is very little difference between the three active filter operating costs (AF Costs) since the additional cost of power consumed to operate the active filter is small. The operating costs of the active filter were based on an efficiency of 95%, losses assumed proportional to the square root of the load THD and the supply current THD being reduced to 5%.

Figure 7.4(b) illustrates the financial savings to the consumer by active filtering. When the charge is solely for kWh consumed, operation of the active filter costs the consumer money as the energy charge is based on the additional real power consumed and not for the reduction in kVA. As can be seen, the greatest savings occur when the consumer is charged for kVAh as the cost of the real power for active filtering is small

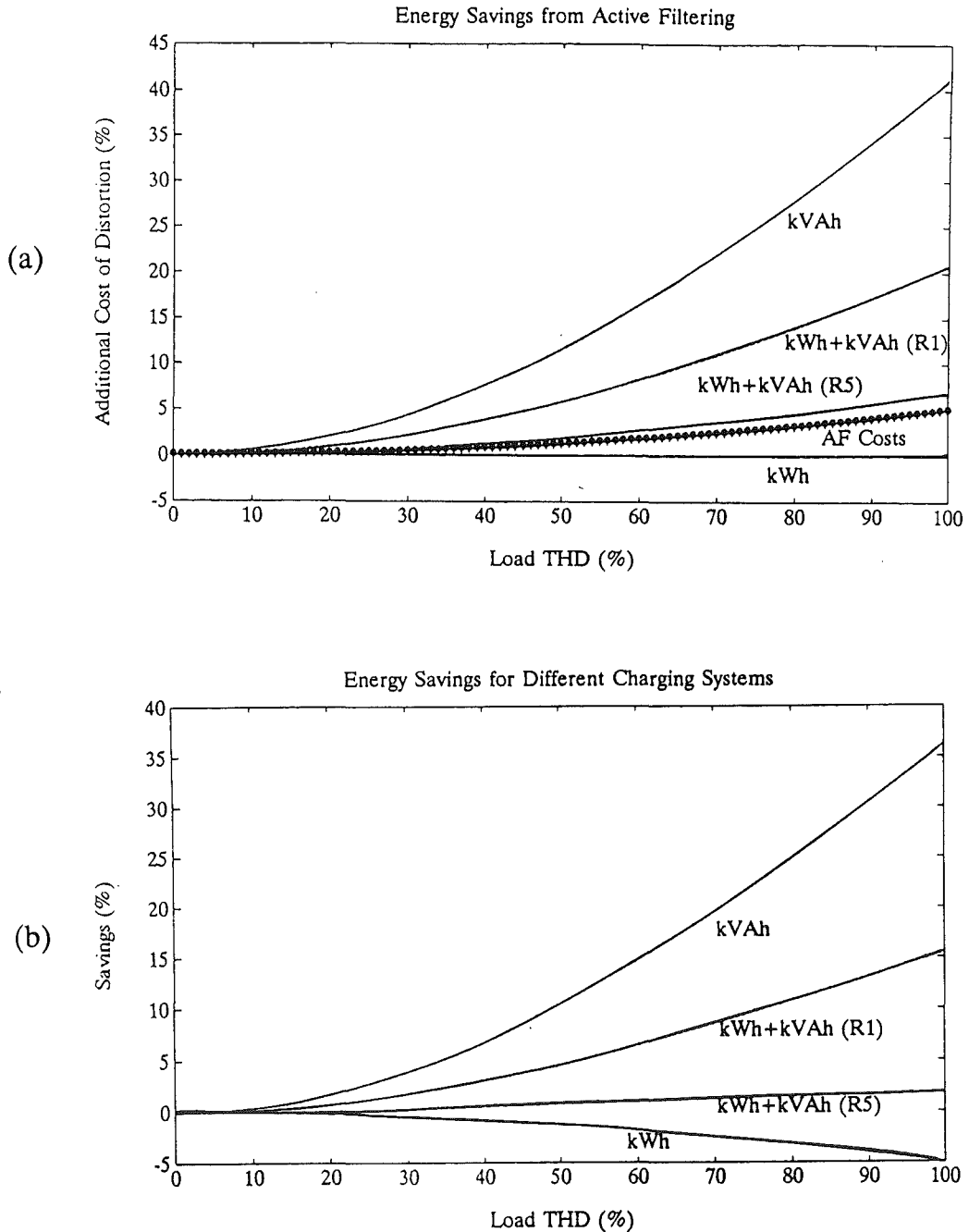


Figure 7.4 Effect of Harmonic Distortion on Energy Cost

compared to the saving in reducing the kVA. Figures 7.4(a) and (b) show that by manipulating the energy cost ratio local authorities could provide an incentive for consumers to limit their harmonic power drawn from the supply.

Figure 7.5(a) is produced from experimental measurements of the savings made from active filtering for different energy cost ratios using the load described in Section 7.1. Under the New Zealand energy cost ratio of five to one, small savings occur at low

bus voltages for this particular load. By decreasing the energy cost ratio the savings increase because the cost of the reduced kVA is less than the cost of the additional real power which is consumed by active filtering. At low bus voltages, Figure 7.5(b) shows that full compensation is not being achieved since the supply current THD is large due to the inability to reinject the required compensating current. When the energy cost ratio is 0.2, the maximum savings occurs at a bus voltage of at least 220 V. At this bus voltage full compensation is being achieved for the bridge rectifier type of load (Section 4.1.1.2). At lower bus voltages less savings occur as the load distortion is not being fully compensated for and at higher bus voltages the active filter produces excessive losses and the savings are reduced.

7.1.3 Setting the Maximum Allowed Supply Current THD

By considering the financial savings it is possible to set the operating conditions of bus voltage and switching frequency to gain the maximum savings from active filtering. For the previous case of a load current with 78% THD, a energy cost ratio of five and operating at the maximum savings point the supply current would still contain 41.2% THD (Section 7.1.1). In certain cases it may be desirable that the active filtering system be operated so as to achieve a minimum level of supply current THD. The IEEE-519 harmonic standard specifies that for supply voltages of 2.4 kV to 69 kV the current THD at the point of common coupling must be less than 5% [Duffey et al. 1989]. Using an appropriate ratio reinjection transformer it would be possible to connect an active filter to the point of common coupling for these supply voltages and reduce the current THD to less than 5%.

The cost formulation provides a surface in which the operation of the active filter can be altered to achieve the greatest possible savings. However the IEEE-519 standard specifies a level of supply current THD to be achieved. Therefore a required level of supply current THD must be incorporated into the calculation of the savings surface.

It is possible to decrease the level of the supply current THD when active filtering by making the reduction of distortion worth more than the additional cost of the power consumed by the active filter. This can be achieved by continually altering the energy cost ratio to achieve the required level of supply current THD. By adjusting the energy cost ratio, the savings level achieved has no direct relationship to the actual financial savings. An alternative to this is to add a penalty to the savings curve to ensure that the supply current THD is lower than a set maximum allowable value (THD_{MAX}). This can

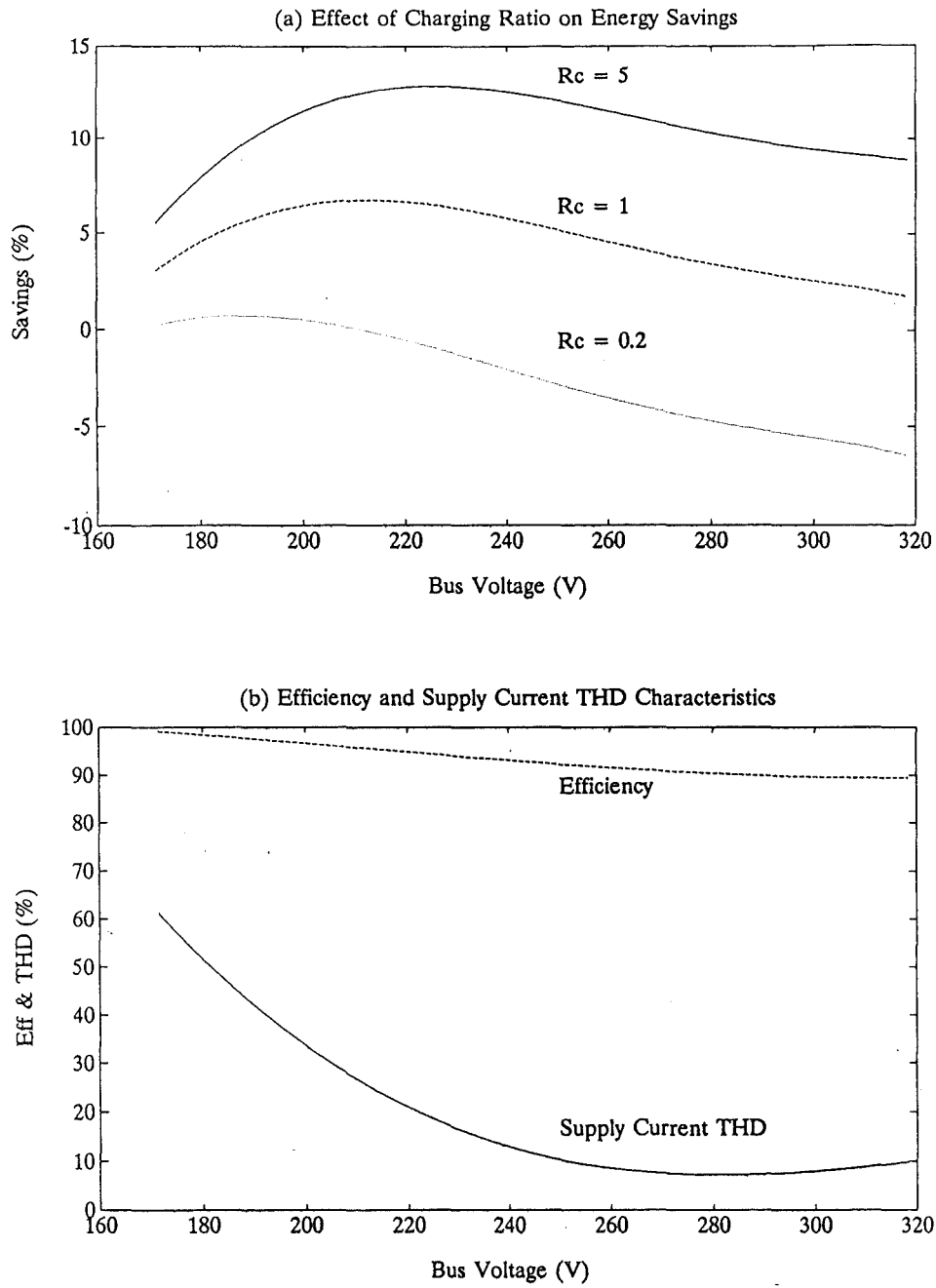


Figure 7.5 Effect of Energy Cost Ratio R_C

be described by Equ. (7.11).

$$\begin{aligned}
 \text{PEN} &= \text{SAV}_R + \sigma \text{THD}_s \mathcal{F}(\text{THD}_s) \\
 \text{where } \sigma &< 0 \\
 \text{and } \mathcal{F}(\text{THD}_s) &= \begin{cases} 1: \text{THD}_s - \text{THD}_{\text{MAX}} > 0 \\ 0: \text{THD}_s - \text{THD}_{\text{MAX}} \leq 0 \end{cases}
 \end{aligned} \tag{7.11}$$

The penalty term only operates when the supply THD (THD_s) is greater than the set maximum THD value (THD_{MAX}). This penalty term is proportional to the amount of supply THD present, which produces a larger deviation the further the supply current THD is away from THD_{MAX} . The scaling term, σ , is negative such that the penalty function reduces the savings and forces the maximum savings point to a region where the supply current THD is less than that specified by THD_{MAX} .

The effect of such a penalty function is shown in Figure 7.6. The savings curve (dotted lines) is for a single phase bridge rectifier, capacitor and resistive load and an energy cost ratio of one. The maximum savings operating point without any penalty imposed is at 207 V and 5 kHz. At this point the efficiency of the active filtering system is 96% and the supply current THD is reduced from 78.0% to 23.4% (Figure 7.1). The maximum allowed supply current THD (THD_{MAX}) is set to 10% for this particular example. When the supply current THD is outside THD_{MAX} , a penalty is added using a scaling term σ of -0.5 which produces a penalty surface (solid lines) in Figure 7.6. The shaded region in Figure 7.6 is where no penalty is added to the savings surface because the supply current THD is less than THD_{MAX} and therefore the savings and penalty surfaces are the same. The maximum savings point for the supply current THD to be less than 10% occurs at a bus voltage of 231 V and switching frequency of 18 kHz. At this point the active filtering system operates with an efficiency of 92.8% and the supply current THD is reduced from 78.0% to 9.8%.

7.2 MAXIMISATION OF SAVINGS

A savings function has been derived which calculates the possible savings available to the consumer by active filtering. The active filter's operating conditions can be altered to achieve a maximum savings point. Therefore an automatic search procedure is required to find a maximum savings point independent of the type of load and THD_{MAX} level. Since more than one operating condition can be adjusted to move about on the savings surface, a multidimensional optimisation algorithm is required. Unlike the more traditional optimisation problems in which the shape of the surface is known, the savings surface is unknown prior to active filtering. The surface is only measured when the optimisation algorithm steps towards the maximum savings point. The active filtering produces the savings surface from measured data which is continually changing due to time varying loads. The optimisation algorithm must therefore continue to explore the area surrounding the maximum savings point in order to find new maximum points over

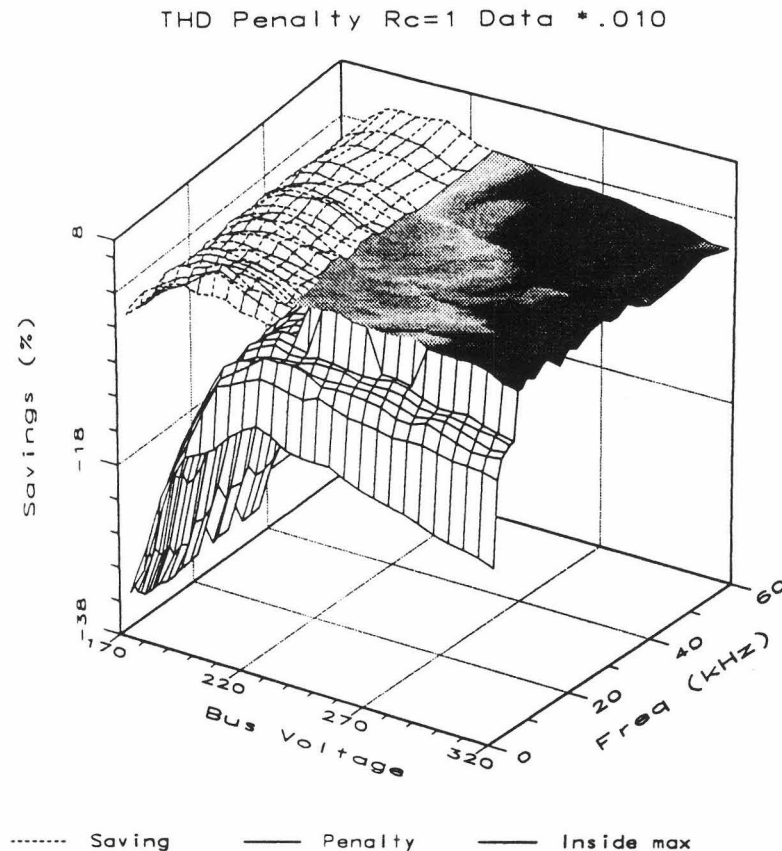


Figure 7.6 Effect of setting maximum allowed THD

time.

There are two classes of optimisation techniques available [Beightler et al. 1979], the direct and indirect methods. The indirect method takes a classical approach to solve equations which describe the problem rather than searching for an optimum. The direct method starts at an arbitrary point and proceeds in a stepwise fashion towards the maxima or minima by successive improvements. The indirect methods are not suitable for finding the maximum savings point as they require the surface to be well defined and with this problem the shape of the savings surface is unknown prior to starting the optimisation search.

Many different types of direct methods are available, however these all fall into two categories. Firstly, methods using the first derivative information such as the conjugate gradient and variable metric methods [Press, Flannery, Teukolsky, Vetterling 1986]. Secondly, methods that don't need to compute the first derivative, such as the direction-set and the simplex method [Press et al. 1986]. For the first derivative methods, the derivative information is obtained by additional sampling of the surface. Since the savings surface is unknown the use of first derivative methods requires the operating point of the active filter to be altered for each measurement. Once the maximum savings

point has been reached, the derivative methods require a larger number of new measurements of the operating conditions of the active filter to make sure the maxima is maintained. A method which does not use the first derivative is therefore employed to determine the maximum savings point.

The simplex method was used to find the optimum operating point because it moves towards a maxima in a straightforward fashion that makes no assumptions about the surface [Press et al. 1986]. Although the simplex method tends to be slow it can be very robust. The simplex method is based on using the geometric figure called a simplex, consisting of $N+1$ vertices (for N dimensions). In two dimensions the simplex is a triangle and in three dimensions it is a tetrahedron [Dixon 1972].

The simplex method is started with a single starting point P_0 and the vertices of the initial simplex are given by Equ. (7.12).

$$P_i = P_0 + \xi e_i, \quad i = 1, 2, \dots, N \quad (7.12)$$

where e_i are orthogonal unit vectors and ξ is some arbitrary length scale. The simplex method can take a series of four different steps towards the optima. These steps are graphically depicted in Figure 7.7 for a three dimensional ($N=3$) case [Beightler et al. 1979, Press et al. 1986]. Initially the measured data from the four starting points is sorted and the highest and lowest points are determined. The first step is taken by moving the lowest point through the opposite face of the simplex (see Figure 7.7(a)). This step is called a reflection. If this new point has a higher value then the reflection length is expanded (Figure 7.7(b)). If the new point is higher again then this point is accepted otherwise the previous point is used. The old low point is now disregarded. However if the first reflected point is worse than the second lowest point then the simplex will contract along one dimension (Figure 7.7(c)). If this contraction does not yield an improvement the simplex contracts itself in all directions, pulling itself in around its highest point (Figure 7.7(d)).

The simplex algorithm [Press et al. 1986] is implemented in the PC which then controls the TMS320C30 (Section 6.2) to set the operating conditions in order to achieve the maximum savings point for the required supply current THD.

7.3 RESULTS OF OPTIMISATION

To show that the simplex algorithm correctly finds the point of maximum savings this section will present results showing the simplex algorithm starting at two different

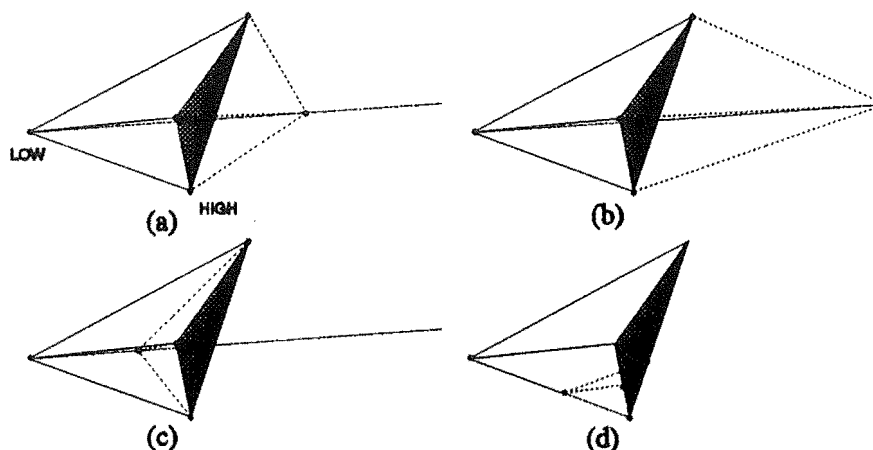


Figure 7.7 Modes of the Simplex Algorithm [Press et al. 1986]

points and climbing to the same maximum point. The operation of the simplex algorithm will also be shown during load changes. In both of these cases, a surface of savings and the track of the simplex algorithm will also be displayed. It is important to note that the simplex algorithm has no prior knowledge of the savings surface and the surface is only present to give the reader an indication of the simplex algorithm in operation. The surface of maximum savings has been previously collected by measuring the efficiency, supply current THD and savings at various discrete bus voltages and average switching frequencies.

7.3.1 Changing the Starting Point

The simplex climbing algorithm should not be affected by variations in starting point. Figure 7.8, which illustrates this, displays the savings surface for a single phase bridge rectifier load (Section 7.1) with an energy cost ratio of one. From a starting point (1) of 236 V and 16 kHz the simplex algorithm tracks (solid line) the surface until a maximum value of 5.8% savings is reached at 201 V and 16 kHz. Another starting point (1*) of 284 V and 32 kHz is used and the dashed line shows the track towards the optimal point also at 201 V and 16 kHz.

There is the possibility that the simplex algorithm could get stranded at a local maxima. This could occur along the ridge of switching frequencies at the optimal bus voltage. These local maxima are produced because the switching frequency of the active filter does not have a large effect on the savings for small shifts in frequency. The position of this ridge is dependent on the type of load being compensated for and the

Operating Characteristic of the AF

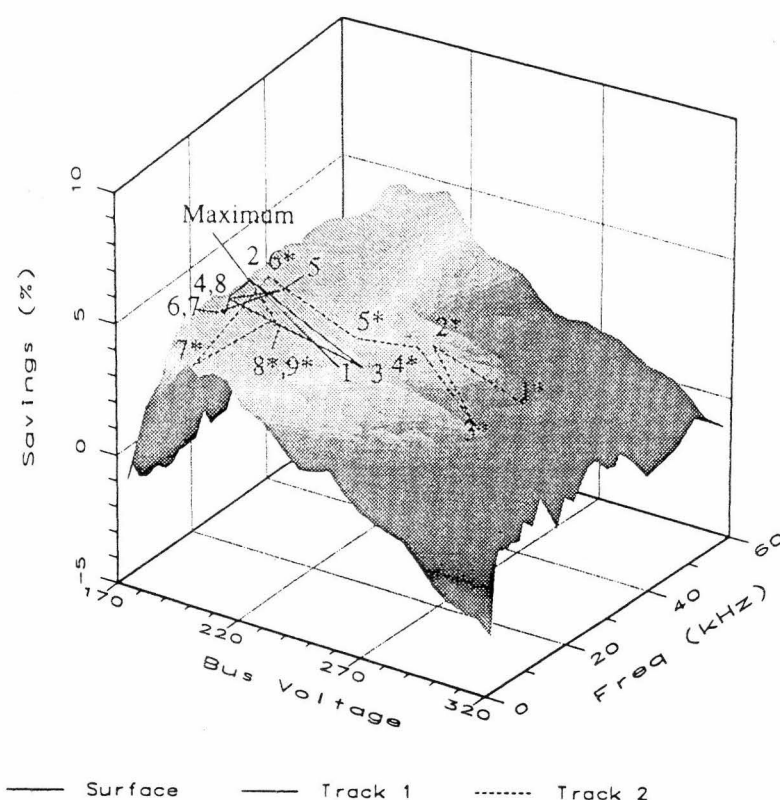


Figure 7.8 Climbing the Savings Surface from Two Different Starting Points

distribution of switching frequencies produced by the active filter's power amplifier. The simplex algorithm operates in such a way that the algorithm always continues to try and find an improved maxima. Small fluctuations in the supply voltage and magnitude of the synthetic sine wave are sufficient to push the simplex algorithm off any local maxima and make it head towards the global maxima. The difference between local maxima savings value along the ridge is usually very small and therefore finding the exact global maxima may not be critical.

7.3.2 Effect of Load Changes

The simplex algorithm is dependent on history terms (existing vertices) to calculate the next step of the algorithm towards the point of maximum savings. These history terms can cause a problem when the savings surface changes due to a new load combination, cost ratio or maximum supply current THD. If the savings surface rises due to such a change, the simplex algorithm will continue to try and find a new maximum and thus track the new surface. However in the case where the new savings surface is lower, the simplex algorithm will not find the new maximum because the history terms

have not changed and they contain the old high values.

To enable the simplex algorithm to follow these changes in the savings surface, the load current RMS and THD values are measured. When a variation (presently 10%) is detected in either term the simplex algorithm remeasures the history terms and starts the optimisation search again.

The operation of the simplex algorithm due to a load change is illustrated in Figure 7.9. Initially the load consists of a single phase bridge rectifier, capacitor and resistor drawing $7.2 A_{RMS}$. This results in a savings surface as shown in Figure 7.9(a). The simplex algorithm measures the three starting points 1, 2 and 3. Based on these three points the simplex measures a new point 4 and then recalculates and measures another point at 5. At point 5 the load increases due to an additional resistive ($3 A_{RMS}$) component being connected in parallel with the bridge rectifier load. The surface now decreases to that in Figure 7.9(b). The history terms now have to be remeasured. The three history terms are the three previous highest savings values which are 1, 2 and 4 on Figure 7.9(a). The bus voltage and switching frequency values of 1, 2 and 4 correspond to the new savings value for points 6, 7 and 8 on Figure 7.9(b). The simplex algorithm now continues searching until it discovers that the maximum savings occur at point 11.

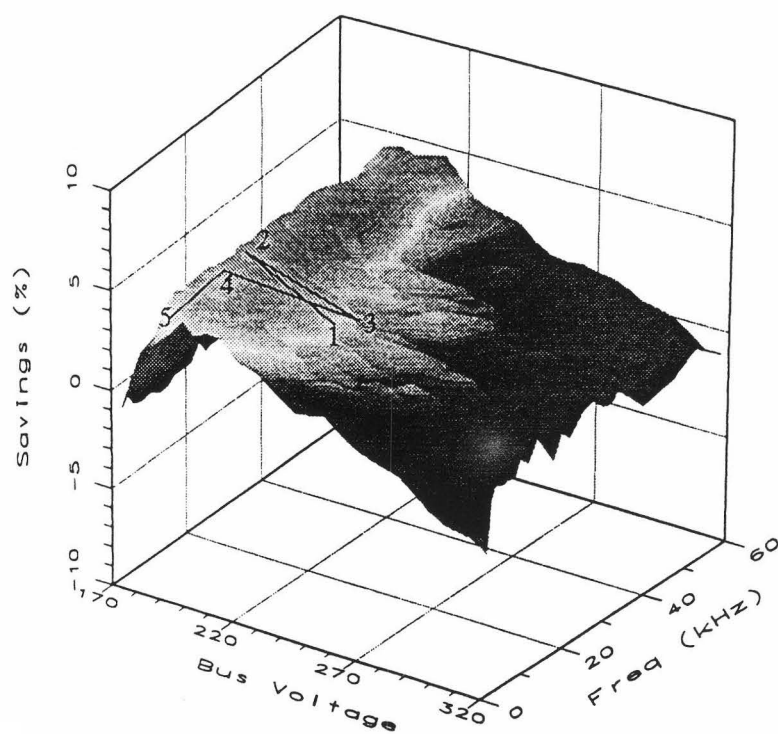
7.4 POWER FACTOR CORRECTION

The ability of the active filter to provide reactive power was discussed in Section 5.1.2. The SPU on the analogue controller had a limited amount of control in adjusting the phase displacement of the supply current. With the digitally controlled active filter the displacement power factor can be adjusted in 0.7 degree steps which allows a greater level of control over the amount of displacement compensation. This section initially considers the effect of displacement compensation, followed by both displacement and distortion compensation on the savings surface. The ability of the simplex algorithm to correctly find the optimum saving point for displacement loads is also considered.

7.4.1 Displacement Correction

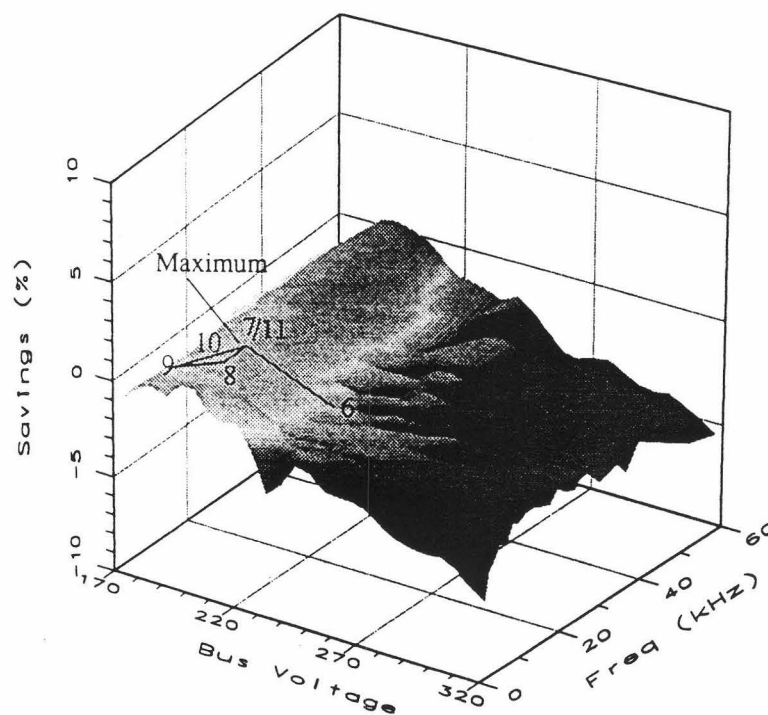
To compensate for displacement distortion the synthetic sinusoid generated by the digital controller is referenced to the supply voltage zero crossings. The synthetic sinusoid is then displaced from the supply voltage zero crossings depending on the level of

(a) Savings Before Load Change



— Surface — Track

(b) Savings After Load Change



— Surface — Track

Figure 7.9 Tracking Maximum under Load Change (a) Track before load change.
(b) Track to maximum after load change.

reactive power that is required to be compensated for.

To illustrate the effect of displacement distortion compensation, a linear load is used and the results are shown in Figure 7.10. The linear load consists of a resistor in parallel with an inductor. The current (Figure 7.10(b)) being drawn by the load is $5.5 \text{ A}_{\text{RMS}}$ and is phase displaced from the supply voltage (Figure 7.10(a)) by 80 degrees. When the active filter is operating, the supply current is shifted towards unity displacement power factor by 30 degrees as in Figure 7.10(c). The supply current has now fallen to $2.6 \text{ A}_{\text{RMS}}$, however the waveform contains 12% THD. Figure 7.10(d) shows the supply current shifted to unity power factor by the active filter. The current has been reduced to $1.8 \text{ A}_{\text{RMS}}$, but the THD has increased to 20%. As the supply current shifts towards a unity displacement power factor the RMS level of current decreases. To reduce the level of reactive power drawn from the supply the power amplifier must supply a relatively large compensating current. Any small error in the generation of the compensating current, either produced by the SPU and/or power amplifier, may become significant compared to the low level of supply current. These errors introduce additional distortion in the supply current as complete compensation of the reactive power is not occurring. The increase in supply current distortion at improved displacement power factors can also be attributed to the reinjection transformer's magnetising current. At $240 \text{ V}_{\text{RMS}}$ the magnetising current of the reinjection transformer is $0.32 \text{ A}_{\text{RMS}}$ and contains a relatively high 3rd harmonic component. The 3rd harmonic component results in a peak current of 0.6 A for the magnetising current. The addition of the magnetising current to the low level of supply current increases the THD as unity displacement power factor is achieved.

Using the active filter technique, it is possible to shift the supply current waveform so that it is leading the supply voltage. This however is not a very economical situation, as there are no additional gains for a leading power factor, and the active filter system requires a greater amount of real power for compensation. Figure 7.10 shows that the RMS supply current is reduced by 53% for a 30 degree shift and is only reduced by 67% for an 80 degree shift to unity power factor. The additional gain in reduced line current by shifting the supply current an extra 50 degrees is small compared to the initial reduction in line current for a 30 degree shift.

The experimental savings for distortion compensation are shown in Figure 7.11. These were measured by adjusting the resistive and inductive components of the previous load configuration such that the total load current remained constant. For these measurements the DC bus voltage was maintained at 240 V and the average switching

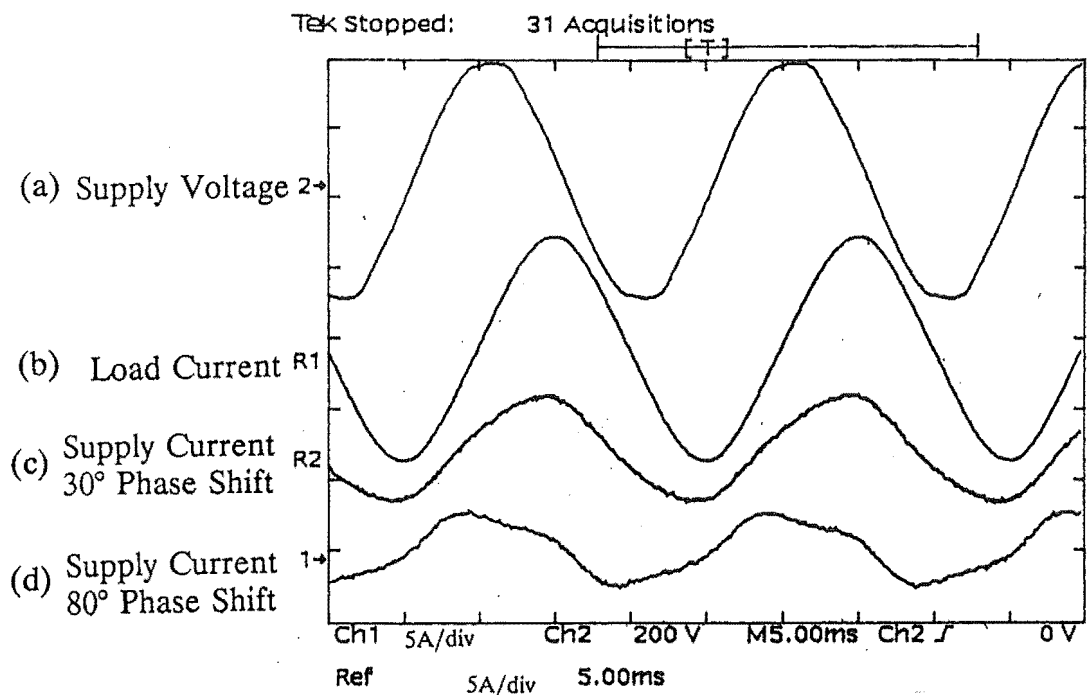


Figure 7.10 Displacement Correction by the Digitally Controlled Active Filter

frequency was set to 22 kHz. Four cases are illustrated, each with a different amount of displacement and the supply current is corrected so it does not exceed unity power factor in each case.

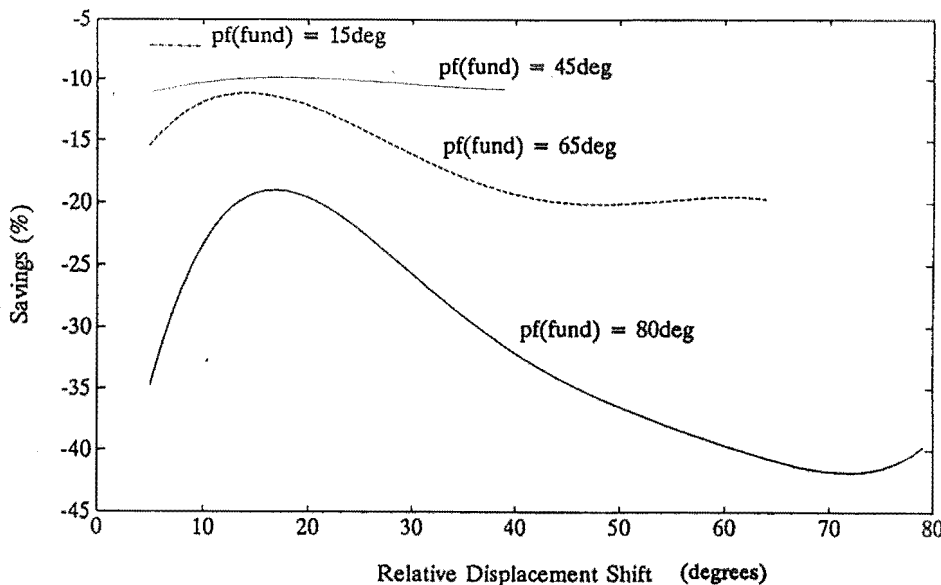


Figure 7.11 Possible Savings by Displacement Correction for various Resistive and Inductive Loads.

In the case where the displacement of the load is 80 degrees it is possible to get the greatest benefit (savings of -19%) by shifting the waveform 18 degrees. If the supply current is shifted beyond 18 degrees the cost of shifting the waveform starts to outweigh the benefit from the reduction in line current. As the initial displacement of the load gets closer to zero degrees, the savings made by shifting the power factor are smaller as the savings are offset by the cost of displacement shifting.

It is possible to shift a displaced load current back in phase with the supply voltage, however economically there is a limit on how far this shift should be. For large displacements it may be worth shifting the waveform up to 30 degrees.

7.4.2 Distortion and Displacement Correction

When the load current contains both harmonic and displacement components the active filter can provide total power factor correction. This is demonstrated in Figure 7.12 for a single phase bridge rectifier with capacitor and resistor in parallel with a resistor and inductor combination. The displacement of the resistor and inductor combination is 80 degrees and the total load has a displacement of 56 degrees with a load current THD of 40.3%, which results in a total power factor of 0.630 using Equ. (7.9).

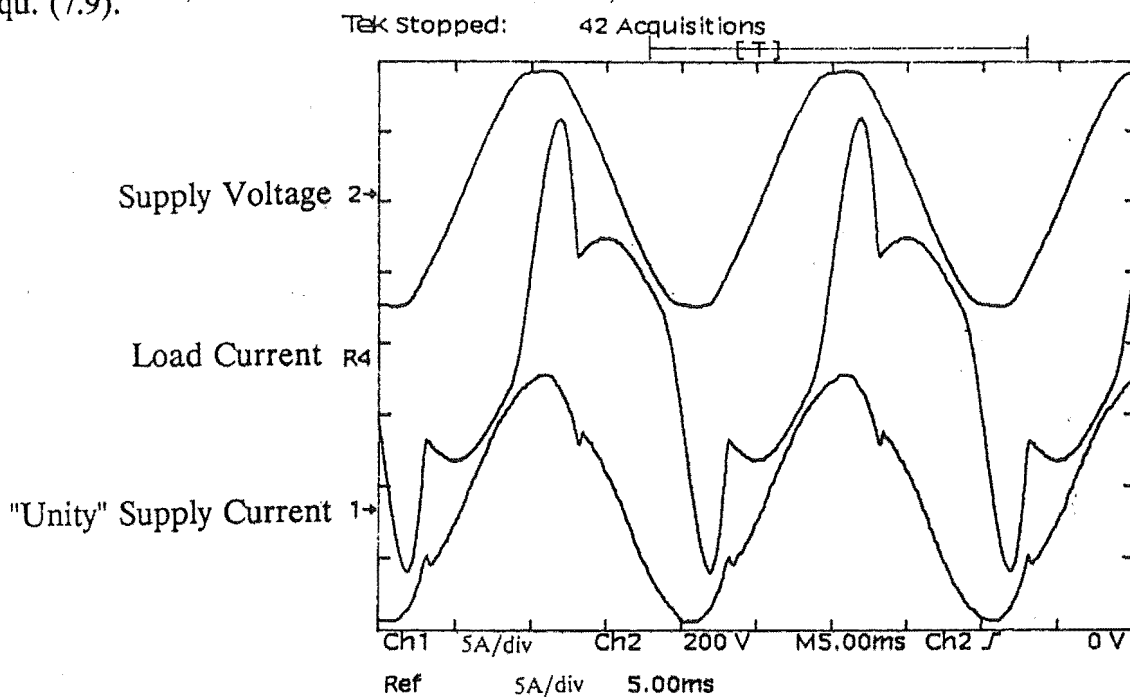


Figure 7.12 Distortion and Displacement Compensation

When the active filter is operated the supply current THD is reduced to 9.1%, with a displacement of 0 degrees, and a resultant power factor of 0.991. The supply current has a value of 5.8 A_{RMS} compared to the load current value of 8.5 A_{RMS}. Operating at 240 V_{DC} and 22 kHz the active filter has an efficiency of 71.4%.

The savings characteristic for variable DC bus voltages and fundamental power factors at a constant average switching frequency of 13 kHz for this load is displayed in Figure 7.13. Shifting the displacement from 56 degrees to 54 degrees and operating at a bus voltage of 195 V produces the greatest amount of saving of -5.0%. However at this low bus voltage the supply current contains 20.0% THD. Therefore by using the THD maximum setting it is possible for the system to optimise itself to the point of greatest savings while maintaining a required level of supply current distortion.

Savings from Displacement Correction R5

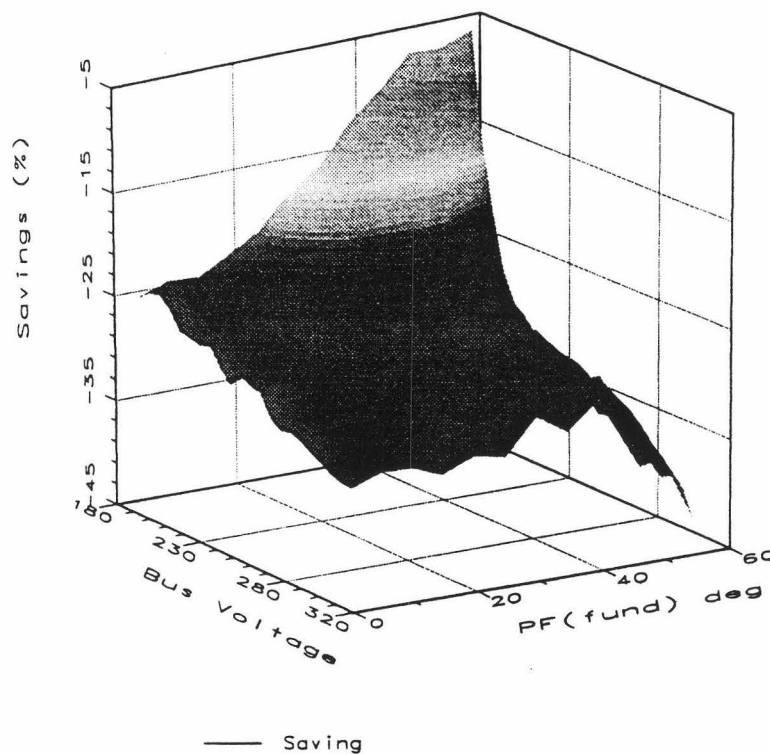


Figure 7.13 Savings for Performing Power Factor Correction at a Cost Ratio of Five

7.4.3 Three Variable Optimisation

The active filtering system has the ability to manipulate the DC bus voltage, average switching frequency and fundamental power factor to achieve the greatest savings for any particular load. The simplex optimisation algorithm is well suited to

multidimensional problems [Press et al. 1986]. In the case of three variables, the number of starting points is now increased to four. It is difficult to graphically represent a four dimensional savings surface to show the operation of the optimisation algorithm as it steps towards the maximum savings point. The track to the optima is shown in Figure 7.14 by displaying the three variables and the tracking sequence between them.

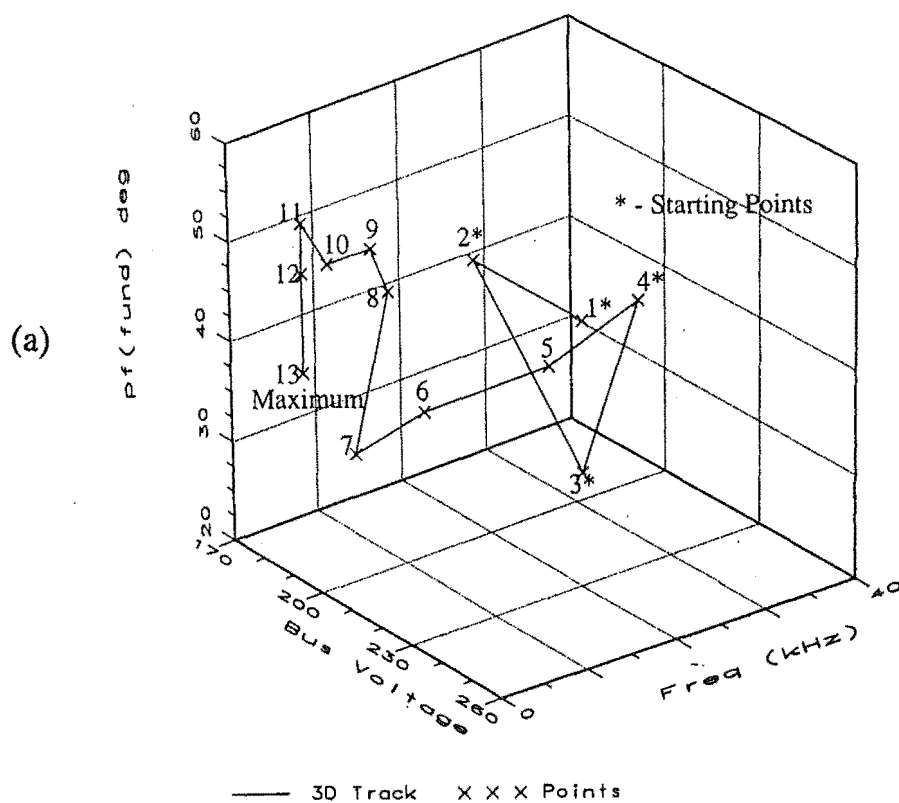
Figure 7.14(a) shows the track leading to the maximum savings point for the load as described in Section 7.4.2. The starting point is at 242 V, 16 kHz and 49 degrees. Three other points are measured and the simplex algorithm then tracks to a maximum point of 4.9% at 189 V, 2 kHz and 54 degrees. At the low bus voltage of 189 V and low switching frequency of 2 kHz, the supply current has not been fully compensated for as the supply current THD is 29.9%. By introducing a required level of supply current THD to be achieved (10% in this case), the maximum savings point has now altered. Figure 7.14(b) illustrates the track to this new maximum savings point of -21.6%. The four starting points are identical to the case in Figure 7.14(a) and the active filtering system now tracks to this maxima at 212 V, 12 kHz and 44.5 degrees which results in a supply current THD of 9.9%.

7.5 SUMMARY

A savings equation using the cost of electricity consumed by non active filtering and active filtering distorted loads has been developed in this chapter. This savings equation is based on the energy cost ratio of real to apparent power. By adjusting the energy cost ratio it is possible for the local supply authorities to charge consumers more for drawing distortion. The savings function is used to produce a savings surface for active filtering distortive loads. An optimisation algorithm is then used to automatically find the operating point of the active filter which produces the greatest savings. The maximum savings achieved, using a energy cost ratio of five and a single phase bridge rectifier load, were negative. The cost of active filtering was greater than the savings made from reducing the distortion. If the energy cost ratio is altered by the supply authorities to charge more for distortion the savings may become positive, thus encouraging consumers to remove the distortion from their supply current.

By adding a penalty to the savings surface it is possible to operate the active filter in a region where maximum savings occur without exceeding a certain level of supply current THD. A simplex optimisation algorithm is used to find the point of maximum savings. The operation of the simplex algorithm for various starting points and load

Three Variable Optimisation - No Penalty



Three Variable Optimisation - Penalty 10%THD

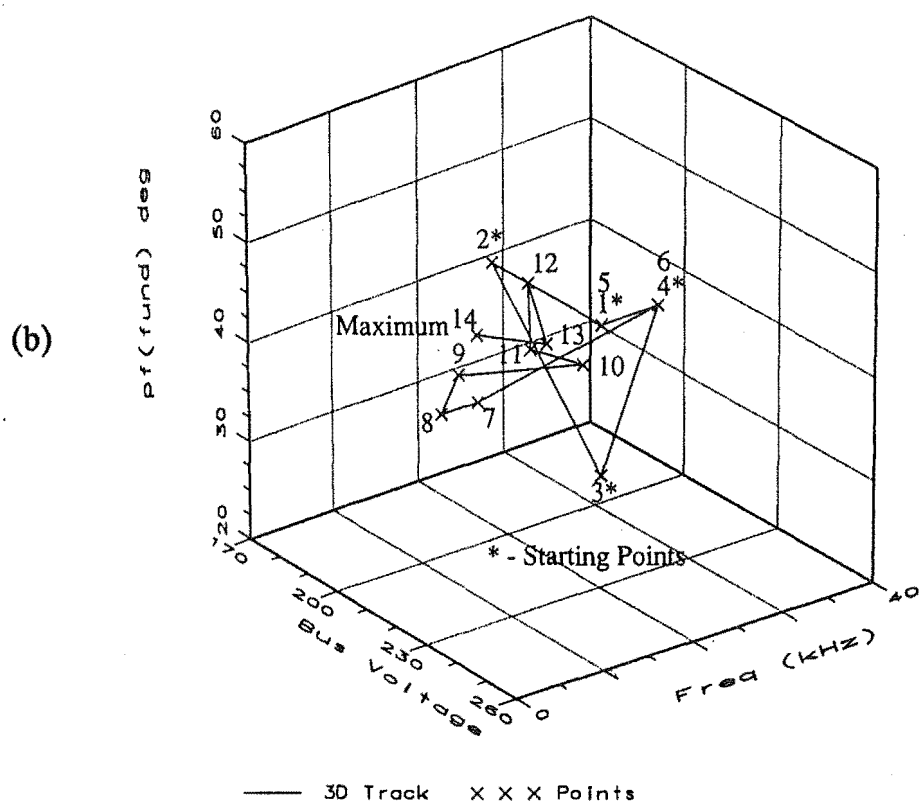


Figure 7.14 Three Variable Optimisation Track (a) No penalty (b) Penalty added, supply current THD must be less than 10%

changes was demonstrated. The simplex algorithm is able to find the maximum savings point regardless of starting point or load type.

The ability of the active filter to perform harmonic and displacement correction was demonstrated. The savings equation was applied to displacement compensation to achieve maximum savings. Using the three variables of bus voltage, average switching frequency and fundamental power factor the optimisation technique can find a maximum savings point.

CHAPTER 8

NOVEL APPLICATIONS OF ACTIVE FILTERING

Previous chapters have shown that the active filter is capable of compensating for current distortion produced by non-linear and phase displaced loads. Two novel applications of active filtering are investigated in this chapter. The first application requires the active filter to compensate for a distortive load operating from a variable frequency generation system. In the second application the active filter is used in conjunction with a three phase diode bridge rectifier-boost converter combination with DC-link current shaping.

8.1 VARIABLE FREQUENCY GENERATION SYSTEMS

Traditionally in an AC power system the generators are operated at a fixed frequency. However there are situations, such as the remoteness of the generation plant, when individual generators may not be connected to the AC network. In these cases the generator does not have to operate at a fixed system frequency. Depending on operating constraints, it may be more efficient to operate at a frequency other than the fixed system frequency. Variable frequency control, to achieve high efficiency operation, can occur in wind and variable head hydro generation systems [Naidu, Mathur 1989, Sankar 1991].

The main purpose of the variable frequency generation may be to supply power to the national grid. However, since each generator is operating at different frequencies, the power must be converted from AC to DC for transmission [Calverley, Ottaway, Tufnell 1973]. To produce DC for transmission from remote AC generation requires rectification, which introduces current distortion. Current distortion in the generator results in overheating and the generator rating may have to be increased to cope with this, therefore the cost of the generation equipment is more expensive. If the generator is part of a relatively weak power system the current distortion can produce a distorted supply voltage.

Passive filters have traditionally been used to remove the current distortion produced by DC converters. However in this particular case, tuned passive filters are not suitable because of the variable frequency generation. An active filter does not have the same frequency limitation as the passive filter, its operation is not fixed to a fundamental frequency. The active filter is able to remove current distortion from a variable frequency supply and in addition improve the supply voltage waveform of a weak power system.

This section describes the application of a three phase active filter to an experimental model of a variable frequency generation system and to a computer simulation of a larger variable frequency generator and DC converter system.

8.1.1 Hardware Model

To demonstrate the principle of variable frequency active filtering a small isolated 10 kW generator and three phase diode bridge rectifier load is used (Figure 8.1). To produce a variable frequency supply, a three phase generator is driven by an induction motor which is controlled by a variable speed drive. A distortive load, in this case a three phase diode bridge rectifier load, and three phase active filter are connected in parallel with the output of the generator.

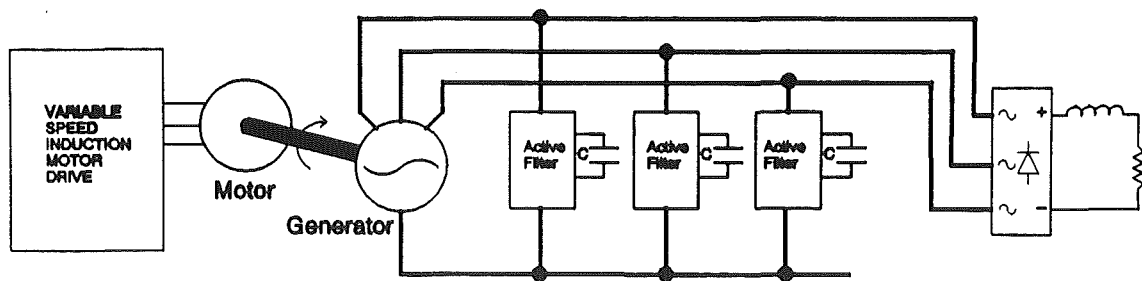


Figure 8.1 Hardware Connection for Active Filtering from a Variable Frequency Generation System

The variable speed drive is operated so that the generator produces a 220 V line to line supply voltage for a range of frequencies from 40 to 60 Hz. The DC load current is 9 A, and Figure 8.2 shows the waveforms obtained for this isolated generator and distorted load connection.

With the frequency of generation at 50 Hz, Figure 8.2(a) and (b) illustrates the generator phase to neutral voltage (128 V) and line current ($7 A_{RMS}$) when no active filtering is occurring. This line current is produced by the three phase bridge rectifier, with its inductive and resistive load, and has a THD of 15.2%. The current harmonics drawn by the load produce a generator output voltage with a THD level of 6.5%.

When the three phase active filter is compensating for the distortion the generator voltage and current become more sinusoidal (Figure 8.2(c) and (d)). The THD of the generator current is now reduced to 0.85% and the generator voltage THD is reduced

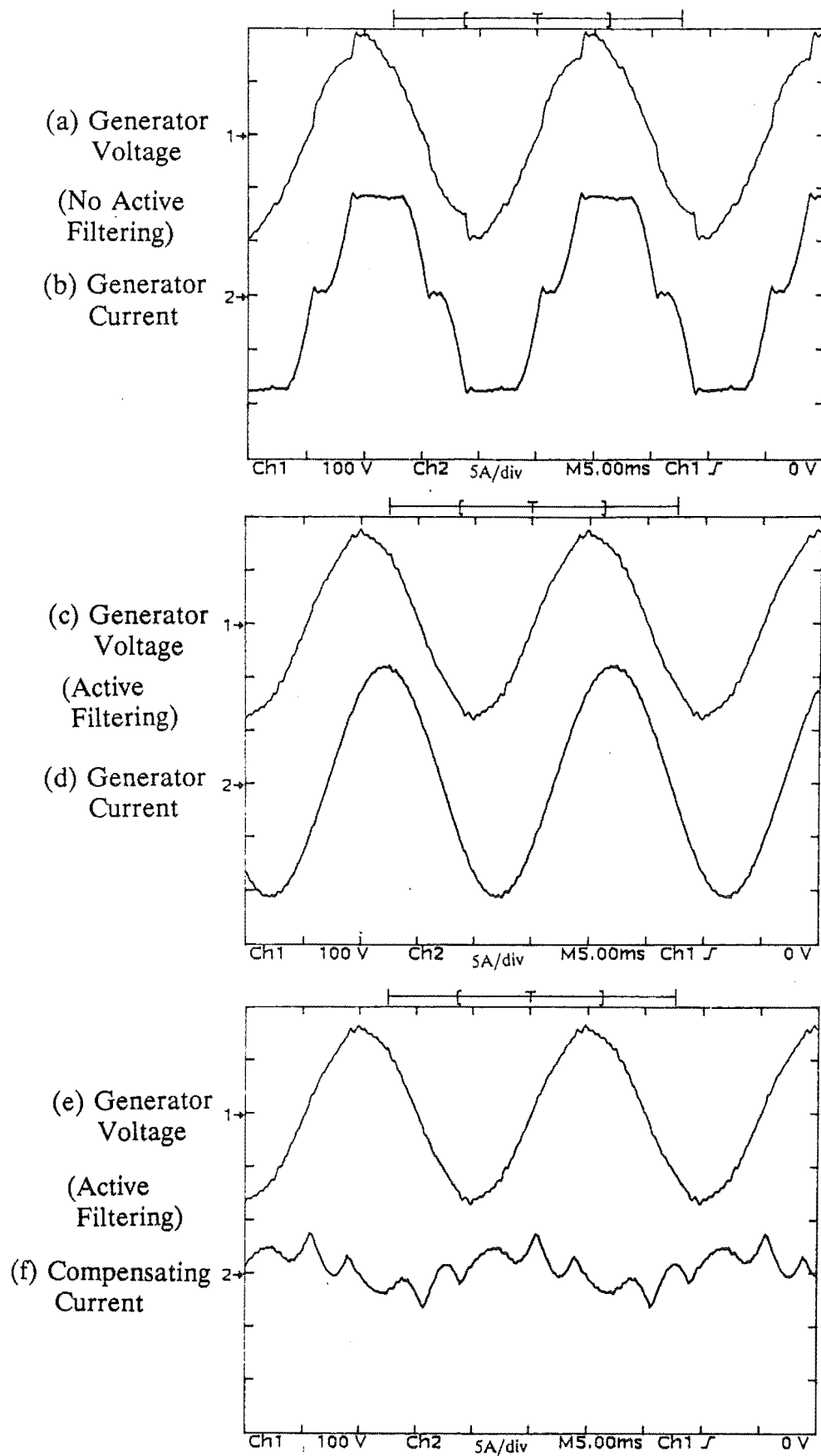


Figure 8.2 Experimental Results of Isolated Generator and Active Filtering System

to 2.5%. In order to compensate at the lower voltages (200 V line to line instead of 415 V) produced by the generator, a reinjection transformer with a turns ratio of one to one is used. For compensation the active filter is operated at a DC bus voltage of 250 V_{DC} and Figure 8.2(e) and (f) shows the compensated generator voltage and the active filter's compensating current respectively. By using the active filter on a weak system with a non-linear load it is possible to compensate for the current distortion and thus improve the quality of the supply voltage.

The ability of the active filtering system to track and compensate for distortion in a system with a changing fundamental frequency is shown in Figure 8.3. Initially the generator frequency is set to 45 Hz and the active filter is not operating. The 5th and 7th current harmonics drawn from the generator by the bridge rectifier load can be seen on the bottom trace. Each trace represents a linear spectrum taken at one second intervals with time increasing from the bottom of Figure 8.3. The frequency of the generator is held at 45 Hz for 4 seconds, then the active filter is started and the current harmonics are reduced. The generator frequency is held at 45 Hz for a further 7 seconds. With the active filter still operating the fundamental frequency is increased to 56 Hz over a time interval of 20 seconds. During this shift in fundamental frequency the active filter is still providing compensation as no current harmonics appear in the generator supply current. Once 56 Hz is reached and the active filter is stopped, the 5th and 7th current harmonics of the new fundamental frequency (56 Hz) appear.

8.1.2 Computer Simulation of a Large Isolated Generation System

The idea of a remote generator system connected to a DC link is not new [Calverley et al. 1973, CIGRE 1988]. With this configuration, the rectifier system introduces current harmonics in the generator and to supply the required power level (up to hundreds of MW), the generator has to be derated, thus increasing the cost and operational losses of the generation plant. By using an active filter to remove the current harmonics the generator would not have to be derated and only the capital and running costs of the active filter have to be considered.

Computer modelling is now used to investigate the feasibility of connecting an active filter to a large isolated generator system. In larger rectifier systems the technique of pulse multiplication is used to reduce the level of harmonic currents (Section 2.2) drawn by the converter. Normally the pulse number is increased from 6 to 12 [Arrillaga et al. 1985]. A 12 pulse rectifier system connected to a remote generator has been

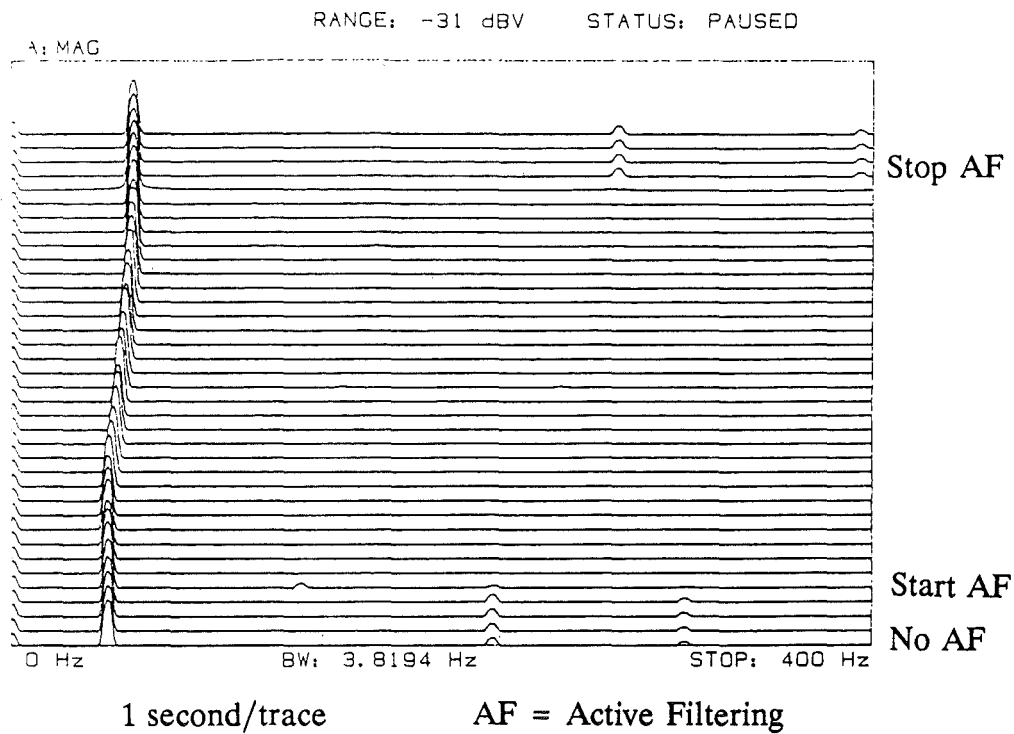


Figure 8.3 Operation of the Active Filter during a Shift in Fundamental Frequency

modelled by Sankar [Sankar 1991]. The 12 pulse configuration (detailed in Figure 8.4) consists of one generator, two fully controlled 6 pulse bridges and two converter transformers with the position of the active filter also detailed.

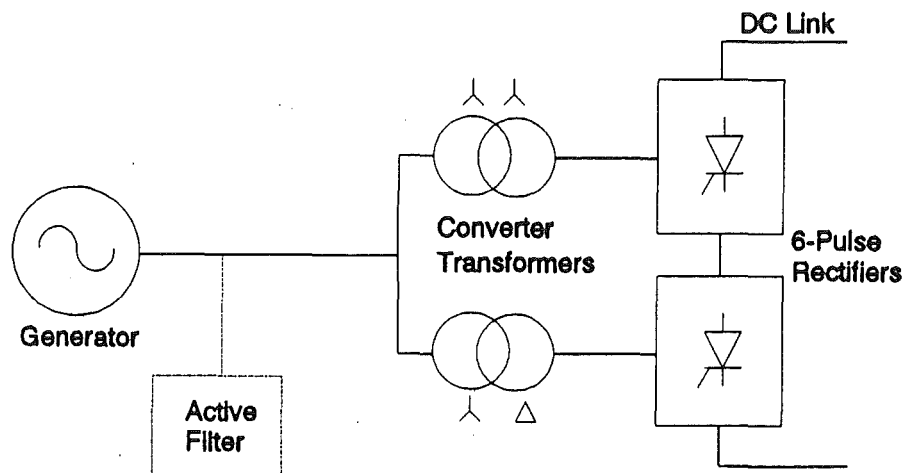


Figure 8.4 12 Pulse DC System Supplied by Isolated Generation

For this 850 kVA system Sankar simulated the load current drawn by the rectifier with a firing angle of 15 degrees. This load current data is then used as an input data file by the active filter simulation. The active filter operates from a 13.8 kV line to line (8 kV phase to neutral) generator, therefore the generator voltage has to be reduced to a level in which the switching devices can operate. The voltage is reduced by a reinjection transformer to 450 V_{RMS} on the amplifier side of the transformer. To achieve this voltage reduction a reinjection transformer with a turns ratio of 17.8:1 and 10% leakage inductance is used. The 10% leakage inductance limits the rate of rise of compensating current, but still ensures that the active filter is able to compensate for the higher order harmonic components. Throughout the simulation the generator voltage is assumed to be sinusoidal. Under these conditions the 12 pulse rectifier system draws a load current of 35 A_{RMS} with a THD of 5.8%, which is mainly produced by the 11th and 13th harmonics (Figure 8.5(a)). When active filtering is being carried out the compensated supply current (Figure 8.5(b)) is nearly sinusoidal with a small amount of transistor switching current superimposed. The THD of the supply current has been reduced to 1.0% and the required compensating current (Figure 8.5(c)) has a current level is 109 A_{RMS}. The average DC bus voltage of 900 V_{DC} to achieve this level of compensation is shown in Figure 8.5(e). A transistor switching time delay of 25 μ s results in an average switching frequency of 7.7 kHz with a switching frequency distribution as shown in Figure 8.5(f).

Using this particular configuration of a remote generator and active filter system it has been shown that it is possible to correct for current distortion produced by a converter of 850 kVA using present IGBT technology. The complexity of this system for a power rating of 850 kVA, is probably not justified due to the expense of two converter transformers and controlled bridges. A more economical system would consist of a generator, such as those used in wind farms, of a rating of say 1 MVA, directly connected to an uncontrolled 6 pulse rectifier system. The use of a diode bridge rectifier is a cheaper alternative to a thyristor controlled rectifier [Bowles 1989]. The 6 pulse rectifier produces around 15% THD in the generator line current and present semiconductor technology could produce an active filter that could compensate for the distortion and operate off a variable frequency.

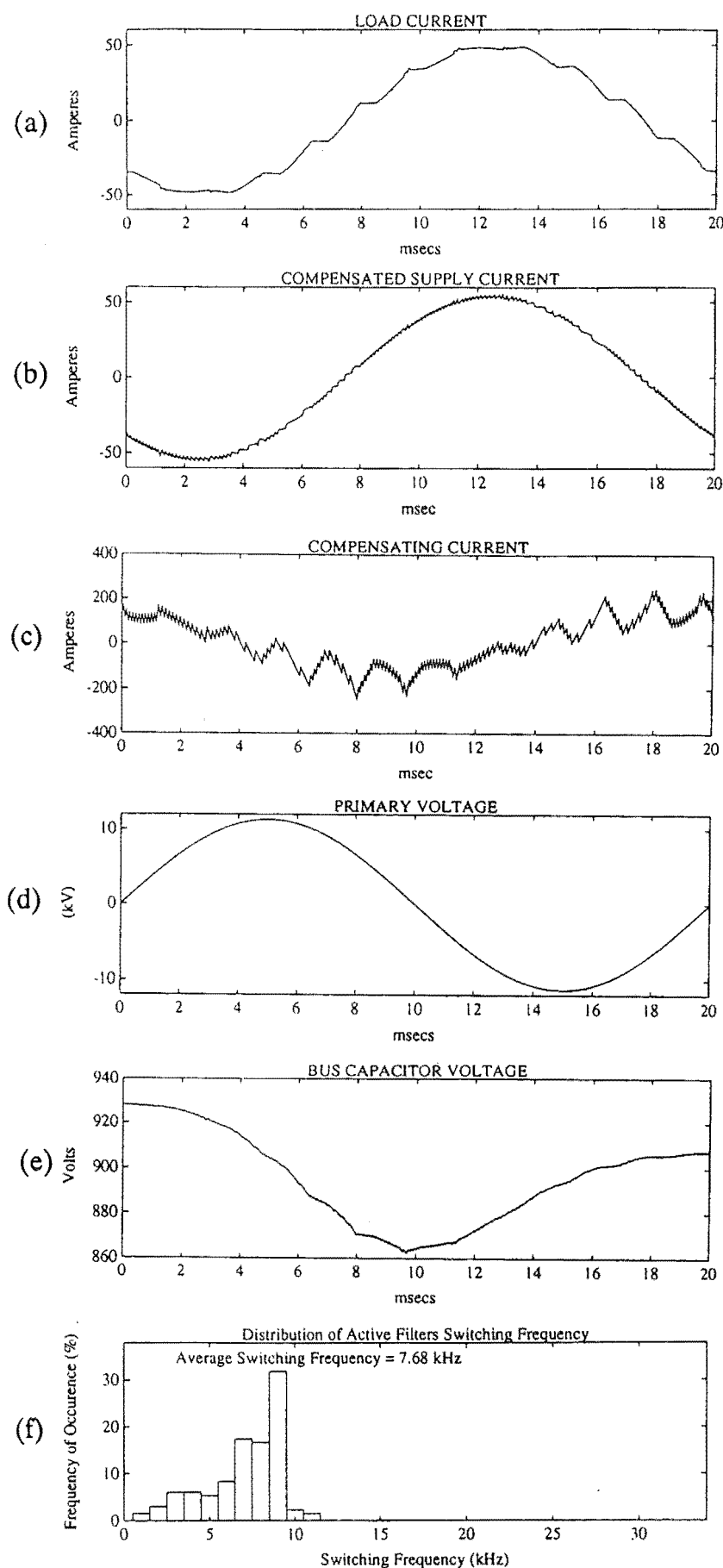


Figure 8.5 Computer Simulation Results of 12 pulse DC Link and Isolated Generator

8.2 THREE PHASE RECTIFIER WITH DC-LINK CURRENT SHAPING

The second application of the active filter is its use in conjunction with a three phase bridge rectifier and DC link shaping system. Traditionally many industrial applications, such as variable speed motor drives and uninterruptible power supplies, use a diode bridge rectifier to convert three phase AC power to DC power. Although this configuration is simple and offers high reliability, the output DC voltage is uncontrolled and has an upper limit which is set by the supply voltage. The input currents to the diode bridge rectifier are also non-sinusoidal.

It is possible to achieve sinusoidal input current by including six controllable switches in the rectifier [Green, Boys, Gates 1988, Ooi, Salmon, Dixon, Kulkarni 1987]. This is an expensive option, when compared to the original bridge rectifier, as each controllable switch is required to have the full power rating of the system.

In power systems where a low supply voltage (110 V) is used there are some applications where it would be desirable that the DC output voltage of a rectifier could be adjusted so it is greater than the limit that can be achieved by using just a three phase diode bridge rectifier. Voltage above this limit can be achieved by using a three phase diode bridge rectifier and boost converter configuration [Kolar, Ertl, Zach 1990] as illustrated in Figure 8.6.

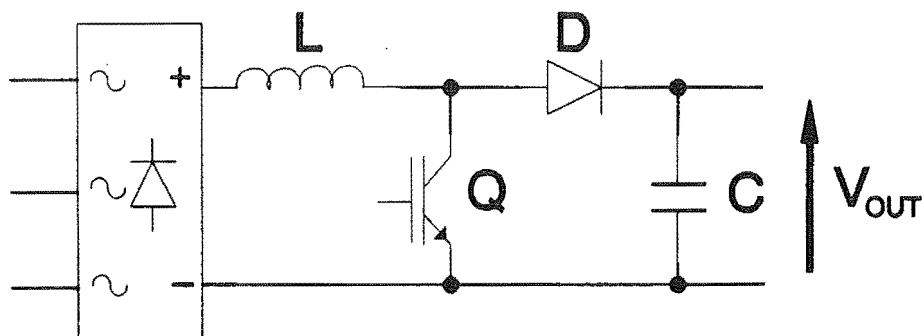


Figure 8.6 Boost Converter Configuration

The boost converter operates by switching transistor Q, such that the current in the inductor L remains at a constant level, which is set by the controller. The output voltage V_{OUT} can be controlled by this level of constant current. Therefore if the output voltage falls below a set value the average inductor current is increased. The use of this controlled current boost converter and diode bridge rectifier combination results in the supply current having the same waveshape as the case of the three phase bridge rectifier

with inductive and resistive load presented in Section 5.2.1 (Figure 5.7). An improvement in supply current distortion can be obtained by using a three phase active filter connected between the supply and the bridge rectifier (Figure 8.7).

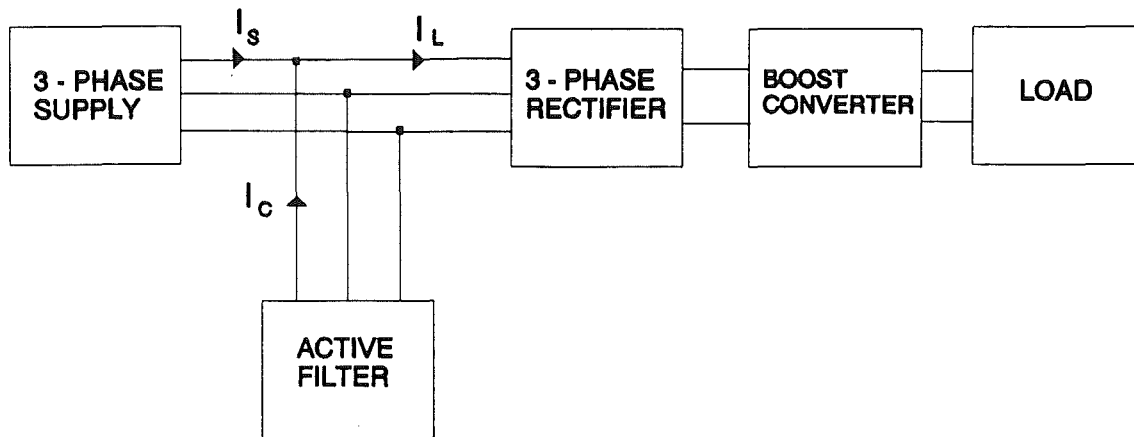


Figure 8.7 Active Filter Connection to the Controlled Current Boost Converter

By active filtering, the supply currents can now be made nearly sinusoidal. This configuration is an economical solution compared to the various controlled switch rectifier configurations, because now only one controllable switch (boost converter transistor) needs to be rated to full output current. The controlled switches in the active filter only have to be rated to 30% of the full output current to ensure complete compensation for the distortion produced by the rectifier and DC link current shaping circuit.

The active filter connection to the controlled current boost converter system is initially computer simulated to gain an understanding of operation and performance, then experimental verification is obtained by the development of a hardware prototype.

8.2.1 Computer Simulation

To simulate operation of the active filtering system compensating for the line current produced by the boost converter system the input line current I_L (Figure 8.7) is calculated as described by Kolar [Kolar et al. 1990]. This calculated line current is used as the load current input to the active filter simulation. From the computer simulation, Figure 8.8(a) shows the 5 A line current for one 50 Hz cycle. The required compensating current I_c is shown in Figure 8.8(b) and the compensated supply current I_s (Figure 8.8(c)) is now nearly sinusoidal, the THD has been reduced from 25.2% to 3.6%. The

small notches which appear in the compensated supply current are due to the inability of the power amplifier of the active filter to reinject current at a sufficient rate to follow the compensating current signal.

The computer simulation results have shown that the active filter connected to the controlled current boost converter will result in a near sinusoidal supply current.

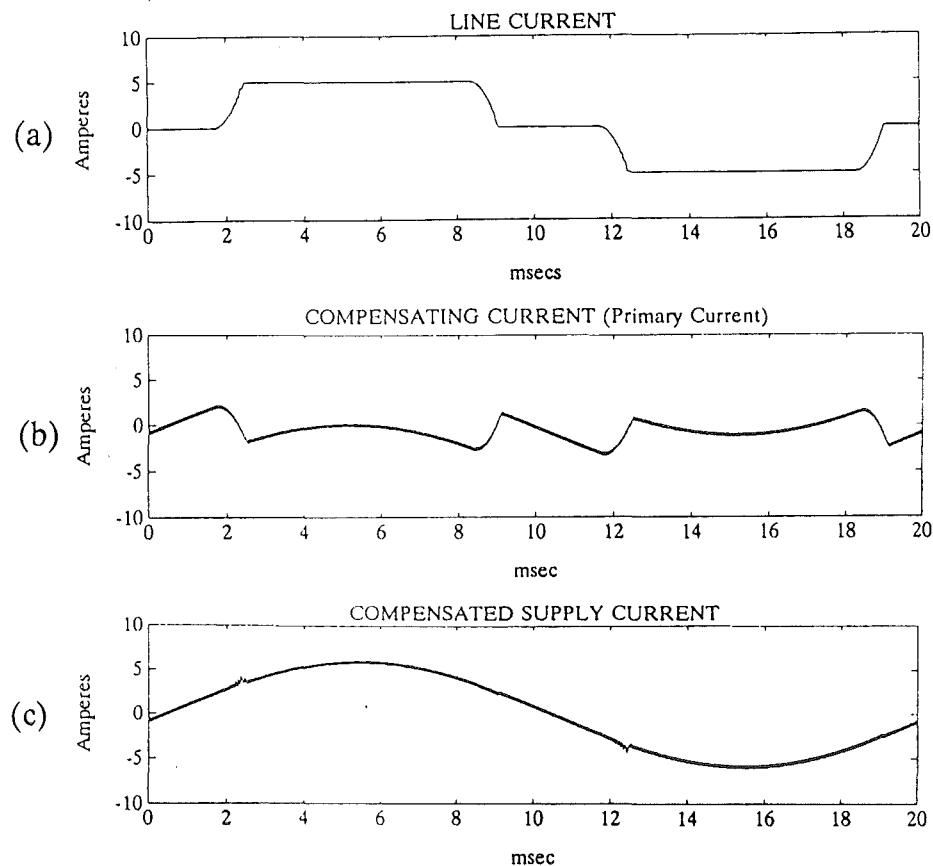
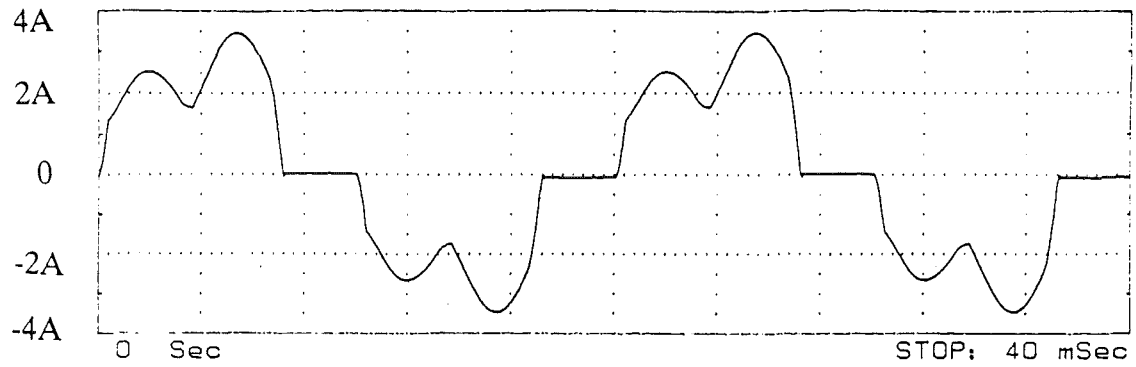


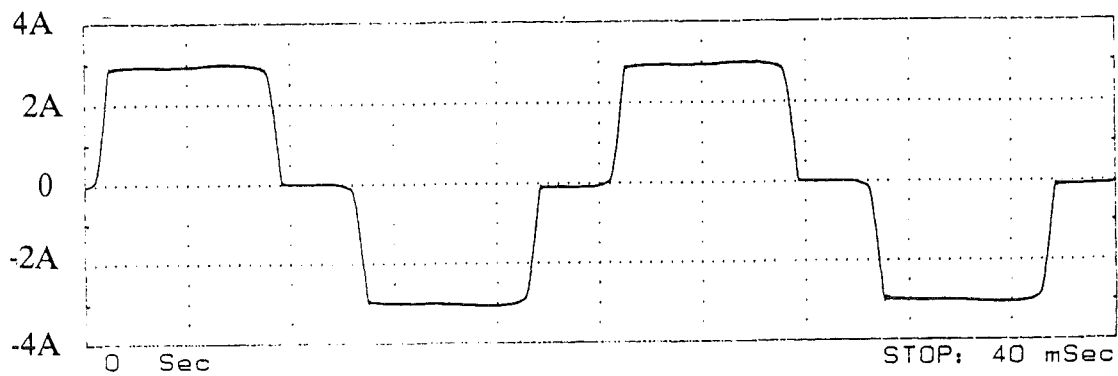
Figure 8.8 Computer Simulation of the Active Filter and Controlled Current Boost Converter

8.2.2 Hardware Model

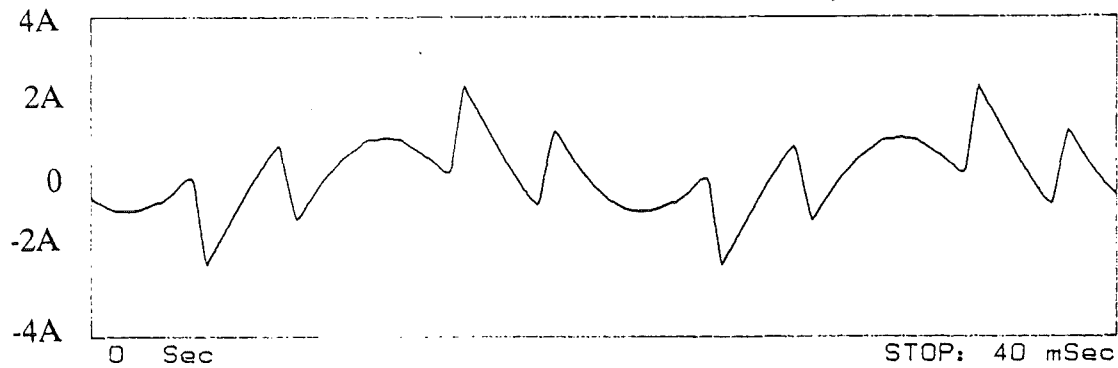
To demonstrate the principle of operation of the active filter and controlled current boost converter system a low supply voltage (50 V line to line) hardware model has been built and tested. When a three phase bridge rectifier with capacitive and resistive load are connected to the power system a double peaked current as shown in Figure 8.9(a) is drawn from the supply. This line current has 34% THD and the DC output voltage is 64 V_{DC}. Connecting a controlled current boost converter between the rectifier and capacitive-resistive load the output voltage can be increased to 85 V_{DC} with



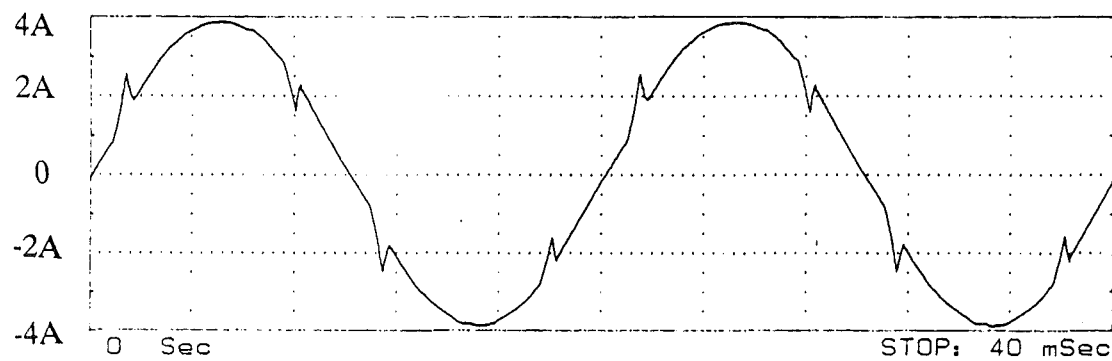
(a) Supply Current (Bridge Rectifier with Capacitor Resistive Load Only)



(b) Supply Current (Boost Converter)



(c) Compensating Current of Active Filter



(d) Supply Current (Boost Converter & Active Filtering)

Figure 8.9 Hardware Test Results of the Active Filter and Controlled Current Boost Converter

the supply current distortion being reduced to 25% as shown in Figure 8.9(b).

When the three phase active filter is connected between the supply and rectifier-boost converter combination the active filter's compensating current, as shown in Figure 8.9(c), is produced. This results in the compensated supply current (Figure 8.9(d)) becoming nearly sinusoidal and the THD has been reduced to 4.9%.

As with the computer simulation in the previous section small spikes are superimposed on the actual compensated supply current during the time the bridge rectifier diodes are commutating. These spikes are due to the active filter's inability to reinject current fast enough to fully compensate.

8.3 SUMMARY

Two new applications of active filtering have been discussed. The first application dealt with filtering a variable frequency system and the second with a three phase bridge rectifier-controlled current boost converter combination.

When a weak power system, such as an individual generator, supplies a load that produces harmonic current distortion, the generator voltage can become contaminated by that distortion. It has been demonstrated experimentally that by connecting an active filter to a weak power system the supply current not only becomes nearly sinusoidal, but the distortion in the supply voltage can also be improved.

The operation of the active filter in a variable frequency system has also been demonstrated. For generation systems that operate over a frequency range in order to operate at their most efficient point, passive tuned filters can not be employed to improve the generator's voltage and current when a non-linear load is connected. The active filtering technique is not frequency dependent and therefore can be used on distortion producing loads at variable supply frequencies.

The second application of active filtering was to achieve a sinusoidal supply current from a three phase bridge rectifier-controlled current boost converter combination. The combination of the active filter and boost converter produces a near sinusoidal supply current and a higher output DC voltage than is possible from just a bridge rectifier operating from the system voltage. A rectifier system using 6 fully controlled switches can produce sinusoidal supply currents and a high DC output voltage. However, such a system requires the use of 6 switches rated at the full load current. Using an active filter with a three phase rectifier and DC link current shaping converter, only one switch rated at full load current is required in the converter while the active

filter switches only have to be rated to 30% of the full output current.

CHAPTER 9

RESONANT LINK ACTIVE FILTER

The active filter, as described in previous chapters, uses a power amplifier with a topology in which the power devices (IGBTs) dissipate power each time they are switched. This power dissipation is known as switching loss. Topologies including power devices which operate in this way are generally known as hardswitched converters. For hardswitched converters in the range of 1 kW to 50 kW, the switching losses can be 30-50% of the total device loss [Divan, Skibinski 1989a].

Device switching losses can be practically eliminated by switching the power devices under zero voltage or zero current conditions [Bose 1992b]. To achieve zero voltage (ZVS) or zero current switching (ZCS) a resonant inductor-capacitor topology is usually implemented. These topologies are commonly known as resonant converters [Mohan, Undeland, Robbins 1989].

The hard switching of semiconductor devices produces high rates of rise of both voltage and current, which result in turn in electromagnetic interference (EMI). By using resonant converters with zero voltage and/or zero current switching, EMI is reduced due to the lower rates of rise of voltage and current.

Operating the hardswitched converters at low frequencies to reduce switching losses results in higher levels of acoustic noise and low bandwidth in the output current waveform [Divan 1989b]. The use of a zero switching loss converter permits the switching frequency to be increased, resulting in an increase in the output current bandwidth and a lowering of the acoustic noise for higher power level converters.

Resonant converter topology can be divided into four main classes [Mohan et al. 1989] and are listed as follows:

- load resonant
- resonant switch
- high frequency link integral half cycle
- resonant DC link

Load resonant converters require an oscillating voltage and current to be applied to the load in order to provide zero voltage and/or zero current switching. Resonant switch converters use an inductor-capacitor topology to shape the switch voltage and current waveform to obtain lossless switchings. The high frequency link uses a high frequency sinusoidal AC waveform to synthesis a lower frequency AC waveform. In resonant DC link converters the output voltage is made to oscillate around a fixed DC input voltage. The output voltage is controlled so that it remains zero for a certain time

and during this time any connected circuit can be zero voltage switched.

A modified resonant DC link converter can be used with the hardswitched active filter to produce ZVS. The resonant action modifies the DC bus voltage and produces a resonant link voltage for the standard active filter configuration as shown in Figure 9.1. The resonant DC link topology used with the active filter only allows a forward current flow. Since the active filter requires a bidirectional power flow to store energy on the DC bus capacitor a reverse current path has to be added.

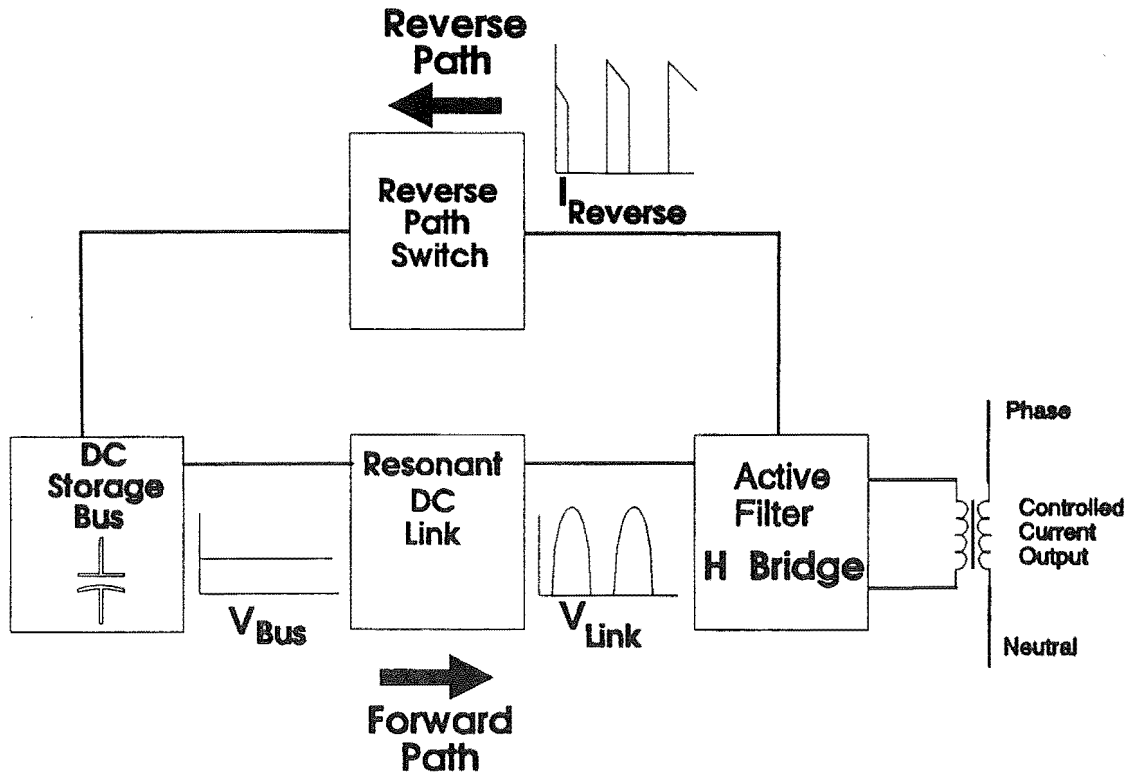


Figure 9.1 Block Diagram of Resonant Link Active Filter

The detail and mathematical analysis of the resonant DC link is presented in the next section. This is followed by descriptions of a hardware model of the resonant DC link, computer simulation of the resonant link active filter and the evaluation of hardware performance of the resonant link active filter.

9.1 ANALYSIS OF RESONANT LINK BEHAVIOUR

The resonant link circuit, shown in Figure 9.2, consists of an energy storage bus capacitor C_B , charged to an initial voltage of V_B , a resonant inductor L , resistor R , and resonant capacitor C_R . A thyristor T , controls the start of the positive resonant cycle and

prevents the negative resonant cycle from occurring. The resistor R , is used to model the losses associated with the conduction of the thyristor, resistance of the inductor and the equivalent series resistance of the capacitors C_B and C_R . Initially it is assumed that the thyristor T is off, C_R is discharged and that a load current I_L is freewheeling through the diode D . Throughout one resonant cycle the load current is assumed constant since it is flowing through an inductive load (reinjection transformer in the active filter) and therefore can be represented as a constant current source. The bus capacitor is usually much larger than the resonant capacitor and therefore over one resonant cycle the voltage on the bus capacitor would only fall a small amount. To mathematically analyse the resonant cycle (a full mathematical analysis is contained in Appendix A), the bus capacitor is assumed to be a voltage source V_B .

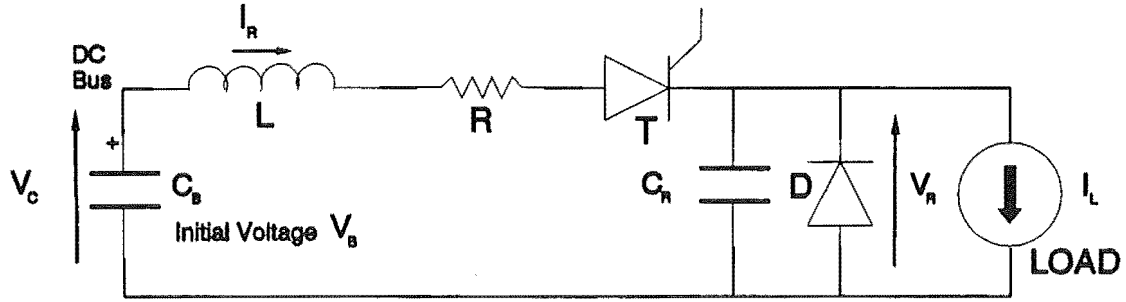


Figure 9.2 Resonant Link Converter Circuit for Active Filter

When the thyristor is turned on at time $t=0$, the diode continues to freewheel and the resonant current I_R increases as defined by Equ. (9.1).

$$i_R(t) = \frac{V_B}{R} (1 - e^{-\frac{R}{L}t}) \quad (9.1)$$

When the resonant current is equal to the load current, $i_R(t) = I_L$, the diode turns off, allowing the resonant capacitor to charge. The diode turns off at a time t_1 , which is defined by Equ. (9.2).

$$t_1 = -\frac{L}{R} \ln \left(1 - \frac{I_L R}{V_B} \right) \quad (9.2)$$

The inductor and resonant capacitor form a resonant circuit when the thyristor is on and the current flowing in the inductor is greater than I_L . The resonant current which flows in this circuit for time greater than t_1 is defined by Equ. (9.3)

$$\begin{aligned}
 i_R(t) = & \frac{V_B}{\omega L} \frac{1}{\sqrt{1-\delta^2}} e^{-\delta\omega(t-t_1)} \sin(\omega\sqrt{1-\delta^2}(t-t_1)) \\
 & + I_L \left(1 - \frac{1}{\sqrt{1-\delta^2}} e^{-\delta\omega(t-t_1)} \sin(\omega\sqrt{1-\delta^2}(t-t_1) + \phi) \right) \\
 & - \frac{I_L}{\sqrt{1-\delta^2}} e^{-\delta\omega(t-t_1)} \sin(\omega\sqrt{1-\delta^2}(t-t_1) - \phi)
 \end{aligned} \tag{9.3}$$

where $\phi = \tan^{-1} \frac{\sqrt{1-\delta^2}}{\delta}$

and where

$$\omega = \sqrt{\frac{1}{LC_R}} \text{ and } \delta = \frac{R}{2} \sqrt{\frac{C_R}{L}} \tag{9.4}$$

A resonant voltage builds up across C_R once the resonant current flowing in the inductor is greater than the load current and the freewheeling diode has turned off. The time it takes for the positive resonant current cycle is dependent on the value of inductance L , and the resonant capacitor C_R . From Equ. (9.3) it can be seen that the peak value of current in the inductor is also dependent on the combination of the inductor and resonant capacitor values. The resonant voltage, $v_R(t)$ can be calculated from Equ. (9.5) using ω and δ as defined in Equ. (9.4).

$$\begin{aligned}
 v_R(t) = & (V_B - I_L R) \left(1 - \frac{1}{\sqrt{1-\delta^2}} e^{-\delta\omega(t-t_1)} \sin(\omega\sqrt{1-\delta^2}(t-t_1) + \phi) \right) \\
 & \text{where } \phi = \tan^{-1} \frac{\sqrt{1-\delta^2}}{\delta}
 \end{aligned} \tag{9.5}$$

When the thyristor turns off, once the resonant current goes negative, the resonant capacitor has reached a value which is greater than V_B . The resonant voltage then falls linearly until the resonant capacitor has been discharged to zero volts. At this point the freewheeling diode starts to conduct the load current and zero voltage remains on the resonant capacitor until the thyristor is turned on again and the resonant cycle restarted. Since zero voltage exists on the resonant capacitor any device connected to the output of the resonant DC link is able to switch under zero voltage conditions.

Using a value of $125 \mu\text{H}$ for the inductor and $3 \mu\text{F}$ for the resonant capacitor it is possible to calculate the resonant current and voltage waveforms produced for various load currents and initial bus voltages using Equ.s (9.1), (9.3) and (9.5). A resistor R , of one ohm, is used as an estimation of the thyristor conduction and resonant link resistive losses. The calculated resonant current and voltage for an average load current of 2 A and an initial DC bus voltage (V_B) of 60 V are presented in Figure 9.3.

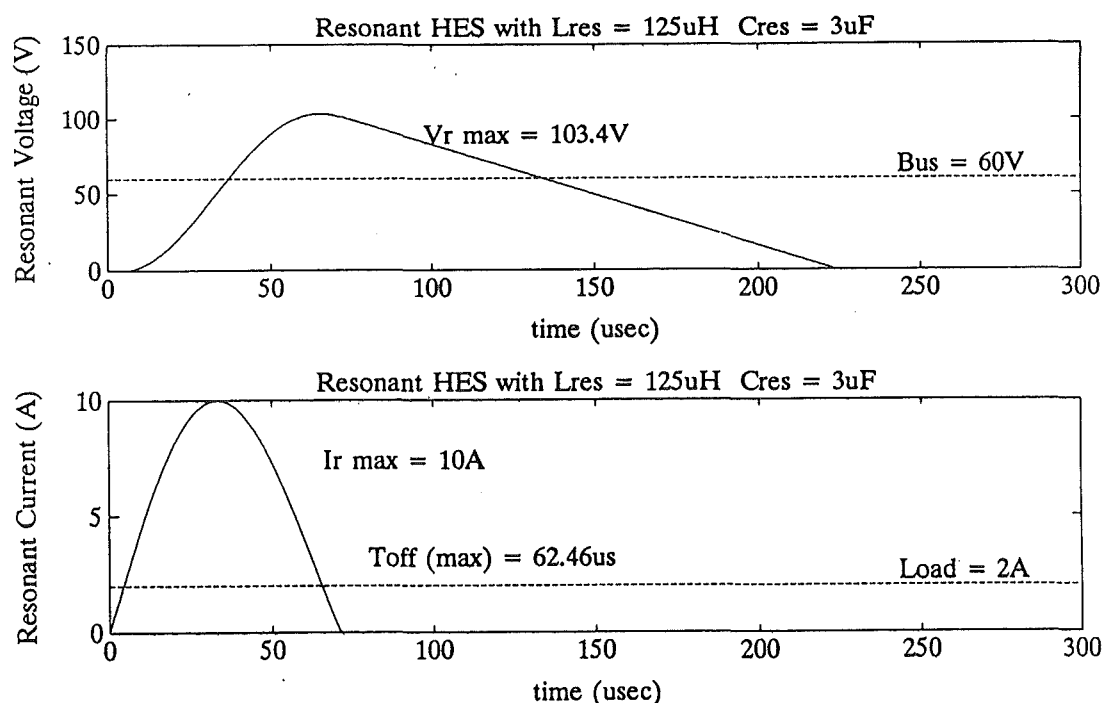


Figure 9.3 Resonant Current and Voltage Analytically Calculated

From the initial bus voltage of 60 V_{DC} , the resonant voltage reaches a peak of 103.4 V in $65.1 \mu\text{s}$, while the positive resonant current pulse lasts for $71.6 \mu\text{s}$. The peak of the resonant current is 10.0 A, which is high in comparison to the average load current of 2 A. This illustrates the disadvantage of this particular resonant link configuration where high pulse currents flow in the resonant components when a relatively low load current is supplied. The resonant voltage across C_R discharges linearly once the thyristor

turns off at 71.6 μs and reaches a level of zero volts after a further 152.4 μs . Therefore the total resonant period lasts for 224.0 μs , which allows a maximum repetition frequency of 4.4 kHz for the 2 A load current.

The peak of the resonant current is mainly determined by the first term in Equ. (9.3). Since the initial bus voltage is fixed, the peak current can be limited by the resonant frequency and inductance term (ωL). This term ωL is dependent on the square root of the ratio of L and C_R (Equ. (9.6)) and is known as the characteristic impedance Z_0 [Mohan et al. 1989]. Therefore if the inductor is too small then the resonant current has a very high peak. This increases the conduction losses and the resonant components have to be designed to handle these peak levels, which are much greater than the average level.

$$\omega L = \sqrt{\frac{L}{C_R}} = Z_0 \quad (9.6)$$

A further consideration is the operating frequency of the resonant cycle as defined in Equ. (9.4). The inductor and resonant capacitor values determine the resonant frequency. Ideally for the active filter application, high frequency operation without the high inductor peak currents is required. This would allow the resonant link to produce sufficient current to follow a fast changing compensating current signal. If the resonant capacitor is large, the discharge time to achieve zero voltage switching for a given load current is longer, thus reducing the possible switching frequency of the resonant circuit.

The positive resonant current cycle occurs only when the thyristor is conducting. Once the resonant current attempts to flow in a negative direction the thyristor switches off. Under certain conditions it is possible that the thyristor becomes continuously forward biased because the voltage on C_R becomes less than the voltage on C_B before the resonant current reaches zero. Therefore the thyristor will never switch off and the resonant converter will lose resonance, a resonant failure.

A resonant failure is caused by excessive load current discharging the resonant capacitor below the voltage level of the DC bus capacitor before the thyristor turns off. This resonance failure is predicted by the mathematical analysis and is shown in Figure 9.4. Using the same condition as in the previous example, with the exception that the load current is increased to 6 A. Resonance fails because the resonant current in Figure 9.4(b) does not reach zero (allowing the thyristor to turn off) before the resonant voltage becomes less than the bus voltage. The thyristor remains forward biased and allows the resonant current to start to increase. Resonance continues until the resonant oscillations

damp out and the resonant voltage tends toward the bus capacitor voltage and the resonant current tends towards the constant load current. To regain resonant operation the resonant capacitor's voltage has to be increased or the bus capacitor's voltage lowered to reverse bias the thyristor and force it to turn off.

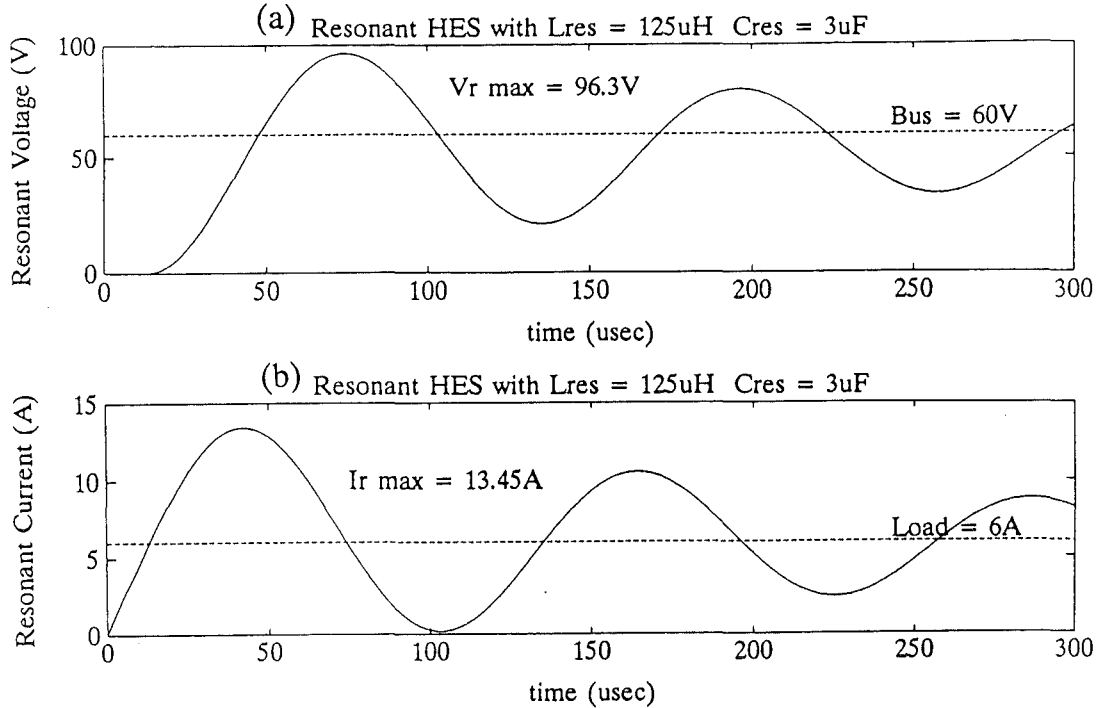


Figure 9.4 Failure of the Resonant Cycle due to the Thyristor being Continually Forward Biased

To ensure that resonance does not fail, a turn off time must exist when the current in the inductor has reached zero, to allow the thyristor to reverse recover before becoming forward biased. If high current and frequency operation is required a fast thyristor must be used with a short turn off time. A MOS Controlled Thyristor (MCT) could be used, it has a fast turn off time and forced turn off capability via gate control [Bose 1992b]. So if a resonant failure did occur the control circuitry would have the ability to restart resonance without having to discharge the bus capacitor.

9.2 HARDWARE MODEL

A hardware model of the resonant link is used to investigate the actual performance of the thyristor controlled resonant link topology. The resonant link is connected to an inductive and resistive load as shown in Figure 9.5. The power for the resonant link is supplied by a 60 V_{DC} external source. A controller turns on the thyristor

when the resonant voltage is zero and the load current is below some preset level. The resonant circuit consists of $125\ \mu\text{H}$ and $3\ \mu\text{F}$, the same component values which were used in the mathematical analysis in the previous section. The decision in choosing the resonant components is complex, as there are many possible trade-offs between peak currents and/or voltages, resonant frequency and maximum switching frequency of the thyristor [Divan 1991].

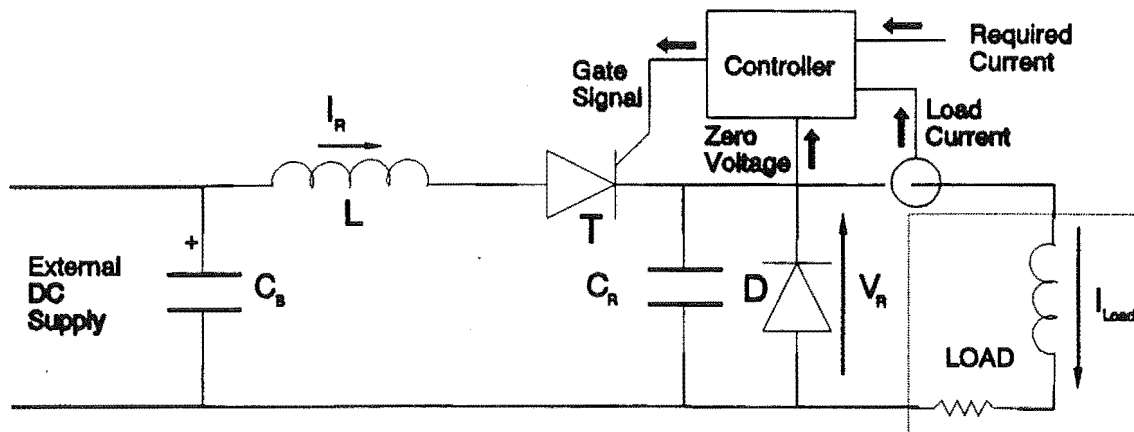


Figure 9.5 Hardware Implementation of Resonant Link Model

Initially the thyristor is turned off, the resonant voltage is zero and a controlled average current of 2 A flows in the load circuit. When the thyristor is fired, the inductor current follows a half resonant cycle as shown in Figure 9.6(a). The inductor current lasts for $96\ \mu\text{s}$ and has a peak of 10 A. The resonant capacitor voltage (Figure 9.6(b)) builds up to a maximum of 100 V with the voltage falling before the end of the resonant current pulse. The resonant voltage falls because the load current is greater than that supplied from the resonant inductor and the additional current is drawn from the resonant capacitor. Once the thyristor switches off the resonant capacitor discharges into the load and the voltage falls linearly. The total resonant cycle time from zero voltage on the resonant capacitor to zero voltage again is $192\ \mu\text{s}$ or a possible maximum repetition frequency of 5.2 kHz for this particular constant load current level.

As the level of load current changes, the frequency at which the resonant link operates also changes as illustrated in Figure 9.7. When the load current is increased from zero to 2 A, the discharge time of the resonant capacitor becomes smaller. Resonant operation stops when the set level of current (2 A) is achieved in the load. The peak of the resonant voltage decreases as the load current increases. This occurs because the freewheeling diode does not turn off until the resonant inductor is supplying a current greater than the load current. Therefore at higher load current levels, the peak

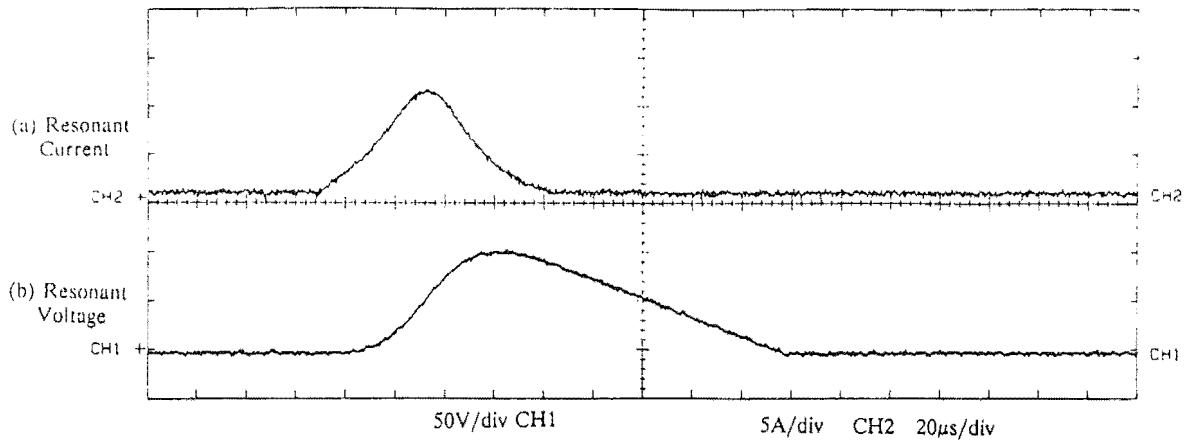


Figure 9.6 Resonant Switching Cycles for the Hardware Model

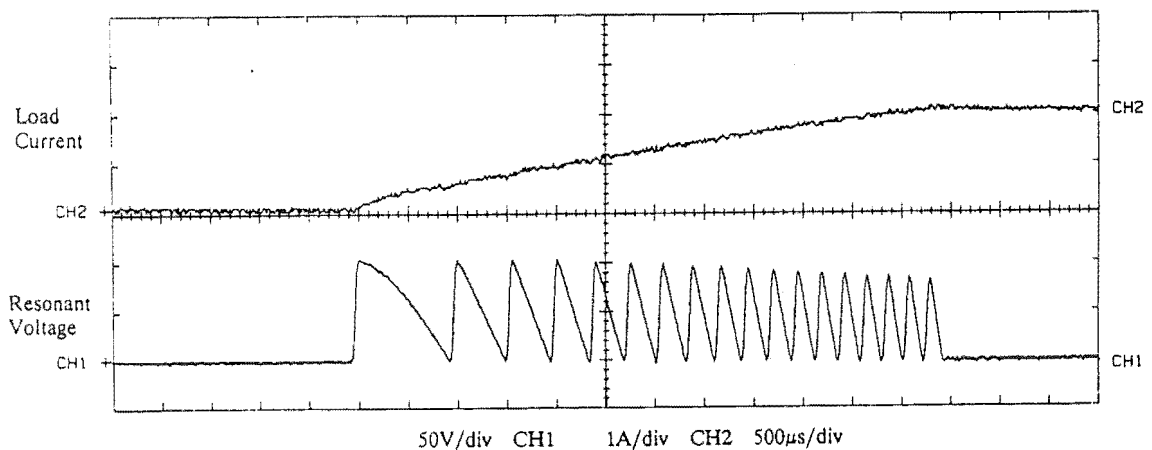


Figure 9.7 Operation of the Resonant Capacitor Voltage as the Load Current Ramps Up

voltage on the resonant capacitor is always less than twice the DC supply voltage.

For the resonant link configuration to operate with the active filter there must be an opportunity for zero voltage switching and the ability of the resonant link to produce sufficient current to follow the compensating current signal. For example, the ability of the resonant link converter to follow a rectified sinusoidal current signal is presented in Figure 9.8. The resonant link is able to provide a current which follows the required 50 Hz rectified sinusoidal waveform. Once the current in the load has increased past the reference level due to the resonant cycle, the load current decreases by freewheeling through the diode D , and the energy stored in the load inductor is dissipated in the load resistor. The rate of current fall in the load is controlled by the load inductor and resistor combination and not by the resonant link. At low load current levels the output current of the resonant circuit overshoots the required current level. At high current levels the resonant link circuit is able to better follow the required current signal.

To follow the required current signal accurately at lower current levels, the

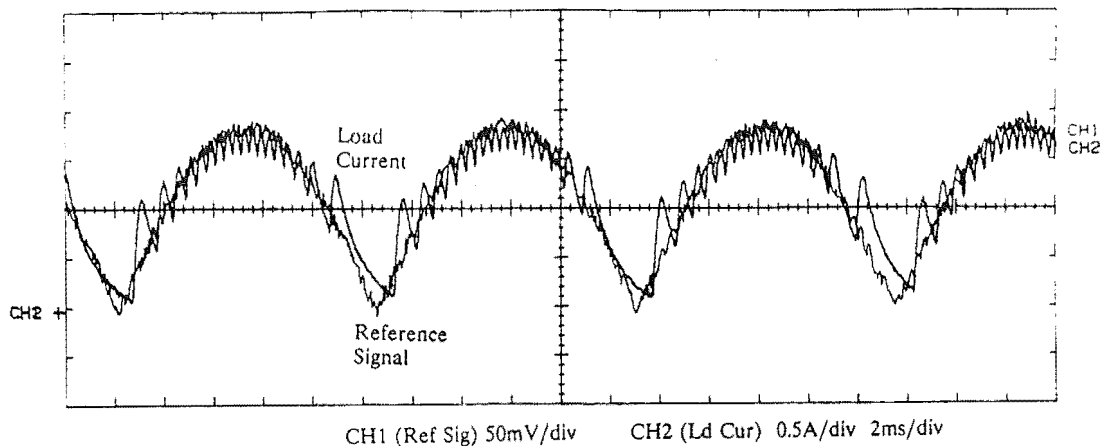


Figure 9.8 Ability of Resonant Link Converter to follow an Arbitrary Waveform

resonant inductor value needs to be increased to reduce the peak current. However this limits the maximum amount of load current that the resonant circuit can provide before the resonant action fails. To overcome this limitation it would be possible to construct a resonant converter with multiple inductors and thyristors as shown in Figure 9.9. If the inductor L_1 has a larger value than inductor L_2 , the resonant combination of L_1 and C_R (controlled by firing T_1), results in the resonant cycle having a lower peak current and lower frequency. This multiresonant link circuit would be able to follow more accurately the lower current levels of the compensating current signal waveform, while the L_2 and C_R combination would be used to supply higher level currents.

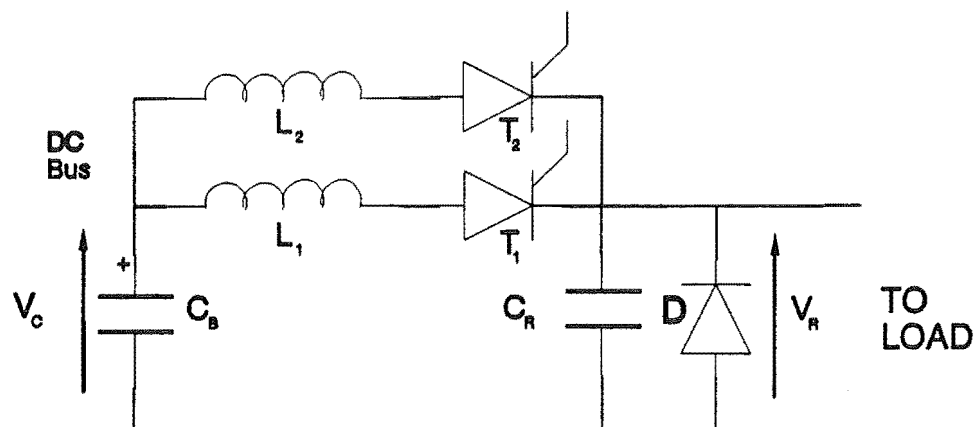


Figure 9.9 Multiresonant Link Circuit to Improve Performance at Low Load Current Levels

9.3 COMPUTER SIMULATION OF A RESONANT ACTIVE FILTER

As has been shown, the resonant link converter is able to provide a resonant DC bus to enable zero voltage switching. The computer simulation technique described in Chapter 3 is used to investigate the feasibility of incorporating a resonant link into an active filter.

The active filter has a bidirectional power flow and therefore a reverse path to supply power to the bus capacitors is required (Figure 9.1). This reverse power flow and the resonant operation adds to the complexity of the required computer model. In Chapter 3 (Section 3.2) it was shown that only two topologies were required to model the active filter. To model a resonant link active filter requires these two topologies in association with another three resonant topologies. A resonant topology is required for the resonant current cycle when the thyristor is on, another topology for the period while the resonant capacitor is discharging and another topology for the period while the load current is freewheeling. This results in a total of six topologies being required to simulate the resonant link active filter.

The resonant link active filter is computer simulated for steady state operation. Compensation is provided by the active filter for the current drawn by a single phase bridge rectifier with a capacitive and resistive load. The load current (Figure 9.10(a)) has a peak of 8 A and a THD of 103%. To compensate for this particular load the resonant link is operated with a DC bus voltage of 350 V_{DC}, resonant inductor of 125 μ H and resonant capacitor of 0.47 μ F. The compensating current shown in Figure 9.10(b) is referred to the amplifier side of the reinjection transformer (see Figure 4.1) and has a peak current of 10 A. When the compensating current is low the resonant link produces large current excursions. At high levels of compensating current, double resonant cycles are needed to reach the required compensating current level. Reinjecting this compensating current, the compensated supply current is shown in Figure 9.10(c). The compensated supply current now follows a fundamental sinusoidal waveform, however it contains a number of low switching frequencies. The THD of the compensated supply current has been reduced to 31.2% compared to the 7.0%, which is possible with the standard active filter (operating with an average switching frequency of 25 kHz) for this particular load.

The resonant current and voltage are shown in Figures 9.10(d) and (e) respectively. To supply a compensating current of up to 10 A, the resonant current reaches levels of 30 A, with an average peak current level of 25 A, and the resonant

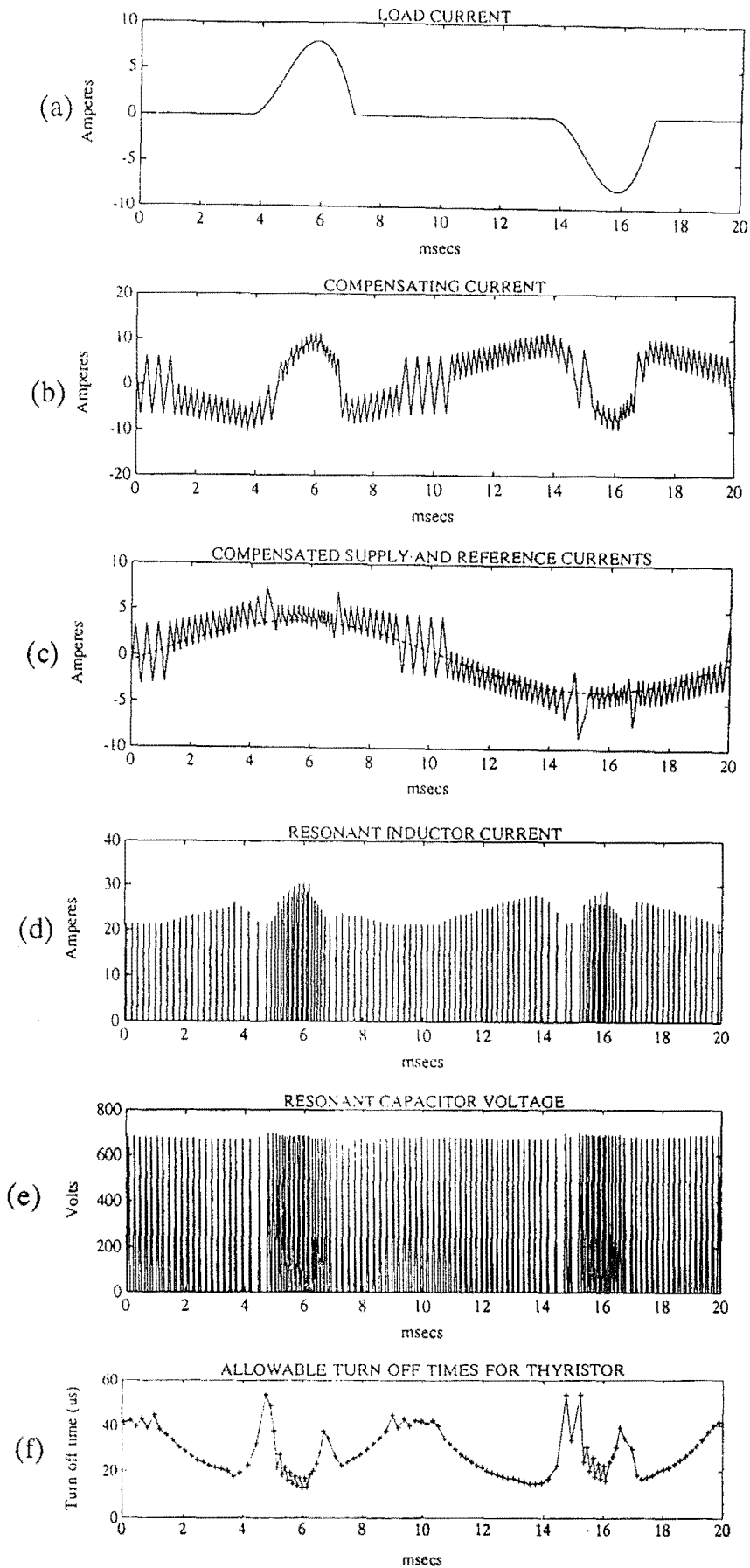


Figure 9.10 Computer Simulated Performance of the Resonant Active Filter

capacitor voltage reaches a peak of $680 V_{DC}$. The disadvantage with this resonant link configuration is the high level of resonant voltage, which increases the required voltage rating of the power devices in the active filter.

An important aspect to consider in the resonant active filter is the prevention of resonance failure due to excessive compensating current requirements. Therefore the turn off time of the thyristor has to be less than the time between reaching zero resonant current and the thyristor becoming forward biased. Figure 9.10(f) presents the turn off times available to the thyristor through out the compensating process. During the time when the resonant link has to supply the greatest amount of compensating current, 5 to 7 ms and 15 to 17 ms, the shortest time is available for the thyristor to turn off. For this particular load type, the turn off time of the thyristor must be less than $12 \mu s$ to prevent a resonant failure. This level of turn off time is only available in the smaller thyristor devices and therefore a MCT would be a more suitable device as its turn off times are less than $3 \mu s$ for higher rated devices [Bose 1992b].

The advantage of implementing a resonant link active filter is that the switching losses are reduced due to zero voltage switching. Using the computer simulation, the active filter was simulated under the same conditions for operation with and without a resonant link. The losses produced by various components in both resonant and non resonant active filtering modes are presented in Table 9.1.

The switching losses in the active filter have been reduced by using the resonant link. However the resonant link itself has introduced additional losses. Overall the additional losses of the resonant link are smaller than the reduction in switching loss, therefore it could be beneficial to incorporate the resonant link in the active filter from an efficiency point of view. However the additional cost of the resonant link would have to be investigated before the full benefit (if any) of the resonant link as an addition to the active filter could be made.

TABLE 9.1 Comparison of Losses with and without a Resonant Link Converter

TYPE OF LOSS	Active Filter (Avg Frequency $\approx 25\text{kHz}$)	Resonant Active Filter (Avg Frequency $\approx 7\text{kHz}$)
IGBT - Conduction	10.7	8.6
IGBT - Switching	71.6	12.5
Diode - Conduction	7.4	9.6
Diode - Switching	1.9	0.1
Transformer & R_{SENSE}	15.1	21.3
Thyristor - Conduction	-	3.7
Thyristor - Switching	-	0.5
Resonant Inductor	-	5.3
TOTAL LOSS (W)	106.7	61.6

9.4 HARDWARE IMPLEMENTATION OF THE RESONANT LINK ACTIVE FILTER

The implementation of a low voltage (100 V_{DC}) resonant link active filter was carried out by Laird [Laird 1992a] as part of a Masters degree project. Laird designed and constructed the control circuitry and carried out modifications to the power circuitry in order to operate the active filter in both resonant and non resonant modes.

A hardware schematic of the resonant link active filter system is shown in Figure 9.11. During the course of this work it was discovered that additional components were required for the resonant link to operate with the active filter. Diodes D5 and D6 along with thyristor T_{Ret} are required to provide the return path of current to the main energy storage capacitor C_{Bus} . This allows the resonant link active filter to have a bidirectional power flow. The thyristor T_{Ret} allows the current to flow only when the freewheeling of the compensating current is required and blocks the possible current path back to C_{Bus} during a resonant cycle. Diodes D7 and D8 are required to prevent the freewheeling load current from flowing into the resonant capacitor. Additional control was necessary to co-ordinate the active filter and the resonant link.

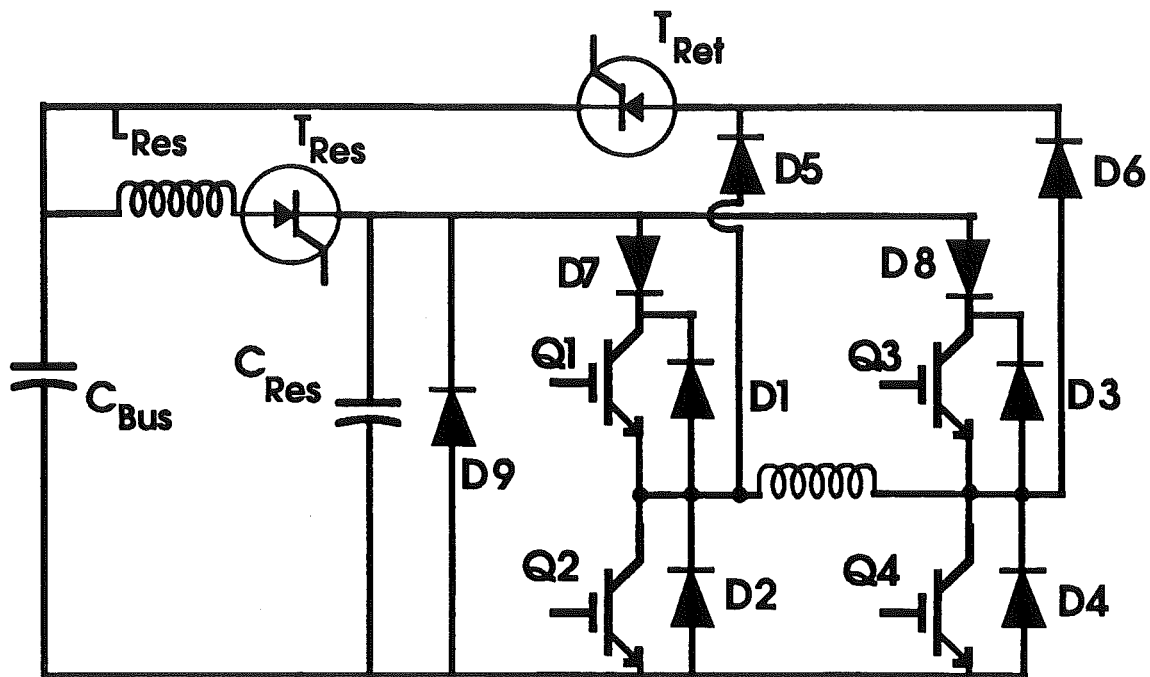


Figure 9.11 Final Hardware Implementation of the Resonant Link Active Filter [Laird 1992a]

The resonant link requires a fast thyristor T_{Res} (short turn off times) to operate the active filter for higher compensating current levels. Ideally a MCT would be a good choice for the resonant thyristor, however these devices are not yet commercially available in New Zealand. Laird constructed a hardware model of a MCT using conventional IGBTs, diodes and discrete control circuitry [Laird, Duke 1992b]. This hardware model is functionally equivalent to the MCT, but has a larger on state voltage drop. Operation of the resonant link active filter, with a similar load to that used in the computer simulation in the previous section, is illustrated in Figure 9.12.

The compensating current (Figure 9.12(a)) has large excursions at low current levels. These large current excursions result in low frequency components in the supply current (Figure 9.12(b)). The supply current has a sinusoidal form and the THD has been reduced from 51.5% to 16.8%. The waveforms presented here have a very similar characteristic to those obtained from the computer simulation illustrated in Figure 9.10.

The efficiency of operation for the resonant link active filter was measured at 66% compared to the operational efficiency of the non resonant active filter of 82% for the same load current [Laird 1992a]. The losses produced by the additional components required to construct the resonant active filter greatly outweigh any benefits from the reduction of switching loss. If an actual MCT with a lower on state voltage was

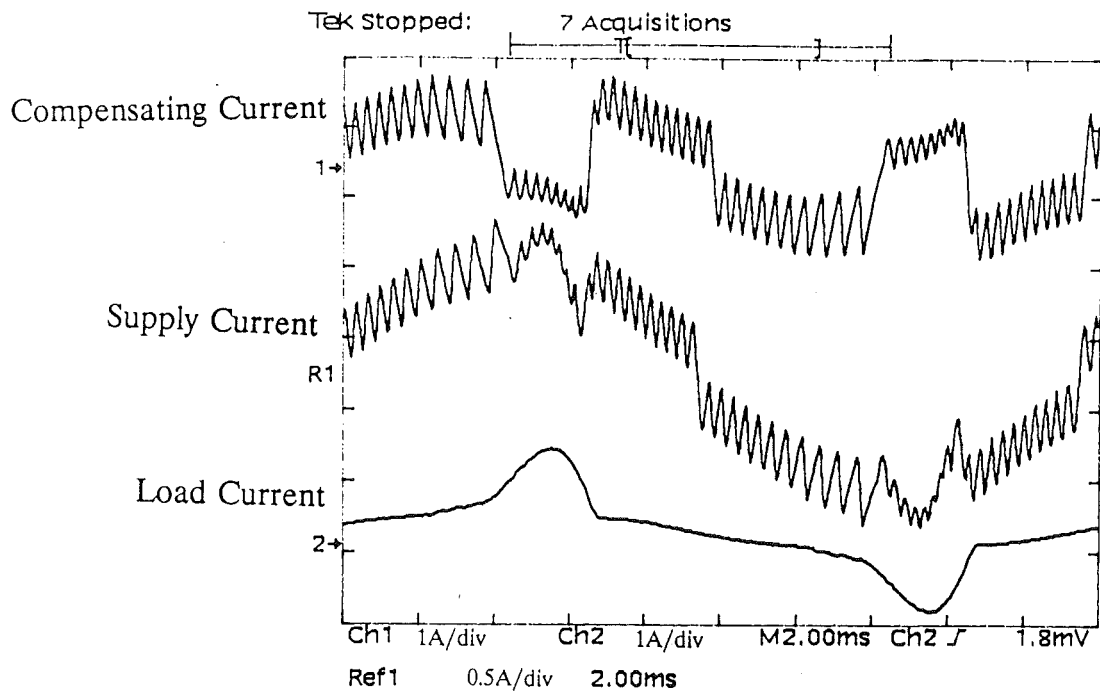


Figure 9.12 Supply, Compensating and Load Currents during Operation of the Resonant Link Active Filter

substituted for the MCT model an improvement in the resonant link active filter's efficiency could be made.

9.5 SUMMARY

To reduce the switching losses of the hardswitched active filter described in previous chapters, a resonant link active filter has been proposed. The resonant current and voltage of the resonant link were mathematically defined and operation of the resonant link described. Operation of the resonant link has been demonstrated, showing that zero voltage switching can occur.

A computer simulation of the resonant link active filter was developed to investigate the possible reduction in switching loss. The computer simulation results also showed that the resonant link active filter was able to compensate for harmonic distortion produced by nonlinear loads.

A hardware version of the resonant link active filter was constructed as part of a Masters project. Due to the extra complexity of the circuit and the use of a MCT model, the efficiency of the operation of the resonant active filter is lower than the equivalent hardswitched active filter. The use of an actual MCT would increase the

efficiency of the resonant link active filter which might make the additional complexity worthwhile in reducing switching losses at higher bus voltages.

CHAPTER 10

DISCUSSION and CONCLUSION

10.1 FUTURE WORK

The ability of single and three phase analogue active filters to remove supply current distortion has been demonstrated. Based on the performance of the analogue single phase active filter a digitally controlled active filter was constructed. The digital controller automatically adjusted the operation of the active filter to optimise the financial savings gained by reducing the current distortion.

During this work many different types of load current waveforms have been compensated for, many more than could be presented in this thesis. The active filter has been able to remove the harmonic and displacement components from the supply current for all of these cases. A limitation exists on the ability of the active filter to compensate for fast changing load current waveforms. If a load current waveform contains a sharp discontinuity, such as a triac controlled resistive load, the active filter system cannot completely compensate at the instant of the discontinuity [Henderson 1989]. A certain time delay occurs before the active filter can continue to provide full compensation. Such fast changing waveforms however usually have a small effect on the active filter's total compensation ability.

During these tests other interesting ideas and performance measurements could be carried out, but time has limited the study of these. This section presents some of the possibilities for future work related to both analogue and digital versions of the active filter for both single and three phase loads.

10.1.1 Optimisation Techniques

The digitally controlled active filter is operated so it can reduce supply current distortion, while operating with a high level of efficiency. To achieve this, a savings function was derived and an optimisation procedure to find the point of maximum savings was implemented.

The simplex optimisation technique was implemented, however this method has the disadvantage that history terms are used in the calculation of the path to the maxima. In conditions of changing load current, the savings surface also changes. The simplex method may be unable to independently track these changes because the history terms are invalid. Once a load change is detected by the existing controller the history terms

are recalculated and the optimisation procedure then starts to head towards the new maximum savings point.

It would be more efficient if the history terms could be used in such a way that they speed the search to the maxima, without impeding the search after a load change. A possible alternative once the load change is detected is for the optimisation algorithm to remeasure only one of the history terms. The other history terms can then be scaled depending on the difference between the old and new remeasured history term value. This technique should be tested to ensure it is suitable for this application. Other optimisation procedures exist, such as the direction-set method [Press et al. 1986], which may be more suitable for the optimisation of savings for load changing systems.

10.1.2 Bus Voltage Control

The DC voltage on the power amplifier bus capacitor is used to control the magnitude of the synthetic sinusoid. A proportional-integral controller has been implemented which provides an adequate transient response (within a few fundamental cycles) to step changes in load current. An improvement can be made to the transient response of this controller by an additional feed forward controller.

The feed forward controller used a differentiator to detect load current changes. However the differentiator can produce false outputs due to noise contamination on the input signal. A suggestion for future work, to improve the noise immunity of the feed forward controller, is to replace the differentiator with a suitable bandpass filter. This bandpass filter would have a high frequency cutoff which would reject switching noise, but still be able to detect load current changes.

In the present implementation of the feed forward controller a fixed threshold level is used to determine if a load change has occurred. A fixed threshold level can produce errors when low levels of load currents are being drawn. A fixed threshold level is determined so that the output of the differentiator is not above the threshold level for the greatest value of steady state load current. For low current levels, a step change in load may occur and the feed forward controller may not detect this change as the output of the differentiator is not greater than the set threshold. To overcome this limitation an adaptive threshold system could be investigated which would adjust the level of threshold depending on the level of, say, RMS load current. This adaptive threshold system would improve the performance of the feed forward controller.

An alternative method to detect whether a load change has occurred is to store

the data from the previous load current period and then compare it with the present period measured load current data. An appropriate filter would have to be used to ensure noise contamination of the sampled data does not falsely operate the feed forward controller.

10.1.3 Phase Balancing

The three phase active filter can be used to balance the supply currents in each phase for an unbalanced harmonic load. However, by increasing the level of current in one phase and decreasing the current level in another phase it is not possible to fully compensate for the harmonic distortion. A trade off situation exists for balancing the phase currents (reducing the neutral current) and fully compensating for the harmonic and displacement distortion. This problem needs to be fully analysed and the benefits for phase balancing and current distortion reduction investigated. An optimisation technique similar to that described in Chapter 7 could be used to determine the optimum operating point for phase balancing and distortion reduction.

10.1.4 Adaptive Fundamental Tracking Filter

Compensating for current distortion in a variable frequency supply system using an active filter has been demonstrated. The frequency range in which the active filter can accurately operate is limited by the bandpass filter which extracts the fundamental load current or supply voltage component. The bandpass filter is designed to have a 180 degree phase delay at the fundamental frequency of 50 Hz. As the system frequency changes an error will occur in the phase information of the generated synthetic sinusoid. This error causes the supply current to be phase displaced from the actual phase of the fundamental of the load current or supply voltage. Thus causing an incorrect amount of phase angle displacement correction.

To accurately track the phase of the fundamental of a variable frequency system the bandpass filter characteristic would need to be adjustable. Using the DSP based digital controller a bandpass filter could be implemented as an adaptive filter. Adaptive filtering techniques have been implemented in signal processing fields [Oppenheim et al. 1989] and should be suitable for this application.

10.2 CONCLUSION

Harmonic currents drawn by an increasing number of nonlinear loads are beginning to create problems in the power system. It has been demonstrated that an active filter can reduce the supply current distortion by converting the distorted current drawn from the power system into a nearly sinusoidal current. This thesis has presented single phase active filters, with analogue and digital controllers, and an analogue three phase active filter which can be used to achieve both harmonic and phase displacement (reactive power) compensation.

A computer model, based on a state space formulation, has been developed for the active filter. The switching strategy for the active filter's power amplifier uses a controlled current, time delay switching technique. This time delay technique effectively produces a spread spectrum of switching frequencies. The computed results have been verified against the actual hardware system and found to be an accurate representation.

The generation of the compensating current signal is based on a time domain approach, where a synthetic sinusoid controls the real power flow into the active filter to compensate for the operational losses. Initially the magnitude of this synthetic sinusoid was controlled manually, by measuring the fundamental component of the load current, and then controlled by the voltage level of the DC bus capacitor. After investigating these techniques a proportional-integral bus voltage controller, which has a response within a few fundamental cycles for step load changes, was implemented.

A three phase active filter was able to reduce harmonic distortion and balance the supply currents of unbalanced harmonic loads. Such phase balancing of unbalanced harmonic loads however does not reduce the neutral current to zero. Complete compensation of the harmonic components in the phase which draws the largest current is not possible. The residual harmonic current flows in the neutral, however this neutral current magnitude is less than the uncompensated supply's neutral current.

The active filter's performance has been shown to be affected by the power amplifier's bus voltage and average switching frequency. These two parameters are used to adjust the efficiency of operation of the active filter and to regulate the possible reduction in supply current THD.

A digitally based controller, using a TMS320C30 DSP, was constructed for a single phase active filter. Such a digital controller makes possible the implementation of "intelligent" control of the active filter's operational characteristic. To achieve this "intelligent" control, a savings equation was developed to represent the benefits of active

filtering. A simplex optimisation technique was implemented to enable the active filter to automatically find the point of maximum savings. This technique was able to set a new bus voltage, average switching frequency and phase displacement correction angle to achieve a maximum savings point in the operation of the active filter. Results were presented which showed that the optimisation algorithm would find the maximum savings point, when started from different points and for load changes which altered the shape of the savings surface.

The application of active filtering to a weak, variable frequency power system was investigated. In a variable frequency system only an active filtering technique is available to remove harmonic currents, since tuned filters are designed to operate at a fixed frequency. It was shown that the active filter could compensate for harmonic currents during a change in supply frequency. For a weak power system (results based on a single generator) supplying a nonlinear load, the supply voltage and current become distorted. The active filter can compensate for this distortion, resulting in both the supply voltage and current becoming nearly sinusoidal.

Another novel application was the connection of the active filter to a three phase diode bridge rectifier-boost converter combination. The boost converter provides a higher DC voltage than was possible by simply rectifying the three phase voltage supply. This boost converter was operated so that the current drawn by the bridge rectifier was similar to a six pulse rectifier with a large inductive load. The three phase active filter was then used to compensate for this distorted supply current and produced a nearly sinusoidal supply current waveform. Such an active filter and boost converter combination results in only one fully rated power switch, with the rating of the active filter devices being 30% of full load. This solution would be more economical than a technique which uses six fully rated power switches to force the rectifier to draw sinusoidal current.

An active filter using a resonant DC link to reduce the switching losses by using zero voltage switching was investigated. The extra complexity and components involved in producing the resonant link active filter resulted in its efficiency being lower than the hardswitched active filter. Resonant configurations for different applications are being investigated internationally to reduce switching losses. The idea of incorporating a resonant technique into an active filter is attractive to improve the system efficiency for high power level applications.

The active filter proposed in this thesis has been shown to reduce the level of harmonic and displacement distortion drawn from the power system by single and three

phase loads. The three phase active filter has the additional capability of performing phase balancing for unbalanced distorted loads. A digital controller for the active filter has been developed which incorporates an "intelligent" optimisation technique to reduce supply current distortion while operating with a high level of efficiency. The optimisation technique uses a simplex algorithm to automatically maximise the possible financial savings, independent of time varying loads, made by reducing the harmonic and displacement distortion drawn from the power system.

REFERENCES

- AKAGI H., NABAE A. and ATOH S. (1986): "Control Strategy of Active Power Filters Using Multiple Voltage-Source PWM Converters", IEEE Trans. Industry Applications, vol. IA-22, no. 3, pp. 460-465.
- ARRILLAGA J. (1982): "Harmonic Elimination", Int. Journ. of Elect. Eng. Education, vol. 19, no. 2, pp. 125-144.
- ARRILLAGA J., BRADLEY D.A. and BODGER P.S. (1985): "Power System Harmonics", John Wiley and Sons, New York.
- ARRILLAGA J. and DUKE R.M. (1980): "A Static Alternative to the Transformer On-Load Tap-Changer", IEEE Trans. Power App. and Sys., vol. PAS-99, no. 1, pp. 86-91.
- ARRILLAGA J., JOOSTEN A.P.B and BAIRD J.F. (1983): "Increasing the Pulse Number of a.c.-d.c. convertors by current reinjection techniques", IEEE Trans. Power App. and Sys., vol. PAS-102, no. 8, pp. 2649-2655.
- ARRILLAGA J., YONGHE L., CRIMP C.S. and VILLABLANCA M. (1992): "Harmonic Elimination by D.C. Ripple Reinjection in Generator-Convertor Units Operating at Variable Speeds", Private Correspondence Paper, University of Canterbury, New Zealand.
- ASTROM K.J. and WITTENMARK B. (1984): "Computer Controlled Systems: Theory and Design", Prentice-Hall, Englewood Cliffs, USA.
- BEIGHTLER C.S., PHILLIPS D.T. and WILDE D.J. (1979): "Foundations of Optimization", Prentice-Hall, Englewood-Cliffs.
- BHATTACHARYA S., DIVAN D.M and BANERJEE B. (1991): "Synchronous Frame Harmonic Isolator using Active Series Filter", European Power Electronics Conf., Firenze, vol. 3, pp. 30-35.
- BOSE B.K. (1992a): "Recent Advances in Power Electronics", IEEE Trans. Power Electron., vol. PE-7, no. 1, pp. 2-16.
- BOSE B.K. (1992b): "Evaluation of Modern Power Semiconductor Devices and Future Trends of Converters", IEEE Trans. Industry Appl., vol. IA-28, no. 2, pp. 403-413.
- BOWLES J. (1989): "HVdc Unit Connected Generators- Receiving End Control", paper no. IV-07, International Colloquium on HVdc Power Transmission, 13-15 August, Recife, Brazil.
- BRIGHAM E.O. (1974): "The Fast Fourier Transform", Prentice-Hall, Englewood-Cliffs.

- CALVERLEY T.E, OTTAWAY C.H. and TUFNELL D.H.A. (1973): "Concepts of a Unit Generator Convertor Transmission System", IEE Conference on High Voltage DC and/or AC Power Transmission, no. 107, pp. 53-59, London.
- CHOE G.H., PARK M.H (1988): "A New Method for AC Harmonic Elimination by Active Power Filter", IEEE Trans. Industrial Electronics, vol. IE-35, no. 1, pp. 141-147.
- CHOE G.H., PARK M.H (1989): "Analysis and Control of Active Power Filter with Optimized Injection", IEEE Trans. Power Electronics, vol. PE-4, no. 4, pp. 427-433.
- CIGRE (1988): "Records of Meetings of SC-11 and SC-14", CIGRE, Paris, France.
- CONVERSE A.O. (1970): "Optimization", Holt, Rinehart and Wiston Inc, New York.
- DIVAN D.M. and SKIBINSKI G. (1989a): "Zero-Switching-Loss Inverters for High-Power Applications", IEEE Trans. Industrial Appl., vol. IA-25, no. 4, pp. 634-643.
- DIVAN D.M. (1989b): "The Resonant DC Link Converter - A New Concept in Static Power Conversion", IEEE Trans. Industry Appl., vol. IA-25, no. 2, pp. 317-325.
- DIVAN D.M. (1991): "Resonant Link Converters", High Power Soft Switching Inverters Tutorial, Power Elect. Spec. Conf.
- DIXON L.C.W. (1972): "Nonlinear Optimisation", English University Press, London.
- DOULAI P. and LEDWICH G. (1990) "Microcontroller-based Strategy for Reactive Power Control and Distortion Compensation", IEE Proc., vol. 137, pt. B, no. 6, pp. 364-372.
- DUFFEY C.K., STRATFORD R.P. (1989): "Update of Harmonic Standard IEEE-519: IEEE Recommended Practices and Requirements for Harmonic Control in Electric Power Systems", IEEE Trans. Industry Appl., vol. IA-25, no. 6, pp. 1025-1034.
- DUKE R.M. and ROUND S.D. (1990): "Novel Use of a Synthetic Sinusoid in the Measurement of Power System Harmonics", Proc. 6th Conf. on Power Electronics and Motion Control, vol. 2, pp. 368-373.
- DUKE R.M., ROUND S.D. and HENDERSON K.C (1990): "An Active Filter for Current Distortion Compensation in Power Systems", Proc. 4th Intl. Conf. on Harmonics in Power Systems, Budapest, Hungary, pp. 367-373.
- ENSLIN J.H.R and VAN HARMELEN G.L. (1990): "Real-Time, Dynamic Control of Dynamic Power Filters in Supplies with High Contamination", Proc. of Power Electronic Specialists Conf., pp. 887-894.

- GATLAND B. (1992): "Ziegler-Nichols Refined", Journal of the Institute of Measurement and Control (NZ) Inc., April, pp. 28-29.
- GREEN A.W., BOYS J.T. and GATES G.F. (1988): "3-Phase Voltage Sourced Reversible Rectifier", IEE Proc., vol. 135, Pt.B, no. 6, pp. 362-370.
- GYUGYI L. and STRYCUŁA E.C. (1976): "Active AC Power Filters", IEEE Industry Applications Society Annual Conference, vol. 19-C, pp. 529-535.
- HANG C.C, ASTROM K.J and HO W.K. (1991): "Refinements of the Ziegler-Nichols Tuning Formula", IEE Proceedings-D, vol. 138, no. 2, pp. 111-118.
- HAYAFUNE K., UESHIBA T., MASADA E. and OGIWARA Y. (1984): "Microcomputer Controlled Active Power Filter", Int. Conf. on Industrial Electronics, Control and Instrumentation, Tokyo, pp. 1221-1226.
- HAYASHI Y., SATO N. and TAKAHASHI K. (1991): "A Novel Control of a Current-Source Active Filter for ac Power System Harmonic Compensation", IEEE Trans. Industry Applications, vol. IA-27, no. 2, pp. 380-385.
- HENDERSON K.C. (1989): "The Development of a High Performance Active Filter for Current Distortion Compensation in Power Systems", M.E. Project Report, University of Canterbury, Christchurch, New Zealand.
- IEC-555-2 (1982): "Disturbances in Supply Systems Caused by Household Appliances and Similar Equipment", International Electrotechnical Commission IEC Standard.
- KOLAR J.W., ERTL H. and ZACH F.C. (1990): "Realization Considerations for Unidirectional Three-Phase PWM Rectifier Systems with Low Effects on the Mains", Proc. 6th Conf. on Power Electronics and Motion Control, Budapest, Hungary, vol. 2, pp. 368-370.
- LAIRD H.D. (1992a): "An Investigation into a Resonant DC Link Shunt Active Filter for the Power System", M.E. Thesis, University of Canterbury, Christchurch, New Zealand.
- LAIRD H.D. and DUKE R.M. (1992b): "A MOS Controlled Thyristor Hardware Model", Proc. National Electronics Conference, vol. 29, Wellington, New Zealand, pp. 167-172.
- LÊ T.N. (1991): "Performance of Voltage-Source Active Filters", European Power Electronics Conference, Firenze, vol. 3, pp. 1-5.
- LEGGETT J. (1992): "Running Down to Rio", New Scientist, vol. 134, no. 1819, pp. 38-42.
- LIN K.S., FRANTZ G.A and SIMAR R. (1987): "The TMS320 Family of Digital Signal Processors", Proceedings of the IEEE, vol. 75, no. 9, pp. 1143-1159.

- MADANGOPAL S. and CATHEY J.J. (1990) "Suppression of Converter Introduced Harmonic Currents using a Forced-Commutated Cycloconverter", IEEE Trans. Energy Conversion, vol. EC-5, no. 4, pp. 632-639.
- MALESANI L., ROSSETTO L. and TENTI P. (1991): "Active Power Filter with Hybrid Energy Storage", IEEE Trans. Power Electronics, vol. PE-6, no. 3, pp. 392-397.
- MOHAN N., PETERSON H.A., LONG W.F., DREIFUERST G.R. and VITHAYATHIL J.J. (1977): "Active Filters for AC Harmonic Suppression", presented at the IEEE/PES Winter Power Meeting, no. A77026-8.
- MOHAN N., UNDELAND T.M. and ROBBINS W.P. (1989): "Power Electronics: Converters, Applications, and Design", John Wiley and Sons, New York.
- MOLER C., LITTLE J. and BANGERT S. (1987): "PC-MATLAB for MS-DOS Personal Computers", The Math Works Inc, USA.
- NAIDU M. and MATHUR R.M. (1989): "Evaluation of Unit Connected Variable Speed Hydro-Power Station for HVdc Power Transmission", IEEE Trans., Power Systems, vol. 4, no. 2, pp. 668-676.
- NAKAJIMA T., MASADA E. and OGIHARA Y. (1987): "Compensation of the Cycloconverter Input Current Harmonics using Active Power Filter", 2nd European Conf. on Power Electronics and Applications, Grenoble, pp. 1227-1232.
- OPPENHEIM A.V. and SCHAFER R.W. (1989): "Discrete-Time Signal Processing", Prentice-Hall, Englewood Cliffs.
- OOI B.T., SALMON J.C., DIXON J.W. and KULKARNI A.B. (1987): "A Three-phase Controlled-Current PWM Converter with Leading Power Factor", IEEE Trans. on Industry Applications, vol. IA-23, no. 1, pp. 78-84.
- PAPAMICHALIS P. (Ed.) (1990): "Digital Signal Processing Applications with the TMS320 Family", vol. 3, Texas Instruments Inc., Houston, pp. 31-52.
- PENG F.Z., AKAGI H. and NABAE A. (1990): "A New Approach to Harmonic Compensation in Power Systems - A Combined System of Shunt Passive and Series Active Filters", IEEE Trans Industry Appl., vol. IA-26, no. 6, pp. 983-990.
- PENNY J.R. (1986): "The Development of a Controlled-Current Inverter System for use in High Performance AC Motor Speed Controllers", M.E. Project Report, University of Canterbury, Christchurch, New Zealand.
- PRESS W.H., FLANNERY B.P, TEUKOLSKY S.A. and VETTERLING W.T. (1986): "Numerical Recipes the Art of Scientific Computing", Cambridge University Press, Cambridge.

- QUINN C.A., MOHAN N. (1992): "Active Filtering of Harmonic Currents in Three- Phase, Four-Wire Systems with Three-Phase and Single-Phase Non-Linear Loads", Applied Power Electronics Conference, Boston, pp. 829-836.
- RAJAGOPALAN V. (1987)" "Computer-Aided Analysis of Power Electronic Systems", Marcel Dekker Inc., New York, pp. 1-25,344-346.
- SANKAR S. (1991): "Dynamic Simulation of AC/DC Systems with Reference to Converter Control and Unit Connection", Ph.D. Thesis, University of Canterbury, Christchurch, New Zealand.
- SASAKI H., MACHIDA T. (1971): "A New Method to Eliminate AC Harmonic Currents by Magnetic Flux Compensation - Considerations on Basic Design", IEEE Trans. Power App. Sys., vol. PAS-90, no. 5, pp. 2009-2019.
- SHEPHERD W. and HULLEY L.N. (1987): "Power Electronics and Motor Control", Cambridge University Press, Cambridge, pp. 209-211.
- SIMAR R. and DAVIS A. (1988): "The Application of High Level Languages to Single-Chip Digital Signal Processors", Proc. Int. Conf. Acoustics, Speech, and Signal Processing. pp. 1678-1681.
- SOUTHPOWER. (1991): "Electricity Pricing Schedule", Southpower, Christchurch, New Zealand.
- TESSAROLO A. (1991): "Fast FFT Algorithm for TMS320C30", Texas Instruments, Sydney, Australia.
- TEXAS INSTRUMENTS (1991): "TMS320C3X Users Guide", Houston, Texas.
- WILLIAMS S.M. and HOFT R.G. (1991): "Implementation of Current Source Inverter for Power Line Conditioning", IEEE Trans Industry Applications, vol. IA-27, no. 4, pp. 773-779.

APPENDIX A

MATHEMATICAL ANALYSIS OF RESONANT LINK

The resonant link converter analysis is based on the connection shown in Figure A.1. The resonant cycle is analysed only when the thyristor T, is on. Initially it is assumed that T is off and that the load current I_L is freewheeling through the diode D. The voltage across the resonant capacitor C_R is at zero for this particular time. When the thyristor is off no current flows through the inductor L. The DC bus capacitor C_B is initially charged to a voltage V_B . The resistor R is used to model the losses associated with the conduction of the thyristor, resistance of the inductor and the equivalent series resistance of capacitors C_B and C_R .

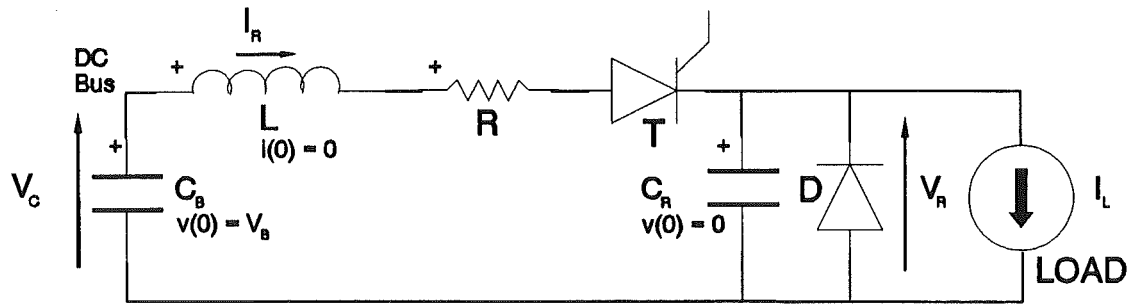


Figure A.1 Resonant Link Configuration used in Resonant Cycle Analysis

In this analysis it is assumed that the load current and bus capacitor voltage are constant during one resonant cycle and can therefore be represented by a constant current source I_L and voltage source V_B respectively. When diode D is freewheeling, the resonant capacitor is effectively removed and the resonant link can be simplified to the circuit as shown in Figure A.2. At time $t=0$, the thyristor is turned on and the resonant current starts to build up. The diode remains conducting until the resonant current I_R is greater than the load current I_L .

The resonant current, when the thyristor is on and the freewheeling diode is conducting, can be determined using a complex frequency domain representation of Kirchoff's Voltage Law (KVL) as in Equ. (A.1).

$$\frac{V_B}{s} - I_R(s)(R+sL) = 0 \quad (A.1)$$

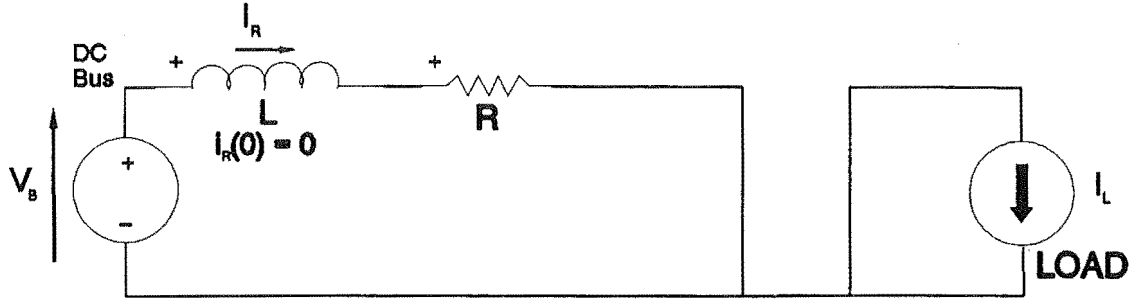


Figure A.2 Simplified Resonant Link Configuration when diode D is freewheeling ($I_R < I_L$)

Using an inverse Laplace transform, a time domain representation of the resonant current can be derived as described by Equ. (A.2).

$$i_R(t) = \frac{V_B}{R} (1 - e^{-\frac{R}{L}t}) \quad (\text{A.2})$$

When $i_R(t) = I_L$ the freewheeling diode turns off at time t_1 , as defined by Equ. (A.3).

$$t_1 = -\frac{L}{R} \ln \left(1 - \frac{I_L R}{V_B} \right) \quad (\text{A.3})$$

For all times greater than t_1 , the diode is off and the resonant capacitor C_R begins to charge. This can be represented by another simplified configuration which is shown in Figure A.3.

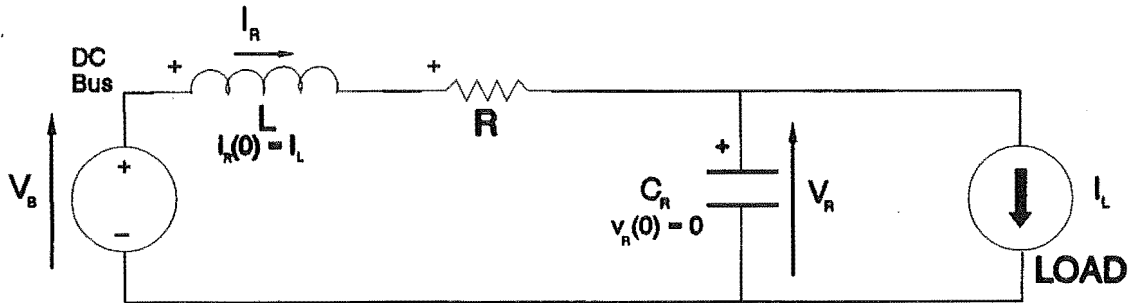


Figure A.3 Simplified Resonant Link Configuration when Diode D is off ($t > t_1$)

The resonant current I_R is determined using KVL and the initial inductor current $i_R(0)$ (where $i_R(0) = I_L$) as described by Equ. (A.4). To simplify the analysis it is assumed that t_1 is effectively $t=0$.

$$\frac{V_B}{s} - I_R(s)(R + sL) + Li_R(0) - \left(I_R(s) - \frac{I_L}{s} \right) \frac{1}{sC_R} = 0 \quad (\text{A.4})$$

Solving for I_R results in Equ. (A.5).

$$I_R(s) = \frac{\left(\frac{I_L}{sLC_R} + \frac{V_B}{L} - sI_L \right)}{s^2 + s\frac{R}{L} + \frac{1}{LC_R}} \quad (\text{A.5})$$

and using Equ. (A.6), which are definitions of resonant frequency ω and damping δ , gives Equ. (A.7).

$$\omega = \sqrt{\frac{1}{LC_R}} \quad \text{and} \quad \delta = \frac{R}{2} \sqrt{\frac{C_R}{L}} \quad (\text{A.6})$$

$$I_R(s) = \frac{\frac{V_B}{L}}{s^2 + 2\delta\omega s + \omega^2} + \frac{\frac{I_L}{LC_R}}{s(s^2 + 2\delta\omega s + \omega^2)} + \frac{sI_L}{s^2 + 2\delta\omega s + \omega^2} \quad (\text{A.7})$$

Taking the inverse Laplace transform of Equ. (A.7) and substituting the correct time back in gives the time domain form of the resonant current I_R as described by Equ. (A.8).

$$\begin{aligned} i_R(t) = & \frac{V_B}{\omega L} \frac{1}{\sqrt{1-\delta^2}} e^{-\delta\omega(t-t_1)} \sin(\omega\sqrt{1-\delta^2}(t-t_1)) \\ & + I_L \left(1 - \frac{1}{\sqrt{1-\delta^2}} e^{-\delta\omega(t-t_1)} \sin(\omega\sqrt{1-\delta^2}(t-t_1) + \phi) \right) \\ & - \frac{I_L}{\sqrt{1-\delta^2}} e^{-\delta\omega(t-t_1)} \sin(\omega\sqrt{1-\delta^2}(t-t_1) - \phi) \end{aligned} \quad (\text{A.8})$$

where $\phi = \tan^{-1} \frac{\sqrt{1-\delta^2}}{\delta}$

Now solving for the resonant voltage V_R , using KVL, it is possible to determine Equ. (A.9).

$$\frac{V_B}{s} - I_R(s)(R + sL) + Li_R(0) - V_R(s) = 0 \quad (\text{A.9})$$

substituting for I_R as given by Equ. (A.10)

$$I_R(s) = sC_R V_R(s) + \frac{I_L}{s} \quad (\text{A.10})$$

results in Equ. (A.11)

$$V_R(s) = \frac{\frac{V_B - I_L R}{sLC_R}}{(s^2 + s\frac{R}{L} + \frac{1}{LC_R})} \quad (\text{A.11})$$

and then using ω and δ , as defined by Equ. (A.6), results in $V_R(s)$ being defined by Equ. (A.12).

$$V_R(s) = (V_B - I_L R) \frac{\omega^2}{s(s^2 + 2\delta\omega s + \omega^2)} \quad (\text{A.12})$$

Taking the inverse Laplace transform of Equ. (A.12) gives the time domain expression of the resonant voltage V_R as described by Equ. (A.13).

$$v_R(t) = (V_B - I_L R) \left(1 - \frac{1}{\sqrt{1-\delta^2}} e^{-\delta\omega(t-t_1)} \sin(\omega\sqrt{1-\delta^2}(t-t_1) + \phi) \right) \quad (\text{A.13})$$

where $\phi = \tan^{-1} \frac{\sqrt{1-\delta^2}}{\delta}$ (as before)